MAGISTERARBEIT

Titel der Magisterarbeit

„M-Type Stars and their Space Weather“

Verfasserin

Traude Rochowanski Bakk.[a] rer. nat.

angestrebter akademischer Grad

Magistra der Naturwissenschaften (Mag. rer. nat.)

Wien, 2012

Studienkennzahl lt. Studienblatt:	A 066 861
Studienrichtung lt. Studienblatt:	Astronomie
Betreuer:	Univ.-Prof. Dr. Arnold Hanslmeier

To those who never stop questioning

Table of Contents

1 Introduction

1.1 M-Type Stars

When searching for habitable planets outside the Solar System, stars below two solar masses are the best candidates, as their lifetimes are long enough for the evolution of life. About 95% of stars between 0.1 and 2 $M_\odot$ are M-type stars (*Scalo et al.* 2007, and references therein). Although M star masses are so small, they make up about half of the total mass of all stars in the Milky Way (*Reid & Hawley,* 2005).

M-type stars are very small and faint, ranging in mass from about 0.075 to 0.6 solar masses. In the Hertzsprung-Russell diagram they lie between K-type stars and brown dwarfs. A consequence of their very low masses are relatively low temperatures, which are between about 2300 K and 3800 K (e.g. *Reid & Hawley,* 2005). Furthermore, stars of spectral type M are divided into three subgroups: early-type (M0-M3), mid-type (M3.5-M6) and late-type (M6.5-9.5).

Looking at an M star's spectrum, the titanium oxide (TiO) absorption bands are the defining features. For a long time it was believed that M dwarfs are the lowest extremities of the hydrogen-burning main sequence. But photometric surveys have become more sensitive and led to the discovery of even fainter and cooler stars, which have spectral characteristics that do not fit spectral class M. Hence, a new spectral class was defined, class L. This class is separated from M dwarfs through decreasing strength of TiO. Early-type L stars seem to be a mixture of brown dwarfs and hydrogen-burning stars, despite their very low masses. In addition, spectral class T was established. Objects of this spectral class are brown dwarfs with substellar masses. Their temperatures are too low to initiate hydrogen burning.

A distinctive feature of M-type stars is not only their large number but also that this spectral class of stars is the only one below 2 $M_\odot$ (AFGKM) that has two different modes of energy transport depending on their mass. From M0-M3.5 they behave similar to the Sun, having a radiative zone surrounded by a convective envelope.

Between these zones there exists what *Barnes* (2003) calls the *interface*, a region comparable to the Sun's tachocline[1]. The convective zone increases with decreasing stellar mass until stars below ≈ 0.35 $M_\odot$ become fully convective (e.g. *West & Basri,* 2009). This means that all M dwarfs later than M3.5 are fully convective, which seems to change their behavior in several ways. This point will be discussed in more detail in section 1.3.2.

As their emission maximum lies in the infrared, M-type stars are also called red dwarfs. In this work the expression “M dwarf” respectively “red dwarf” stands for all stars with absolute visual magnitudes fainter than $M_V > 8$.

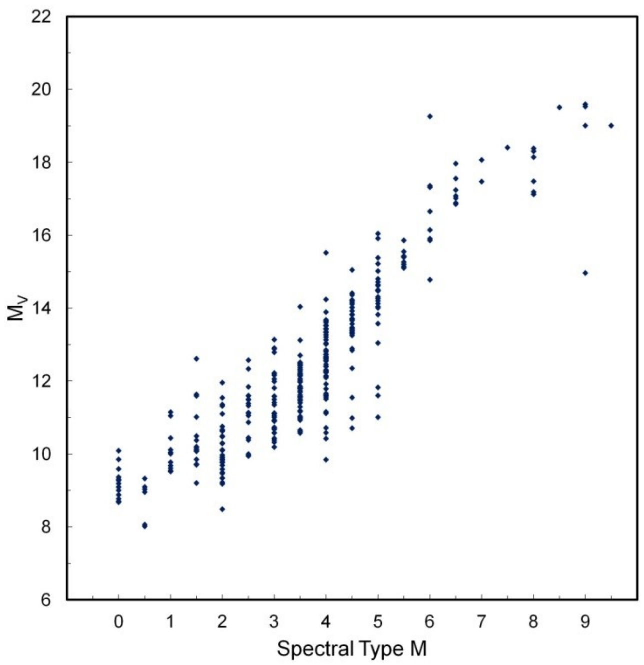

Figure 1.1. The relationship between spectral subtype and visual absolute magnitude of all M stars studied in this work.

Figure 1.1 shows the visual absolute magnitudes of the M stars sample studied in this work as a function of spectral subtype. It can be clearly seen, that the later the subtype, the fainter is the star's visual absolute magnitude.

[1] The tachocline is a thin transition region between the Sun's radiative and convective zone. Since the radiative zone exhibits a solid-body rotation and the convective zone rotates differentially, this leads to shear effects that are believed to induce the activity cycle of the Sun.

1.2 Space Weather

The term s*pace weather* stands for all effects caused by the Sun's activity, that may have an influence on space-born or ground-based technological systems, as well as on organisms. It is also believed that the solar variability, among other effects, might influence changes of the Earth's climate. By observing the Sun, it is attempted to find periodicities in photospheric, chromospheric and coronal events and thus make such events predictable. A further goal is to understand the evolution of the Sun from its birth until the current era.

The Sun continuously emits a stream of charged particles, known as the solar wind. These charged particles form a bubble around the Solar System, the heliosphere. It protects the Solar System from energetic cosmic rays coming through the local interstellar medium. Due to the activity of the Sun, the solar wind is variable and hence also the size of the heliosphere. As the solar wind is modulated by the Sun's activity, its strength follows the well-known eleven year solar cycle.

In addition to the solar wind, there are many other solar activity phenomena, e.g. prominences, faculae, coronal holes, etc., but for this work the most interesting effects of space weather are sunspots, flares and coronal mass ejections (CME) as they can also be observed on other stars. The mentioned phenomena occur in the stellar atmosphere, which is composed of the photosphere, the chromosphere and the corona.

Sunspots are dark areas on the Sun's photosphere (Fig. 1.2). When referring to other stars than the Sun they are called starspots. They often arise in groups. Concerning the Sun, they only appear at lower latitudes on both sides of the equator but never close to the poles (*Hanslmeier,* 2007). This is different for stars of spectral class M (*Mullan*, 1974). Starspots are darker than the rest of the star's surface due to their lower temperature. The darkest region is in their centers, the umbra. The penumbra surrounds this region and is less dark. These two regions are embedded a little deeper into the surface of the surrounding plasma. This phenomenon is called the *Wilson depression* (*Hanslmeier,* 2007).

Through the observation of starspots one can determine a star's rotation period, a parameter that is of highest interest concerning the star's age and activity (see section 1.4).

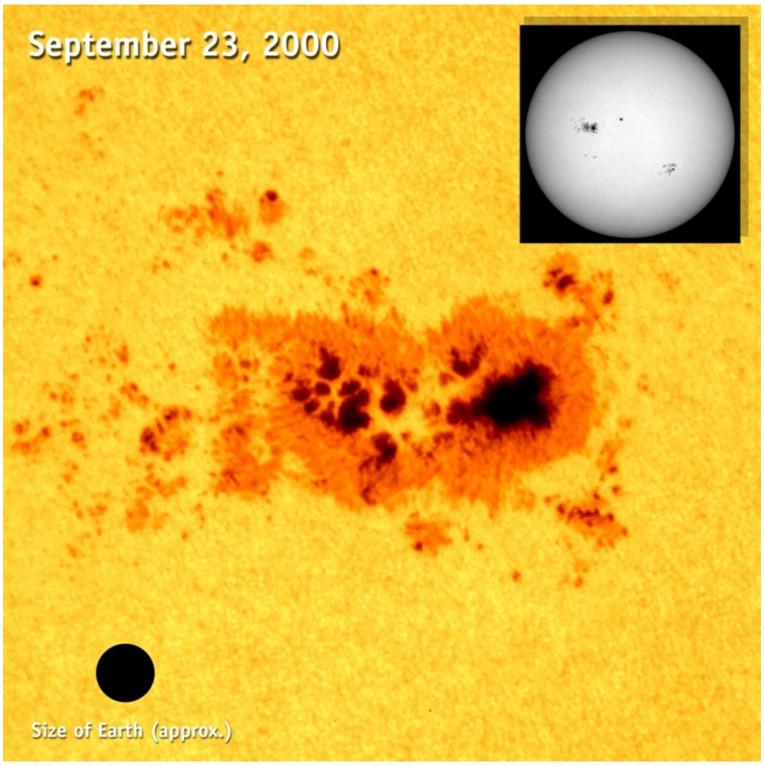

Fig.1.2. Sunspot seen from SOHO satellite in September 2000 with the relative size of the Earth for comparison. Taken from http://sohowww.nascom.nasa.gov/gallery/images/sunspot00.html (January 19th, 2012).

As starspots are cooler than the rest of the stellar surface and temporary phenomena, their existence changes the radiation emitted by the star in different periods of time, which means that planets orbiting the star are exposed to varying radiation intensities.

The origin of starspots is the rise of a magnetic flux tube due to magnetic buoyancy. When the flux tube emerges at the photosphere, a spot becomes visible. Hence this stellar activity phenomenon is related to a star's magnetic activity (*Hanslmeier,* 2007). The number of starspots changes with a period of time, whereupon the Sun is the only star with an identified periodicity, namely eleven years. To study starspots on the photosphere, the Ca II K spectral line can be used as an indicator.

Above the photosphere lies the chromosphere, which has a much higher temperature. This layer is the source of flares, which are eruptions that release large amounts of energy within minutes and thus suddenly brighten a star's surface (Fig. 1.3). During a stellar flare radiation of all wavelengths, from radio waves to gamma rays, is produced, but especially short-wavelength radiation such as UV and X-ray. This strong short-wavelength radiation ionizes molecules in a planet's atmosphere, which can further be eroded by stellar winds if the planetary field is weak, meaning that the planet could lose its atmosphere and would be no longer protected from ionizing short-wavelengths which can be harmful for life.

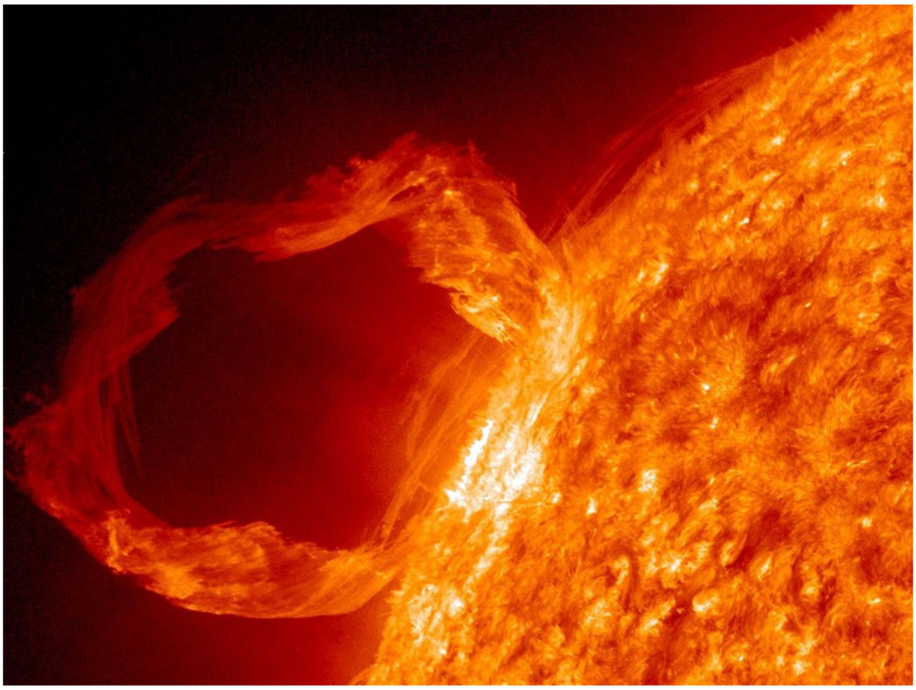

Figure 1.3. Solar flare seen by the SOHO satellite. Taken from http://spacefellowship.com/news/art23691/scientists-unlock-the-secrets-of-exploding-plasma-clouds-on-the-sun.html
(January, 19th, 2012)

Flares appear in regions of higher activity around starspots. To determine the activity of a star's chromosphere, the emission lines H (396.8 nm) and K (393.4 nm) of singly ionized Ca (Ca II) can be used. These lines appear stronger in a star's spectrum when the activity is at maximum (*Hanslmeier,* 2007). Another suitable spectral line to observe the chromosphere is the spectral line Hα (656.3 nm), which will be explained in more detail in section 1.3.2.

The outermost layer of a stellar atmosphere is the corona, which can extend to several solar radii. Its shape changes depending on the solar activity cycle, being more spherical at an activity maximum (*Hanslmeier,* 2007). In this layer the so-called coronal mass ejections (CME) can be observed (Fig. 1.4). A coronal mass ejection is another highly energetic phenomenon, where enormous amounts of stellar material are ejected into a planetary system. Until the 1970's they were unknown because of their poor visibility. The invention of the coronagraph made it possible to cover the solar disk and thus making coronal phenomena observable. At the moment it is not known whether CMEs are connected to flares or not, as CMEs partly appear after a foregone flare, but also separately.

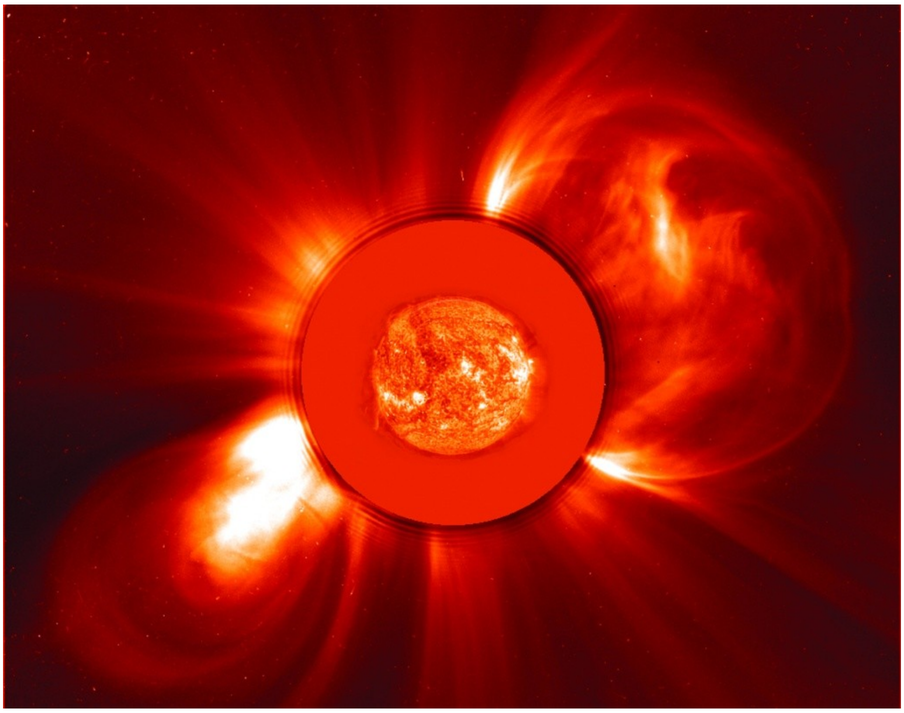

Figure 1.4. Coronal mass ejection seen by SOHO satellite blocking out the light of the solar disk to make the corona visible. Relative size of the Sun shown. Taken from http://sohowww.nascom.nasa.gov/gallery/images/c2eitnov800.html (January, 19th 2012)

1.3 M-Type Stars and their Space Weather

Actually the term *space weather* was created to describe effects caused by the Sun's variability, having an influence on planets in the Solar System's habitable zone[2]. But today, where Earth-like planets are intensively searched and wide-ranging discussions about their habitability are held, space weather becomes also very important for all other stars than the Sun, which are orbited by extrasolar planets. In this work the space weather of M-type stars is examined carefully, which consequently means that their activity depending on their mass, age and spectral subtype was studied.

1.3.1 Internal Structure of M Dwarfs

To understand the different activity phenomena of M-type stars, one has to examine their internal structure. Early-type M stars up to about spectral subtype M3 or stellar masses between 0.35-0.6 $M_\odot$ have a quite similar structure when compared to the Sun (Fig. 1.5). In the center there is a core, which is surrounded by a radiative zone and generates the energy output. Above this layer is the convective envelope, separated from the radiative interior by a transition region, the interface (*Barnes,* 2003). In the convective zone a MHD-dynamo produces a magnetic field, which provokes the heating of the stellar atmosphere that lies above the convective zone and causes various activity phenomena (*Hartmann & Noyes,* 1987, and references therein).

Similar to the Sun, the stellar atmosphere is composed of the photosphere, the chromosphere and the outermost layer, the corona. Between the chromosphere and the corona exists a transition region.

It is believed that all red dwarfs later than M3-M3.5 are fully convective, which means that all energy produced in the core is transported to the outermost layer of the star by convection. Early-types (M0-M3) may have a small radiative core.

---

[2] The so-called habitable zone is a circumstellar region around a star, where liquid water can be maintained on a planet's surface (*Kasting et al*., 1993).

Full convection means further, that helium, which is produced by nuclear fusion of hydrogen, does not accumulate at the core, as it is presumed to happen in Sun-like stars. This leads to a much slower evolution of the star and constant luminosities for hundreds of billions of years. In comparison to the expected long lifetime of M stars, the age of the universe is small. So even when observing an M star older than twelve billion years, it means that the star is investigated somewhere during its initial period on the main sequence.

The point of full convection varies slightly depending on the author. For example, *Barnes* (2007) states that stars become fully convective below 0.3 $M_{\odot}$, *West & Basri* (2009) below 0.35 $M_{\odot}$. In addition, there exist other theories, that place this boundary for young stars with strong magnetic fields and fast rotation around spectral subtype M6-M7 as it is presumed that this behavior can block the transition to full convection (*Chabrier et al.,* 2007). Above this zone the stellar atmosphere is composed in the same manner as in early-type M stars.

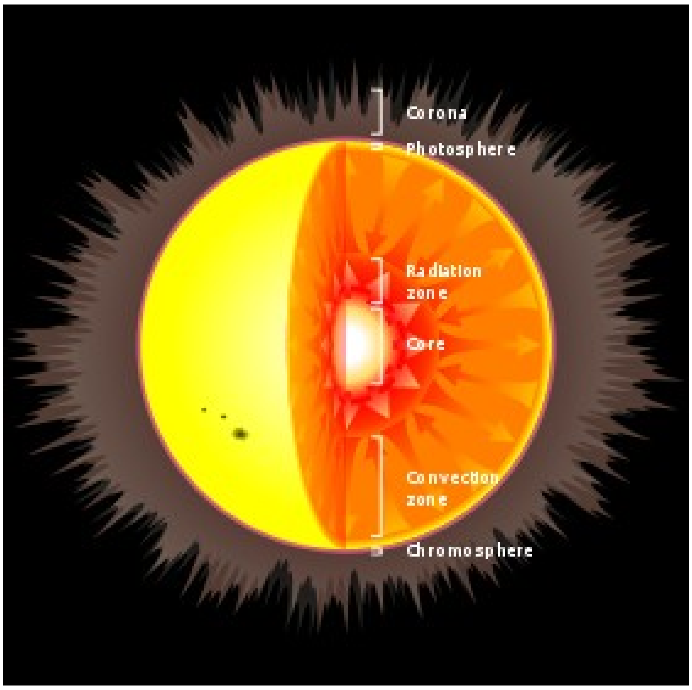

Figure 1.5. Illustration of the internal structure of a Sun-like star showing the different layers except the tachocline. Taken from en.wikipedia.org/wiki/Main_sequence (January 19th, 2012)

1.3.2 Activity of M Dwarfs

Ejnar Hertzsprung was the first, who published an article about M dwarf variability in 1924, where he reported about changes in the brightness of these stars. It took decades to determine that these changes were caused by activity phenomena. Until 1970 about 50 stars showing the same behavior were known and endued with the term *flare star*. *Gurzadyan* (1970) noticed that almost all of these stars belonged to spectral class M, more precisely mid and late M-type stars.

Stellar activity is always connected with the presence of a magnetic field. *Parker* (1955) was the first, who postulated a theory about magnetic field generation in the convective zone of the Sun. His theory of the dynamo mechanism is now known as the $\alpha\Omega$ dynamo. α and Ω are two processes in the generation of magnetic fields.

Reid & Hawley (2005) summarize these processes as follows:
An initial poloidal field generates a toroidal field through shearing forces at the interface. This process is known as the Ω effect. The toroidal field generates through its cyclonic motions a new poloidal field, known as the α effect. Both effects Ω and α are caused by stellar rotation. The twisted magnetic flux lines of the toroidal field occur due to the turbulences in the convective zone. Such magnetic flux lines gathered together build flux tubes, which rise to the surface by magnetic buoyancy and emerge as loop-like structures. The areas, where this happens, are active regions on a stellar surface and can be observed as starspots. M dwarfs' photospheres can be covered with long-lived starspots over a significant fraction of their surface (*Tarter et al.,* 2007, and references therein). In this region the strength of toroidal magnetic fields seems to be amplified and organized causing starspots on the photosphere (*Browning et al.,* 2010). The current belief is that all M stars with masses higher than 0.3 $M_\odot$ generate such a magnetic dynamo at the interface (*Parker,* 1993; *Browning et al*., 2010, and references therein) as they have a similar internal structure as the Sun (see section 1.3.1).

There are indications that the magnetic field generation differs below the fully convective mass limit as the magnetic dynamo cannot work (*Browning et al*., 2010). Another mechanism must exist that explains the existence of a magnetic field.

These authors add that there is evidence of a change in the atmospheric heating mechanism as well.

Bercik et al. (2005) show that the magnetic field of fully convective stars can be generated by turbulent dynamos. This topic is not properly understood at the moment. *Tarter et al.* (2007) claim that there is no obvious transition in the activity behavior of M dwarfs around M3-M4, which is right at the mass where the radiative zone disappears. Several other authors support this presumption that the level of activity is not influenced at the transition from partly to fully convective stars (e.g. *Kiraga & Stépien,* 2007, *Delfosse et al.,* 1998). *West et al.* (2008), however, observed a transition when the stars become fully convective at M3-M4. Firstly, they show that the activity lifetimes are dependent on the spectral subtype and therefore stellar mass. Secondly, he illustrates a dramatic increase in the lifetimes of atmospheric activity below the mass limit of the fully convective model. A similar effect was also noticed in the studied M stars' sample in this work (see section 3.4-3.6).

Several activity properties of M dwarfs are well-studied. M stars at young ages can generate very strong magnetic fields, some of them much stronger than the solar magnetic field (up to several kG), covering almost the entire star (*Tarter et al*., 2007). The stronger a magnetic field, the more intense are space weather phenomena like flares. M stars are known to have extremely strong flaring events, which can brighten the star's surface several times within minutes, emitting X-ray and strong UV radiation. It is still unclear how long the violent flaring period of M dwarfs lasts. The current belief is that younger stars are more likely to flare. *Selsis et al.* (2007) have shown that the duration of intense ionizing radiation, a sign of high activity, increases with decreasing stellar mass.

Rotation and magnetic activity seem to be connected. High stellar activity seems to be linked with rapid rotation (*Kiraga & Stépien,* 2007). *Reiners & Basri (*2009) state that coronal and chromospheric activity saturate at high rotation rates. Furthermore, this relation shows a mass dependency. From early- to mid-type M dwarfs chromospheric and coronal emission is correlated with rotation (*Browning et al*., 2010).

In addition, *Mohanty & Basri* (2003) demonstrated that at mid- and late-type M dwarfs (M5-M9) there appears to be a threshold value where the chromospheric emission is more or less independent from the rotation period. But not all M dwarfs show chromospheric emission, only the more active fraction, which has its maximum around M7 (*West et al.,* 2004). It is still unclear in which way the rotation rate is connected to the strength of dynamo-generated magnetic fields.

In 1972, *Skumanich* claimed that stars rotate rapidly at very low ages and slow down with time through the loss of angular momentum, caused by stellar winds. This process is called rotational braking. The duration depends on the strength and geometry of the stellar magnetic field and thus is linked to the rotation period of the star (*Matt & Pudritz,* 2008). Observations let one presume that the spin down time is strongly connected with stellar mass (*Barnes,* 2003*). Mohanty & Basri* (2003) discussed this topic for M dwarfs and come to the conclusion that for lower mass late-type stars the time needed to spin down is longer than for early-type M stars.

Indicators for stellar activity are the spectral lines in X-ray, EUV, the Hα line, the H and K lines of Ca II and Mg II (*Hanslmeier,* 2007). The ratio between the luminosity in the Hα line and the bolometric luminosity, $L_{\mathrm{H}\alpha}/L_{\mathrm{bol}}$, is a good indicator of chromospheric activity (e.g. *Reid & Hawley,* 2005). *Browning et al*. (2010) add some concerns in using Hα as an activity proxy as they claim that no observable Hα emission can stand for two different activity levels, namely no activity or a moderate amount of activity, as Hα first appears in absorption and then with increasing activity appears in emission. A solution for this problem could be the chromospheric Ca II K and H lines' emission but, as they lie blueward of the most CCD sensitivities, this becomes especially difficult for already faint M-type stars. The corona is formed of high-temperature gas surrounding the star's chromosphere. To determine the coronal activity level, one has to calculate the ratio between the luminosity emitted at X-ray wavelengths and the bolometric luminosity, $L_{\mathrm{X}}/L_{\mathrm{bol}}$ (e.g. *Reid & Hawley,* 2005).

Stellar activity leads to variability of the emitted radiation. This variability has long, but also short timescales. Several programs concentrate on long-term changes in chromospheric activity.

On the long-term side, it is presumed that luminosity changes can be caused through stellar mass loss by stellar winds and coronal mass ejections. The short-term variability is mainly caused by starspots and flares.

Today it is well-known that stars other than the Sun also have activity cycles, but not as precisely determined as that of the Sun (*Soon et al.*, 1993).

1.4 Age Determination for Red Dwarfs

Age is one of the most fundamental parameters of a star. Stellar ages are necessary to gain further knowledge about the star's evolution over time and consequently its activity, but it is especially interesting, for investigating the evolution of a planetary system. The more precise a host star's age can be determined, the more can be concluded about the planets orbiting the star. But estimating the ages of M-type stars is still connected with several challenges and problems. Because of their small masses and consequently slow evolution an extremely long lifetime of up to 200 Gyr or even more can be expected. Most of this time they spend on the main sequence burning hydrogen to helium. As a consequence of their very small masses this process lasts much longer than for stars like the Sun and leads to the presumption of their long lifespan. Nevertheless, it has been attempted to find methods to estimate the ages of M-type stars. There are several methods which are well accepted despite their disadvantages. These methods and their associated problems will be discussed in the following.

Within the last years more than 40 exoplanets orbiting M-type stars have been discovered. Consequently the question arises whether these small, red stars could be hosts for habitable planets. There are several concerns pertaining to their habitability, for example their long-lasting highly ionizing short-wavelength radiation. Further, such planets are exposed to flaring events and other space weather phenomena like coronal mass ejections and strong stellar winds (see section 4.1). Therefore, it is crucial to ascertain more about their evolution over time and how activity parameters change with it. This can be done by estimating the ages of these stars and comparing stars with similar masses at different ages.

1.4.1 Chromospheric Activity- Age Relation

Noyes et al. (1984) showed a relationship between chromospheric emission and age. This method concentrates on the star's chromospheric activity and thus is also known under the term *activity age*. *Donahue* (1998) calculates the chromospheric age *t* [Gyr] calibrated on stars from G0-K7 as follows:

$$\log t_{chromo} = 10.725 - 1.334R_5 + 0.4085R_5^2 - 0.0522R_5^3 \tag{1.1}$$

where $R_5 = 10^5 R'_{HK}$. R'_{HK} is the ratio between the flux of Ca II H and K lines (corrected for the photospheric contribution) and the bolometric flux (*Noyes et al.,* 1984).

Stellar activity declines with age. Depending on the stellar mass, this happens faster or slower. Thus this method is more useful for stars > 1 $M_{\odot}$, as they evolve faster and so long-term changes in their chromospheres can be studied. The advantage of this method is, that only the chromospheric emission in the Ca II H and K lines has to be measured and can be transformed into age without any additional information. Concerning M-type stars, this age-activity-relation leads to several problems as various authors calibrate it for stars for different spectral types, for example *Mamajek & Hillenbrand (*2008) for F7-K2. Using chromospheric emission as an age indicator, one has to consider that several measurements of the same star are essential to compile an average and thus exclude variability from stellar cycles or the rotation itself (*Barnes,* 2007).

1.4.2 Moving Group Ages

This method makes use of the similar kinematics of the individual members of known moving groups, formed in the same star forming region and hence being nearly coeval. Since not many old moving groups are known, this age determination method should be preferred for young stars. Estimating stellar ages with the moving group method can be problematic as stars with different ages having the same kinematics can share a moving group and lead to errors in determining ages, so the membership has to be carefully evaluated (*Lopez-Santiago et al*., 2009).

1.4.3 Isochrone Method

Changes in luminosity and temperature are the primary indicators of isochrone age determination. Therefore, one criterion is to know the exact stellar distances, which leads to inaccuracy in this method when used on field stars (*Barnes,* 2007). For M-type stars this method is generally rather unsuited as their luminosity does not measurably change over a long period of time and hence is more qualified for faster evolving stars.

1.4.4 Rotation-Age Relation

The last age determining method mentioned here, seems to be the most interesting concerning at least a fraction of M dwarfs and will be explained in more detail as all age estimation calculations in this work were done by using this method. It is called *Gyrochronology* and uses the effect, that rotation declines with age (*Barnes,* 2007). This method can be used for low-mass, Sun-like stars (FGKM) on the main sequence, which support a solar dynamo (*Barnes,* 2003).

Barnes (2007) states that the most important activity-related parameter of a star is the rotation period. Firstly, because it is independent of the star's distance. Secondly and even more important, several studies have shown that it orderly changes with time and this change can actually be predicted. This fact is of the highest interest for late-type main sequence stars, for which the isochrone method is not really suitable.

Another advantage of this method is, that rotational periods of stars can be measured rather exactly even for late-type stars with very faint visual luminosities. For example, *Irwin et al.* (2011) give a measured rotation period for a star of spectral class M8, with a mass of about only 0.08 $M_{\odot}$ and at a distance of more than 14 pc.

Barnes (2007) suggests that the rotation period primarily depends on stellar age and mass. Therefore, all stars are classified into two groups (Fig. 1.6): fast/convective/C and slow/interface/I, whereupon he also mentions that there is actually a third group called "g" (gap) that represents stars in transition from I to C. He calls these groups "varieties" and claims that each of them has an individual mass and age dependency.

Variety I (interface sequence stars) is associated with *Skumanich* (1972) and is used in his article to demonstrate the gyrochronology method. *Skumanich* (1972) presented a ratio of a solar-type star's rotational velocity to its age, known as the Skumanich law ($v \sin i \propto 1/\sqrt{t}$). Because of the generally unknown angles of inclination i, this method can lead to large errors in the estimated ages.

The lower a star's mass, the thicker is its convective zone. *Barnes* (2003) presumes that fully convective stars, which do not have an interface, have to be of variety C as they are not able to induce an interface dynamo and thus cannot transform to an I sequence star. Mid- and late-type M stars must have a turbulent dynamo as mentioned in section 3.1.2.

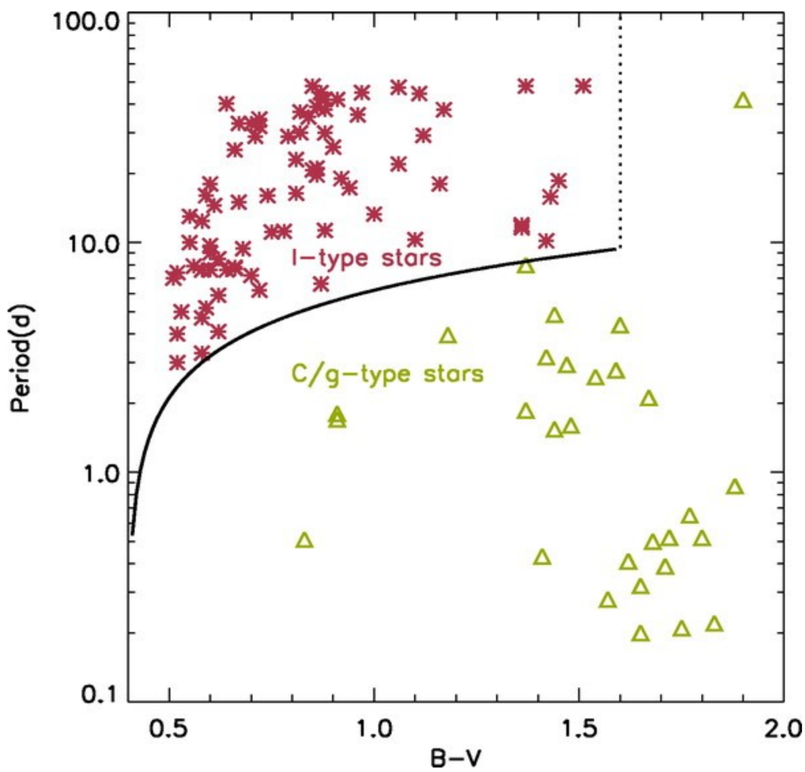

Figure 1.6. Plot taken from *Barnes* (2007) illustrating varieties I and C/g from the *Pizzolato et al.* (2003) stars' sample. The solid line separates the stars of variety I from variety C/g and represents a rotational isochrone for 100 Myr, while the dotted line shows the color at which stars are believed to become fully convective (B-V = 1.6).

Barnes (2003) accentuates that an advantage of gyrochronology is the fact, that rotation periods can be determined with great precision and is only limited by differential rotation of a stellar surface.

The rotation rate can be measured by observing changes in a star's light curve induced by starspots on the surface of solar- and late-type stars (*Barnes,* 2003).

High activity stars seem to be more spotted producing stronger light variations when photometrically studied. That makes it easier to determine their precise rotation periods. Determining the rotation periods of stars can also lead to problems, as the same method is used for detecting extrasolar planets by the transit method. How fast a star spins down seems to depend on its mass. Stars with lower masses spin down faster and higher mass stars spin down slower (*Barnes,* 2003).

It seems to be that estimating stellar ages by using the rotational period leads to the best results. Comparing calculated gyrochronological and chromospheric ages, *Barnes* (2007) and *Odert et al.* (2010) come to the conclusion that these methods are in pretty good agreement in contrast to isochrone ages, where deviations are quite common. Nevertheless, *Barnes* (2007) emphasizes that such a comparison is only then significant and reasonable when the chromospheric emission was measured repeatedly over a longer period of time and only measured and not calculated rotational periods were used without exception.

As a fact, many more rotational periods have to be measured from all different kinds of M dwarfs (from high to low activity levels, from the upper to the lower mass limit, from M0 to M9.5, from both varieties C and I and from slow to fast rotators) to make significant statements possible. The space missions *Kepler* and *CoRoT* were designed to detect exoplanets by using the transit method but also yield the rotation periods of planetary host stars as it is a side effect of all planetary transit missions and thus a large quantity of rotation periods can be expected in the near future.

Of course, there are several more methods for stellar age determination. The above methods were explained as they were mentioned respectively used in this work. For further information concerning this topic *Soderblom* (2010) gives a detailed overview.

2 Data and Methods

2.1 Compiling the Sample

A sample consisting of 355 M-type stars was taken from the PhD thesis "Activity of M-type stars and the influence on planetary atmospheres" (*Odert* 2012, in preparation). From this catalog the stars' names and their trigonometric parallaxes were taken and sorted by increasing right ascension. These stars are all single objects, which are within 15 parsec (pc) of the Sun as measured by trigonometric parallaxes. Using the parallaxes the distances in parsec were calculated by dividing 1000 by the parallax in mas.

Their coordinates were taken from *2MASS*[3] (*Skrutskie et al.,* 2006). Furthermore, the exact spectral subtype (M0-M9.5) was found on *Simbad*[4], where all stars were confirmed as spectral type M. Also the radiation fluxes in apparent magnitudes m in the passbands U, B, V, R and I were taken from *Simbad*. Since *Simbad* does not list a magnitude for each star in each wavelength, additional catalogs were searched to make the sample as complete as possible. All available references will be given in the next chapter. For the photometric bands J, H, and K the apparent magnitudes m were taken from *2MASS* (*Cutri et al.,* 2003), as this catalog contains data for every single star in these three bands.

Additionally the short-wavelengths NUV, FUV, EUV and X-ray as well as the emission of the spectral line Hα were of great interest for this work. NUV and FUV values were taken from *GALEX*[5], EUV from the *EUV Master Catalog*[6], X-ray from *Odert* (2012, in preparation) and finally Hα emission values out of several articles, referenced later.

---

[3] 2MASS stands for Two Micron All Sky Survey and was a mission running from 1997-2001 using two telescopes located in the northern and southern hemisphere to cover the entire sky in the three near-infrared passbands J, H and K.

[4] http://simbad.u-strasbg.fr/ (October 14th, 2011)

[5] *GALEX* stands for Galaxy Evolution Explorer and is an ultraviolet space telescope measuring in NUV and FUV ranges launched in 2003 and still in operation. Data products see: http://galex.stsci.edu/ (November 2nd, 2011) Using the stars' coordinates, *GALEX* objects in GR6 (*GALEX* Data Release 6) within 6" were correlated with stars in the sample as long as no other stellar objects were within 12" of these coordinates. Objects with a distance greater than 6" in GR6 were further correlated with the position of the stars in data from SDSS DR8 (Sloan Digital Sky Survey Data Release 8) and taken, when a GALEX object was within 6" of the SDSS coordinates.

[6] http://heasarc.nasa.gov./W3Browse/all/euv.html

In addition, rotational periods were needed to calculate stellar ages by applying gyrochronology relations. To compare these results, ages determined by the chromospheric activity method were taken from *Odert* (2012, in preparation).

For comparison of the collected M stars' parameters, as well as their calculated ones, a sample of solar-type stars was compiled. Therefore, *Simbad* was used to search for stars with spectral type G2V within 30 pc of the Sun. Twenty-eight stars were found, from which some were not included in this work, because of the fact that only data in two wavelengths was available or the spectral type was not clearly identified. After rejecting those, a list with 22 stars remained. These stars are all included in the HD catalog[7] and are also sorted by increasing right ascension. The aim was to use them in representation of our Sun to compare the radiation and activity differences to M-type stars.

Due to the relatively close distances of all stars in this sample, the effects of interstellar medium absorption and reddening were neglected in all calculations hereafter.

2.2 Calculating Luminosity

2.2.1 Luminosity in the Passbands UBVRIJHK

The apparent magnitudes[8] m were transformed into absolute magnitudes M by using the following formula:

$$M = m + 5 - 5\log_{10}(r) \tag{2.1}$$

where r is the distance in pc. The absolute magnitudes M were needed to determine the stars' luminosities L. Therefore two other parameters had to be calculated, flux density f and frequency range ν.

[7] Henry Draper Catalog

[8] Many apparent magnitudes in R and I were derived from the USNO-B catalog (*Monet et al.*, 2003), a photographic plate sky survey. Use of this data is problematic. Due to a lack of alternatives to convert these values to Johnson UBV, they were processed as described above as other authors have done this as well (e.g. *Schuh et al.,* 2003).

Flux density f is given by (*Reid & Hawley,* 2005):

$$f = f_0 \times 10^{-(M/2.5)} \tag{2.2}$$

where f_0 is the flux density in Jansky[9] at magnitude 0 produced by a star with spectral class A0 and is different for every passband. These f_0 values[10] were also obtained from *Reid & Hawley* (2005).

Frequency range ν was calculated as follows (e.g. *Reid & Hawley,* 2005):

$$\Delta\nu = c/\lambda_{\max} - c/\lambda_{\min} \tag{2.3}$$

where c is the speed of light and $\lambda_{\max}$ resp. $\lambda_{\min}$ are the upper and respective lower limits of each filter's FWHM[11]. The λ values[12] are listed in *Reid & Hawley* (2005).

After computing f and ν in the passbands UBVRIJHK, the luminosities L were calculated. Usually this is done with the formula $L = 4\pi r^2 f$ (e.g. *Karttunen et al.,* 2007).

In this case the formula had to be expanded by ν [Hz] as the flux density f was calculated in the units of Jansky but the result was needed in Watt. Hence the following formula was used:

$$L = 4\pi r^2 f \nu \tag{2.4}$$

to calculate the luminosities in all mentioned wavelengths, where r is 10 pc in meters. Finally, the results were multiplied by 10^7 to receive the units [erg s^{-1}].

For both, M and G stars, data processing was executed with the same method.

---

[9] 1 Jansky = 10^{-26} W m^{-2} Hz^{-1}

[10] f_0: U=1181; B=4520; V=3711; R=3180; I=2460; J=1568; H=1076; K=650. All values in Jansky.

[11] FWHM stands for Full Width at Half Maximum and is an expression of the bandwidth, where less than half of the maximum signal is obtained.

[12] λ_{min}: U=325; B=390; V=500; R=565; I=730; J=1160; H=1490; K=2000. All values in nm.
λ_{max}: U=395; B=490; V=590; R=725; I=880; J=1350; H=1800; K=2300. All values in nm.

2.2.2 Luminosity in the Passbands NUV and FUV

Data from *GALEX* was collected in the form of apparent AB magnitudes[13]. To convert AB magnitudes to luminosity [erg s^{-1}], the magnitudes were transformed into microJansky by calculating the flux density f. For this purpose the formula from *Oke* (1974) $AB = -2.5\log_{10} f - 48.6$ was transformed to:

$$f = 10^{(23.9-AB)/2.5} \tag{2.5}$$

Further, the frequency range ν was determined as it was done in 2.2.1 using equation (2.3). The values[14] for $\lambda_{\max}$ and $\lambda_{\min}$ were calculated using the pivot wavelength[15] ± FWHM/2 given in the *GALEX* observer's guide[16] and finally converted into Jansky by multiplying by 10^6. Using the same formula (2.4) as above, led to the luminosities L [erg s^{-1}] in NUV and FUV. The only difference was, that for r the individual stellar distances [m] were taken, as the initial AB magnitudes had not been converted into absolute values which correlate to the magnitudes at a distance of 10 pc. M and G stars were processed in the same manner.

2.2.3 Luminosity in the Passband EUV

The data in EUV was mainly taken from the *EUV Master Catalog*, which is a compendium of EUV source catalogs, and completed with data from *Hodgkin & Pye* (1994). The *EUV Master Catalog* contains data taken for this work, derived from *EUVE*[17] (filter Lexan/B) and *ROSAT*[18] (filter S1).

---

[13] AB magnitudes differ from the classical magnitude system, in that 0 magnitude in each passband is not defined on the basis of a reference star, i.e. Vega, but rather on the basis of the magnitude zero-point being equivalent to 3631 Jansky. This eliminates possible fluctuations in the luminosity of reference stars and defines the zero-point as an energy level instead of a natural source, and allowing easier calculation of flux densities.

[14] $\lambda_{\min}$: FUV=138.95; NUV=198.9. All values in nm. $\lambda_{\max}$: FUV=165.85; NUV=260.5. All values in nm.

[15] Pivot wavelength is the wavelength of the effective transmission of a filter in a source independent manner and is the same whether expressed in wavelength or frequency.

[16] http://galexgi.gsfc.nasa.gov/docs/galex/documents/galexobserverguide.pdf (November 2nd, 2011)

[17] EUVE stands for Extreme UltraViolet Explorer and was the first satellite mission especially for radiation between 7-76 nm (*Unsöld & Baschek,* 2001). Running from 1992-2001, one of the main goals was to make an all-sky survey in EUV. Lexan/B is a filter sensitive in the range 5.8 - 17.4 nm (*Christian et al.,* 1999).

In certain cases this led to two values in EUV for the same star. All values were given in counts per second [ct s^{-1}]. Using conversion factors[19] (*Hodgkin & Pye,* 1994 for S1; *Wood et al.,* 1995 for Lexan/B), the flux density f was calculated, which transformed the former unit directly to [erg cm^{-2} s^{-1}]. Hence calculating the frequency range ν was not needed in this case.

Finally the luminosity L in EUV was determined applying (e.g. *Karttunen et al.,* 2007):

$$L = 4\pi r^2 f \tag{2.6}$$

where r is the individual stellar distance in centimeters [cm]. These calculations were performed identically for M and G stars.

2.2.4 Luminosity in the Wavelength Range X-ray

Since the calculated X-ray luminosities for the studied M stars' sample were available from *Odert* (2012, in preparation), these values were adopted.
For the G2V stars the data given in [ct s^{-1}] was derived from *ROSAT* bright and faint source catalogs (*Voges et al.,* 1999; *Voges et al.,* 2000). The transformation to [erg cm^{-2} s^{-1}] was performed in the same manner as above (2.2.3) using the conversion factor[20] from *Simon et al.* (1995). Applying equation (2.6) the luminosity L in [erg s^{-1}] was determined.

2.2.5 Luminosity of the Emission Line Hα

The M stars' Hα luminosities were calculated using the equivalent widths in Ångström [Å] of the emission lines. Spectral lines in absorption were not further used. The values were taken from different articles, which will be referenced later.

---

[18] ROSAT stands for Röntgensatellite and was a mission running from 1990-1999 designed to make an all-sky survey in the wavelength ranges X-ray and EUV. Filter S1 is sensitive in the range 6-14 nm (*Pye et al.,* 1995).

[19] Conversion factor for S1 (*Hodgkin & Pye,* 1994): 5×10^{-11} erg cm^{-2} ct^{-1}
Conversion factor for Lexan/B (*Wood et al.,* 1995): 1×10^{-10} erg cm^{-2} ct^{-1}

[20] Conversion factor for X-ray (*Simon et al.,* 1995): 6×10^{-12} erg cm^{-2} ct^{-1}

Walkowicz et al. (2004) give two equations to calculate log (χ), which is the ratio between the flux at Hα ($f_{\mathrm{H\alpha}}$) and the bolometric flux (f_{bol}).
For this case equation (1) from *Walkowicz et al.* (2004) was chosen as it includes the term (I-K) instead of (V-I) (equation (2) in *Walkowicz et al.,* 2004) as there were more K magnitudes than V magnitudes available for the M stars sample allowing more completeness.

$$\log(\chi) = -5.73342 + 3.07439(I-K) - 1.58615(I-K)^2 \\ +0.274372(I-K)^3 - 0.0154537(I-K)^4 \tag{2.7}$$

The ratio $f_{\mathrm{H\alpha}}/f_{\mathrm{bol}}$ was converted to the ratio of $L_{\mathrm{H\alpha}}/L_{\mathrm{bol}}$ by multiplying χ with the equivalent width (*Walkowicz et al.,* 2004). The calculation of the bolometric luminosity L_{bol} follows in section 2.4.

As the χ -factor was only calibrated for M-type stars, the G2V Hα luminosities were processed differently. This was performed using the surface fluxes $F'_{\mathrm{H\alpha}}$, referenced later, with equation (2.6) and setting the radius for all G2V stars equivalent to 1 $R_{\odot}$.

2.3 Calculating Bolometric Magnitude

The bolometric magnitude is needed to calculate the bolometric luminosity. There are different ways to determine the bolometric magnitude. *Veeder* (1974) gives the following equation:

$$M_{\mathrm{bol}} = 1.12 + M_K \times 1.81 \tag{2.8}$$

where M_K is the absolute magnitude in passband K. *Reid & Hawley* (2005) refer to another equation:

$$M_{\mathrm{bol}} = BC_{\lambda} + M_{\lambda} \tag{2.9}$$

where BC_{λ} is the bolometric correction factor and M_{λ} the absolute magnitude at a certain passband.

Depending on the star's spectral subtype there are different methods to determine the bolometric correction factor. *Reid & Hawley* (2005) give three equations to calculate BC using either the V, I or K band.

$$BC_V = 0.27 - 0.604(V - I) - 0.125(V - I)^2 \tag{2.10}$$

$$BC_I = 0.02 + 0.575(V - I) - 0.155(V - I)^2 \tag{2.11}$$

$$BC_K = 0.42 + 1.486(I - K) - 0.22(I - K)^2 \tag{2.12}$$

But these can only be used for the spectral subtypes M0-M6. For subtypes M6.5-M9.5 *Golimowski et al.* (2004) show another relation:

$$BC_K = 3.9257 - 0.3833SpT + 0.053597SpT^2 - 0.002655SpT^3 + 0.000040859SpT^4 \tag{2.13}$$

where SpT stands for the spectral subtype (i.e. M6.5: SpT = 6.5).

It was decided to use the following approach:
For all early- and mid-type M stars (M0-M6), which had a value in both passbands, I and K, equation (2.12) from *Reid & Hawley* (2005) was applied to calculate the bolometric correction factor BC, because its standard deviation (σ) is the smallest of the three presented equations and values in K were available for all stars. Equation (2.9) was then used to calculate the bolometric magnitude M_{bol} for these stars.
For those stars without data in passband I, equation (2.8) (*Veeder,* 1974) was applied and finally for all late-type stars (M6.5-M9.5) equation (2.13) (*Golimowski et al.,* 2004) was taken.

Determining the G2V stars' bolometric magnitudes required using the formula (2.9) (*Flower,* 1996):

$$M_{\mathrm{bol}} = M_V + BC$$

where M_V is the absolute visual magnitude. The bolometric conversion factors BC are listed in *Flower* (1996). Using (*B*-*V*) color, the matching bolometric correction factor could be found in the referenced article and the bolometric magnitude M_{bol} could be determined.

2.4 Calculating Bolometric Luminosity

After calculating the bolometric magnitudes, the modified formula[21] (e.g. *Reid & Hawley,* 2005) was used to determine the bolometric luminosities L_{bol} for both, M and G stars:

$$L_{\mathrm{bol}} = L_{\mathrm{bol}\odot} \times 10^{-(M_{\mathrm{bol}} - M_{\mathrm{bol}\odot})/2.5} \tag{2.14}$$

where the values 3.8503 x 10^{33} erg s^{-1} for $L_{\mathrm{bol}\odot}$ (e.g. *Odert* 2012, in preparation) and 4.72 for $M_{\mathrm{bol}\odot}$ (e.g. *Karttunen et al.,* 2007) were applied.

With these calculated parameters, the logarithmic ratios between the luminosity in each passband and the bolometric luminosity were compiled ($\log L_\lambda/L_{\mathrm{bol}}$) for the diagrams presented in chapter 3.

2.5 Determining Stellar Mass

To determine a star's mass there are several methods. *Delfosse et al.* (2000) give five different mass-luminosity relations employing different passbands, which can be used for all stars with masses smaller than 0.6 solar masses. The following two equations were both applied to compare the results (*Delfosse et al.,* 2000):

$$\log_{10}\left(M/M_\odot\right) = 10^{-3} \times \left(1.6 + 6.01M_J + 14.888{M_J}^2 - 5.3557{M_J}^3 + 0.28518 \times {M_J}^4\right) \tag{2.15}$$

$$\log_{10}\left(M/M_\odot\right) = 10^{-3} \times (1.8 + 6.12M_K + 13.205{M_K}^2 - 6.2315{M_K}^3 + 0.37529{M_K}^4) \tag{2.16}$$

The comparison showed, that the calculated results did not differ until the second decimal place, which is not especially surprising as the passbands lie near to each other. However, interesting was, that nearly all (except three) values calculated using the K passband were smaller than those calculated with J.

---

[21] Original formula (e.g. *Reid & Hawley,* 2005): $M_{\mathrm{bol}} - M_{\mathrm{bol}\odot} = -2.5\log_{10}(L_{\mathrm{bol}}/L_{\mathrm{bol}\odot})$

Ultimately, all M star masses in this work were determined using equation (2.16) as *Delfosse et al.* (2000) come to the conclusion, that the smallest dispersion around the mean relation was observed using the K band.

In particular cases this calculation method led to masses bigger than 0.6 solar masses, which should actually be the upper mass limit for stars of spectral type M.

Taking a closer look, it showed that these stars with masses > 0.6 $M_\odot$ are either of spectral subtype M0 or M0.5 (with one exception: M2), where there is a good chance that those stars are in fact of spectral type K.

The same happened at the other end of the mass limit for M stars which lies at about 0.075 $M_\odot$. Nine stars of the sample lie below this limit, the lowest having a mass of 0.068 $M_\odot$. Potentially these stars could be brown dwarfs.

However, regardless of these concerns the mentioned stars were retained in the sample as different mass calculation methods lead to different results and a certain grade of deviation is acceptable.

The G2V stars' masses were calculated differently, using a relation which is especially applicable for stars with masses between 0.43 $M_\odot$ - 2 $M_\odot$ (*Duric,* 2004):

$$L_{\mathrm{bol}}/L_{\mathrm{bol}\odot} = (M/M_\odot)^4 \tag{2.17}$$

where for $M_\odot$ the value 1 was inserted.

2.6 Estimating Stellar Age

As mentioned in 1.4 age determination is still problematic, especially for M-type stars, which evolve extremely slow. In this work the so-called gyrochronology method by *Barnes* (2007) was used. He shows an improved way of using a star's rotation period connected with its color (B-V) as a clock.

Therefore, rotational periods P_{rot} were collected for both M and G stars from several articles which will be referenced later.

The M and G stars' ages were estimated applying the following formula (*Barnes,* 2007), but with different parameter values[22] in a, b, c and n for the G2V stars (*Mamajek & Hillenbrand,* 2008):

$$\log\ t\ [Myr] = \frac{1}{n}[\log P_{\mathrm{rot}} - \log a - b\log(B - V - c)] \qquad (2.18)$$

as they have revised the parameters of *Barnes* (2007) especially for late F to early K stars and mainly tested them on G stars, which seems to work better for the G2V stars in this sample. *Barnes* (2007) states that his parameters are valid for solar-type (FGKM) stars.

The parameters a and b are fitted constants, c is called the "color singularity" and n represents the time-dependent power law index (*Mamajek & Hillenbrand,* 2008).

The difficulty in using both formulas is that there are many limitations on their use. First *Barnes* (2007) claims that this age determination method is valid for solar-type stars (FGKM), but mentions later in his article that it can only be applied for stars that have an interface and hence are not fully convective, which implies that ultrafast C sequence rotators are excluded. Further, it means that it only works for M stars with masses higher than ≈ 0.35 $M_{\odot}$. The rotation-age relationship for fully convective stars is not well studied yet.

Furthermore, he limits the use of his formula to stars with B-V smaller than 1.55 as in one of his studied samples there are no slow rotators redwards of this color. However, recently *Irwin et al.* (2011) presented new measured rotation periods which showed the opposite, e.g. for the star GJ 1072 (member of the M stars sample studied here) which has a B-V value of 1.95 but a rotation period of 147 days. Additionally, there are eleven other stars with B-V > 1.55 and long rotation periods (> 50 days, most of them above 100 days) in the M stars' sample used here.

[22] *Barnes* (2007): a = 0.7725, b = 0.601, c = 0.40, n = 0.5189.
Mamajek & Hillenbrand (2008): a = 0.407, b = 0.325, c = 0.495, n = 0.566.

Finally, he adds that his formula is not functional until a stellar age of at least 100 Myr is reached, as it takes approximately this time for Sun-like stars to switch from the C- to the I-sequence. This is due to the variability of rotation periods in young stars as they converge during their later evolution.

Mamajek & Hillenbrand (2008) present a different calibration valid for spectral classes from late F till early K type stars.

Concluding it seems that the parameters a, b, c, and n must be defined even more accurately for different stellar mass ranges.

Despite the awareness of many limits to the gyrochronology formula from *Barnes* (2007), it was applied to all stars with rotation periods in the M stars sample as there were only 40 out of 355 available. It demonstrated good correlation with chromospheric ages for the stars that were within the criteria outlined by *Barnes* (2007), but also was able to give crude estimates for young stars or stars with very low masses. All ages estimated by this method, even those where the stars do not meet all criteria, were in good agreement with chromospheric ages and a potential age proxy which will be discussed later.

Out of interest the M stars' ages were also estimated with the parameters given by *Mamajek & Hillenbrand* (2008), which led to many results that were clearly older than the current age of the universe. This cannot be correct but also happened in four single cases when using the parameters given in *Barnes* (2007).

Taking a closer look at these four stars showed that their spectral types are in fact M3.5, M4 or M5, which is right at the border between early- and mid-type M stars and represents a stellar mass around the point where several authors (*Reid & Hawley,* 2005; *Barnes,* 2007; *West & Basri,* 2009) presume the changeover to a fully convective energy transfer, which would mean that these stars are not on the I-sequence and thus making the formula from *Barnes* (2007) not suitable for these stars.

Another reason for the impossibly large ages could be, of course, erroneous rotation periods or errors in measurement of the B or V magnitude.

However, these stellar ages estimated with the parameters of *Barnes* (2007) were kept in the M stars' sample and also included in the compiled diagrams which are presented in the next chapter as there currently exists no dependable gyrochronological method to estimate stellar ages for fully convective stars.

For comparison M star ages calculated with the chromospheric method were taken from *Odert* (2012, in preparation) and can be compared to the gyro ages in Table 2.1 and several diagrams. Furthermore, G2V stars' ages calculated with the isochrone method were taken from *Holmberg et al.* (2009) as only two rotational periods were available and so only for two stars the ages could be estimated using gyrochronology.

Concluding this chapter, Table 2.1 for M-type stars and Table 2.2 for G2V stars summarize fundamental stellar parameters which were either taken from literature or calculated as described above. Included - as far as available - are: number (col. 1), name (col. 2), spectral type (col. 3), right ascension (col. 4), declination (col. 5), parallax (col. 6), B-V (col. 7), bolometric magnitude (col. 8), bolometric luminosity (col. 9), stellar mass (col. 10), rotational period (col. 11), ages calculated using different methods (col. 12 and 13) and references (col. 14).

Table 2.1: M Star Sample

No.	Star	SpT	RA* (J2000)	DEC* (J2000)	Plx° [mas]	(B-V)	M_{bol} [mag]	log L_{bol} [erg s^{-1}]	Mass [$M_{\odot}$]	P_{rot} [d]	t_{gyro} [Gyr]	t_{chromo}° [Gyr]	Reference
1	GJ 1	M1.5	1.350976	-37.357159	230.42	1.46	8.7906	31.9572	0.3858	. . .	. . .	11.1921	SpT(14)
2	GJ 1002	M5.5	1.680230	-7.537419	213.00	1.95	11.9125	30.7085	0.1033	. . .	. . .	. . .	SpT(12)
3	2MASS J00113182+5908400	M5.5	2.882605	59.144455	108.35	1.02	11.9445	30.6957	0.0958	. . .	. . .	. . .	SpT(~)
4	GJ 12	M3.0	3.954983	13.556079	85.85	1.46	10.1170	31.4267	0.2218	78.5	**6.8934**	. . .	SpT(~);P_{rot}(11)
5	GJ 14	M0.5	4.276485	40.948299	66.65	1.42	7.1600	32.6095	0.7206	. . .	. . .	1.0812	SpT(12)
6	GJ 3028	M5.5	5.121767	33.085609	79.30	1.15	11.6991	30.7939	0.1152	. . .	. . .	. . .	SpT(12)
7	NLTT 1261	M9.5	6.102652	-1.972262	82.50	1.78	13.2992	30.1538	0.0734	. . .	. . .	. . .	SpT(12)
8	GJ 1012	M4.0	7.164520	-6.663365	75.40	1.48	9.1750	31.8035	0.3451	. . .	. . .	. . .	SpT(29)
9	GJ 26	M4.0	9.744975	30.616222	80.10	1.54	9.0534	31.8521	0.4241	. . .	. . .	10.6617	SpT(12)
10	GJ 46	M3.0	14.616213	-27.856979	80.95	1.58	9.1118	31.8288	0.3689	. . .	. . .	. . .	SpT(8)
11	GJ 1025	M5.0	15.235159	-4.448930	87.70	1.73	10.6111	31.2291	0.1758	. . .	. . .	. . .	SpT(20)
12	GJ 47	M2.0	15.333610	61.365574	90.90	1.39	9.1092	31.8298	0.3964	. . .	. . .	7.5307	SpT(16)
13	GJ 48	M3.0	15.633880	71.679878	121.41	1.46	8.7387	31.9780	0.4729	. . .	. . .	7.3067	SpT(12)
14	LHS 132	M8.0	15.712504	-37.628841	81.95	. . .	12.7343	30.3798	0.0840	. . .	. . .	. . .	SpT(22)
15	GJ 1028	M5.0	16.223688	-18.124802	99.80	1.87	11.2152	30.9874	0.1370	. . .	. . .	. . .	SpT(~)
16	GJ 1029	M5.0	16.405507	28.492773	79.30	1.88	10.8251	31.1435	0.1666	. . .	. . .	. . .	SpT(12)
17	NLTT 3868	M9.0	17.463218	-3.724007	104.23	1.40	13.6679	30.0063	0.0687	. . .	. . .	. . .	SpT(24)
18	GJ 54.1	M4.0	18.127191	-16.999178	271.01	1.81	11.3518	30.9328	0.1285	. . .	. . .	. . .	SpT(28)
19	GJ 1035	M5.0	19.967825	84.159111	71.60	1.80	10.7963	31.1550	0.1472	. . .	. . .	. . .	SpT(~)
20	NLTT 4623	M	20.825121	-12.939817	97.80	0.98	10.6121	31.2287	0.1470	. . .	. . .	. . .	SpT(~)
21	GJ 63	M2.5	24.590096	57.232536	86.20	3.01	9.5391	31.6579	0.2659	. . .	. . .	. . .	SpT(~)
22	GJ 70	M2.0	25.833995	4.321467	87.62	1.54	8.7983	31.9542	0.4048	. . .	. . .	7.6776	SpT(12)
23	GJ 3113	M3.0	26.653383	-8.649414	70.10	1.58	9.8993	31.5138	0.2518	. . .	. . .	. . .	SpT(29)
24	GJ 3119	M5.0	27.766877	-6.117988	100.78	1.60	11.3714	30.9250	0.1295	. . .	. . .	. . .	SpT(20)
25	GJ 79	M0.0	28.204534	-22.434874	90.86	1.44	7.4152	32.5074	0.6619	15.8	**0.3212**	1.9117	SpT(28);P_{rot}(19)
26	GJ 82	M4.0	29.847914	58.521175	81.65	0.86	9.1133	31.8282	0.3541	. . .	. . .	. . .	SpT(12)
27	GJ 83.1	M4.5	30.053282	13.053120	224.80	1.82	11.1639	31.0079	0.1398	. . .	. . .	. . .	SpT(12)
28	GJ 3126	M4.0	30.397213	63.769970	78.40	1.50	8.7421	31.9767	0.4748	. . .	. . .	. . .	SpT(29)
29	GJ 3125	M4.5	30.475012	73.542229	87.46	1.90	10.8541	31.1319	0.1643	. . .	. . .	. . .	SpT(~)
30	GJ 3128	M6.0	30.567538	10.337137	112.00	2.02	11.9231	30.7043	0.0994	. . .	. . .	. . .	SpT(12)

No.	Star	SpT	RA* (J2000)	DEC* (J2000)	Plx° [mas]	(B-V)	M_{bol} [mag]	log L_{bol} [erg s^{-1}]	Mass [$M_{\odot}$]	P_{rot} [d]	t_{gyro} [Gyr]	t_{chromo}° [Gyr]	Reference
31	GJ 3135	M2.5	31.452461	-30.176697	107.81	1.69	10.3067	31.3508	0.1960	. . .	. . .	. . .	SpT(8)
32	NLTT 7210	~	32.515187	-8.883296	70.20	. . .	9.9967	31.4748	0.2405	. . .	. . .	. . .	SpT(-)
33	GJ 3141	M2.5	32.824913	-63.228142	71.53	1.27	9.5569	31.6507	0.2814	. . .	. . .	. . .	SpT(~)
34	GJ 87	M2.5	33.087121	3.575303	96.02	1.44	8.4451	32.0954	0.4497	. . .	. . .	10.8056	SpT(12)
35	GJ 91	M2.0	33.473298	-32.041191	79.68	1.50	8.1444	32.2157	0.5277	. . .	. . .	. . .	SpT(8)
36	GJ 3146	M6.0	34.124067	13.587127	117.70	1.98	12.0178	30.6664	0.0934	. . .	. . .	. . .	SpT(20)
37	GJ 3147	M5.0	34.291383	35.442505	96.40	0.91	11.6458	30.8152	0.1100	0.276	0.0003	. . .	SpT(12);P_{rot}(11)
38	WT 84	~	34.368565	-59.378777	76.61	0.85	11.8084	30.7502	0.1085	. . .	. . .	. . .	SpT(-)
39	GJ 96	M0.5	35.560968	47.880035	83.75	1.51	7.8167	32.3468	0.6190	. . .	. . .	2.7887	SpT(~)
40	GJ 102	M4.0	38.404882	24.927567	102.40	1.70	10.3859	31.3191	0.2003	. . .	. . .	. . .	SpT(23)
41	GJ 104	M2.0	38.972003	20.219980	73.56	1.51	8.2174	32.1865	0.5150	. . .	. . .	. . .	SpT(14)
42	2MASS J02363244-5928057	M5.0	39.135198	-59.468269	103.72	. . .	11.2600	30.9695	0.1389	. . .	. . .	. . .	SpT(~)
43	HIP 12261	M3.0	39.469945	-58.753056	66.62	1.57	9.3012	31.7530	0.3362	. . .	. . .	. . .	SpT(8)
44	GJ 1050	M2.5	39.961108	-34.132153	93.74	1.59	9.6976	31.5945	0.2592	. . .	. . .	. . .	SpT(~)
45	GJ 109	M3.5	41.064079	25.523609	133.16	1.58	9.1830	31.8003	0.3440	. . .	. . .	9.4734	SpT(12)
46	GJ 3181	M6.0	41.645254	16.419888	121.59	1.95	13.5100	30.0695	0.0680	. . .	. . .	. . .	SpT(12)
47	GJ 114.1 A	M1.5	42.540638	-53.139000	77.19	1.52	8.4757	32.0832	0.4606	. . .	. . .	. . .	SpT(14)
48	GJ 118	M2.5	43.092238	-63.679886	85.87	1.59	9.1031	31.8322	0.3579	. . .	. . .	. . .	SpT(14)
49	2MASS J02530084+1652532	M7.0	43.253536	16.881466	259.25	1.81	12.7099	30.3895	0.0835	. . .	. . .	. . .	SpT(7)
50	GJ 3189	M2.5	44.542553	-12.885187	95.50	1.73	10.8809	31.1211	0.1623	. . .	. . .	. . .	SpT(29)
51	GJ 3198	M3.5	46.018851	-20.378721	67.28	1.59	9.6005	31.6333	0.2967	. . .	. . .	. . .	SpT(~)
52	GJ 1055	M5.0	47.250663	10.023827	83.90	1.71	11.4650	30.8875	0.1227	. . .	. . .	. . .	SpT(12)
53	GJ 1053	M5.0	47.744244	73.771919	83.30	1.79	11.3194	30.9458	0.1227	. . .	. . .	. . .	SpT(~)
54	GJ 130	M1.5	48.123871	-38.089001	79.60	1.51	9.3023	31.7526	0.3270	. . .	. . .	. . .	SpT(~)
55	GJ 1057	M5.0	48.345814	4.774824	117.10	1.83	10.9972	31.0746	0.1563	102	8.0724	. . .	SpT(12);P_{rot}(11)
56	GJ 3208	M6.0	48.551731	28.678099	67.00	2.15	12.1454	30.6153	0.0975	. . .	. . .	. . .	SpT(~)
57	NLTT 10644	M8.0	50.248556	18.906475	65.73	1.29	12.8253	30.3434	0.0816	0.613	0.0007	. . .	SpT(12);P_{rot}(11)
58	GJ 133	M2.0	50.340691	79.967285	71.21	1.59	8.7823	31.9606	0.4188	. . .	. . .	. . .	SpT(~)
59	2MASS J03304890+5413551	M5.0	52.703764	54.231976	103.80	1.34	12.1311	30.6211	0.0923	. . .	. . .	. . .	SpT()
60	GJ 145	M2.5	53.232712	-44.701946	93.11	1.59	9.3526	31.7324	0.3173	. . .	. . .	. . .	SpT(8)

No.	Star	SpT	RA* (J2000)	DEC* (J2000)	Plx° [mas]	(B-V)	M_{bol} [mag]	log L_{bol} [erg s^{-1}]	Mass [$M_{\odot}$]	P_{rot} [d]	t_{gyro} [Gyr]	t_{chromo}° [Gyr]	Reference
61	GJ 1061	M5.5	53.998727	-44.512592	271.92	1.90	11.6504	30.8134	0.1174	. . .	. . .	. . .	SpT(~)
62	2MASS J03360868+3118398	M4.5	54.036169	31.311060	79.60	4.70	10.4864	31.2789	0.1866	. . .	. . .	. . .	SpT(23)
63	2MASS J03393521-3525440	M9.0	54.896749	-35.428913	201.40	. . .	14.2182	29.7862	0.0676	. . .	. . .	. . .	SpT(12)
64	GJ 154	M0.0	56.583832	26.215565	67.80	1.44	7.5454	32.4553	0.6554	. . .	. . .	1.3421	SpT(~)
65	GJ 3250	M4.5	56.837136	8.696234	79.50	1.87	11.1367	31.0188	0.1322	60.3	2.8392	. . .	SpT(~);P_{rot}(11)
66	GJ 1065	M3.0	57.684687	-6.094458	105.40	1.69	10.6190	31.2259	0.1824	. . .	. . .	. . .	SpT(20)
67	GJ 3252	M8.0	57.750195	-0.879244	68.10	1.78	12.4952	30.4754	0.0912	. . .	. . .	. . .	SpT(31)
68	GJ 3253	M4.5	58.173724	17.018246	101.57	1.61	10.7351	31.1795	0.1633	78.8	5.9573	. . .	SpT(~);P_{rot}(11)
69	GJ 162	M1.0	62.155957	33.637066	74.37	1.53	8.0542	32.2518	0.5412	. . .	. . .	. . .	SpT(6)
70	GJ 163	M3.5	62.315307	-53.373737	66.69	1.49	8.8719	31.9247	0.4001	. . .	. . .	. . .	SpT(14)
71	GJ 1068	M4.5	62.617315	-53.602169	143.42	1.93	11.4581	30.8902	0.1228	. . .	. . .	. . .	SpT(~)
72	GJ 3266	M4.0	63.070548	64.732239	84.80	1.39	10.6102	31.2294	0.1765	. . .	. . .	. . .	SpT(~)
73	GJ 3269	M2.0	63.890293	15.706286	26.97	1.28	7.4183	32.5062	0.6538	. . .	. . .	. . .	SpT(6)
74	GJ 169	M0.5	67.250573	21.922634	87.78	1.39	6.9607	32.6892	0.7425	. . .	. . .	2.4447	SpT(14)
75	GJ 170	M4.5	67.605306	39.850014	95.90	1.62	10.9353	31.0994	0.1579	0.718	0.0007	. . .	SpT(21);P_{rot}(11)
76	GJ 173	M1.5	69.424521	-11.038843	90.10	1.51	8.4040	32.1119	0.4740	. . .	. . .	10.4372	SpT(21)
77	LHS 1690	M5.5	69.881828	16.262430	86.60	2.06	11.6800	30.8015	0.1124	. . .	. . .	. . .	SpT(15)
78	GJ 176	M2.0	70.732543	18.957939	107.83	1.54	8.3383	32.1382	0.4928	38.92	**1.6409**	6.4962	SpT(14);P_{rot}(13)
79	GJ 1072	M5.0	72.711801	22.122904	71.10	1.95	11.0347	31.0596	0.1518	147	14.8711	. . .	SpT(~);P_{rot}(11)
80	GJ 179	M3.5	73.023880	6.476566	81.38	1.55	9.2103	31.7894	0.3585	. . .	. . .	. . .	SpT(14)
81	GJ 1073	M4.0	73.143682	40.707088	77.40	1.61	10.4112	31.3090	0.1932	. . .	. . .	. . .	SpT(21)
82	GJ 180	M2.0	73.458165	-17.773216	82.52	1.55	8.7359	31.9792	0.4136	. . .	. . .	10.9124	SpT(14)
83	GJ 3323	M4.0	75.489454	-6.946090	187.92	1.76	10.8436	31.1361	0.1618	. . .	. . .	. . .	SpT(12)
84	GJ 184	M0.0	75.850090	53.128117	73.41	1.42	7.9744	32.2838	0.5483	. . .	. . .	5.8624	SpT(6)
85	2MASS J05102012+2714032	~	77.583841	27.234228	100.70	. . .	12.3765	30.5229	0.0857	. . .	. . .	. . .	SpT(-)
86	GJ 192	M2.0	78.175996	19.665745	81.35	1.56	8.5688	32.0460	0.4434	. . .	. . .	. . .	SpT(14)
87	GJ 1077	M2.0	79.248638	-78.288994	77.50	1.48	9.2807	31.7612	0.3339	. . .	. . .	. . .	SpT(~)
88	GJ 203	M3.5	82.000625	9.643962	113.50	1.64	10.4597	31.2896	0.1868	. . .	. . .	. . .	SpT(14)
89	GJ 205	M1.5	82.863948	-3.676579	176.77	1.48	7.7082	32.3902	0.5960	33.61	**1.3225**	1.9602	SpT(12);P_{rot}(13)
90	GJ 3356	M3.5	83.717185	13.879775	80.60	1.59	9.1243	31.8238	0.3630	. . .	. . .	. . .	SpT(~)

No.	Star	SpT	RA* (J2000)	DEC* (J2000)	Plx° [mas]	(B-V)	M_{bol} [mag]	log L_{bol} [erg s^{-1}]	Mass [$M_{\odot}$]	P_{rot} [d]	t_{gyro} [Gyr]	t_{chromo}° [Gyr]	Reference
91	GJ 213	M4.0	85.537397	12.490350	171.55	1.61	10.2335	31.3801	0.2125	. . .	. . .	. . .	SpT(12)
92	GJ 2045	M5.0	85.552991	-5.465753	80.11	1.86	11.6678	30.8064	0.1120	. . .	. . .	. . .	SpT(12)
93	GJ 218	M1.5	86.918806	-36.328487	66.54	1.46	8.2418	32.1768	0.5009	. . .	. . .	. . .	SpT(14)
94	HIP 28035	M2.5	88.929926	-26.856499	68.57	1.48	8.0853	32.2394	0.5551	. . .	. . .	. . .	SpT(8)
95	GJ 3379	M4.0	90.014630	2.706566	190.93	1.68	10.3583	31.3302	0.2251	1.81	0.0039	. . .	SpT(12);P_{rot}(11)
96	GJ 3378	M3.5	90.296106	59.597450	126.14	1.60	9.8453	31.5354	0.2620	. . .	. . .	. . .	SpT(12)
97	GJ 3382	M3.5	90.594243	-20.329096	71.00	1.75	10.2781	31.3623	0.2052	. . .	. . .	. . .	SpT(~)
98	GJ 3380	M5.0	90.621588	49.865601	107.70	1.84	11.3000	30.9535	0.1278	99.6	7.6484	. . .	SpT(12);P_{rot}(11)
99	HIP 29052	~	91.932308	-25.744841	88.14	1.60	9.5306	31.6613	0.2961	. . .	. . .	. . .	SpT(-)
100	GJ 226	M2.0	92.582422	82.107132	106.69	1.51	9.0110	31.8691	0.4098	. . .	. . .	9.4490	SpT(~)
101	GJ 1088	M3.5	92.720353	-43.404972	87.03	1.59	9.6834	31.6001	0.2798	. . .	. . .	. . .	SpT(~)
102	GJ 3388	M3.5	93.510012	51.668926	70.00	. . .	9.7823	31.5606	0.2366	. . .	. . .	. . .	SpT(~)
103	GJ 231.3	M3.0	94.836609	-6.655973	68.20	1.62	10.0675	31.4465	0.2296	. . .	. . .	. . .	SpT(21)
104	GJ 232	M4.5	96.172184	23.432932	119.40	1.76	10.9147	31.1076	0.1474	. . .	. . .	. . .	SpT(12)
105	HIP 31862	M0.0	99.906839	-55.609718	75.19	1.47	7.8570	32.3307	0.5679	. . .	. . .	. . .	SpT(8)
106	GJ 1092	M4.0	102.272588	37.114826	71.32	1.66	10.3693	31.3258	0.1672	. . .	. . .	. . .	SpT(~)
107	GJ 251	M4.0	103.704276	33.268303	179.01	1.58	9.4547	31.6916	0.3511	. . .	. . .	10.6455	SpT(12)
108	GJ 1093	M5.0	104.869539	19.349373	128.80	1.95	10.9903	31.0774	0.1176	. . .	. . .	. . .	SpT(12)
109	GJ 1096	M4.0	109.075085	33.152882	66.90	1.76	10.6413	31.2170	0.1700	. . .	. . .	. . .	SpT(~)
110	GJ 3438	M0.0	109.534153	39.274876	69.01	1.72	8.2520	32.1727	0.5352	. . .	. . .	. . .	SpT(~)
111	GJ 273	M3.5	111.852091	5.225807	262.98	1.57	9.6325	31.6205	0.2873	. . .	. . .	10.2454	SpT(12)
112	GJ 1097	M3.0	112.189209	-3.297896	81.38	1.57	8.9063	31.9110	0.3998	. . .	. . .	. . .	SpT(14)
113	GJ 1099	M2.5	113.573258	0.985912	68.70	1.47	9.1698	31.8056	0.3382	. . .	. . .	. . .	SpT(~)
114	GJ 277.1	M0.0	113.614581	62.941544	87.15	1.71	8.8520	31.9327	0.3997	. . .	. . .	9.6847	SpT(6)
115	GJ 3452	M2.0	113.841172	54.849724	78.14	1.55	8.9997	31.8736	0.3712	. . .	. . .	. . .	SpT(~)
116	GJ 282C	M	114.029522	-3.110702	70.55	1.48	7.6787	32.4020	0.6174	. . .	. . .	. . .	SpT(~)
117	GJ 3459	M3.0	114.670390	-21.224340	94.31	1.58	9.5423	31.6566	0.2902	. . .	. . .	. . .	SpT(21)
118	GJ 285	M4.5	116.167420	3.552490	167.88	1.61	9.6072	31.6306	0.3066	2.78	0.0095	0.3501	SpT(12);P_{rot}(11)
119	GJ 1101	M1.5	118.974868	83.384720	80.30	1.11	10.0537	31.4520	0.2263	1.11	0.0030	. . .	SpT(~);P_{rot}(11)
120	GJ 1105	M3.5	119.552914	41.303745	116.06	1.63	9.8756	31.5233	0.2545	. . .	. . .	. . .	SpT(12)

No.	Star	SpT	RA* (J2000)	DEC* (J2000)	Plx° [mas]	(B-V)	M_{bol} [mag]	log L_{bol} [erg s^{-1}]	Mass [$M_{\odot}$]	P_{rot} [d]	t_{gyro} [Gyr]	t_{chromo}° [Gyr]	Reference
121	GJ 299	M4.5	122.989896	8.772792	146.30	1.77	11.1360	31.0191	0.1346	. . .	. . .	. . .	SpT(12)
122	GJ 300	M4.0	123.170338	-21.551579	125.60	1.59	9.9732	31.4842	0.2547	. . .	. . .	. . .	SpT(21)
123	GJ 2066	M2.0	124.033270	1.302550	109.62	1.54	8.5274	32.0626	0.4543	. . .	. . .	9.2054	SpT(12)
124	GJ 3497	M4.5	126.470211	69.033783	75.09	2.04	11.2745	30.9637	0.1313	. . .	. . .	. . .	SpT(15)
125	GJ 3500	M3.5	126.799326	-44.989307	72.80	2.05	8.8657	31.9272	0.4131	. . .	. . .	. . .	SpT(~)
126	GJ 1111	M6.5	127.456242	26.776339	275.80	2.06	12.5055	30.4713	0.0891	. . .	. . .	. . .	SpT(12)
127	LHS 2025	M	127.875480	73.062752	81.80	1.65	10.0773	31.4426	0.2118	. . .	. . .	. . .	SpT(~)
128	GJ 2070	M3.0	128.607808	-1.144215	73.40	1.62	10.0526	31.4525	0.2352	. . .	. . .	. . .	SpT(21)
129	GJ 3506	M2.5	128.954826	68.069359	75.37	1.57	9.3619	31.7287	0.3679	. . .	. . .	. . .	SpT(~)
130	GJ 316.1	M6.5	130.123962	18.402550	71.10	1.61	12.3479	30.5343	0.0944	. . .	. . .	. . .	SpT(25)
131	GJ 317	M3.5	130.246829	-23.456470	94.20	1.22	9.5360	31.6591	0.2956	. . .	. . .	. . .	SpT(~)
132	GJ 3512	M5.5	130.333890	59.497387	102.38	1.93	11.4519	30.8928	0.1208	. . .	. . .	. . .	SpT(12)
133	GJ 3517	M9.0	133.400817	-3.492253	109.90	2.00	13.2969	30.1547	0.0730	. . .	. . .	. . .	SpT(12)
134	GJ 333	M1.5	134.882082	-47.436054	72.50	2.07	9.7684	31.5661	0.2504	. . .	. . .	. . .	SpT(~)
135	GJ 3520	M4.0	134.983537	72.960129	72.60	1.71	10.8067	31.1508	0.1486	138	15.9988	. . .	SpT(~);P_{rot}(11)
136	LHS 2090	M6.5	135.098309	21.834843	156.87	1.20	12.4572	30.4906	0.0907	. . .	. . .	. . .	SpT(12)
137	GJ 1119	M4.5	135.135586	46.586601	96.90	1.72	10.4033	31.3122	0.2009	. . .	. . .	. . .	SpT(12)
138	GJ 3526	M4.0	135.720199	68.062889	85.30	1.35	9.9010	31.5131	0.2344	. . .	. . .	. . .	SpT(~)
139	GJ 1123	M4.5	139.272200	-77.823158	110.92	1.64	10.4866	31.2788	0.2008	. . .	. . .	. . .	SpT(~)
140	GJ 341	M0.0	140.406709	-60.281979	95.58	1.49	7.9535	32.2921	0.5508	. . .	. . .	. . .	SpT(14)
141	GJ 1125	M3.5	142.685730	0.322620	103.46	1.59	9.5976	31.6345	0.2889	. . .	. . .	. . .	SpT(14)
142	GJ 353	M2.0	142.984694	36.320271	71.91	1.63	8.1552	32.2114	0.5306	. . .	. . .	3.6862	SpT(6)
143	GJ 357	M2.5	144.006725	-21.660318	110.82	1.57	9.2696	31.7657	0.3256	. . .	. . .	10.2452	SpT(8)
144	GJ 359	M4.5	145.258311	22.024767	79.00	1.77	10.8642	31.1278	0.1471	. . .	. . .	. . .	SpT(12)
145	GJ 361	M1.5	145.293050	13.209568	88.81	1.52	8.4144	32.1077	0.4729	. . .	. . .	4.7447	SpT(16)
146	GJ 1128	M4.5	145.693150	-68.885010	153.05	1.73	10.7482	31.1742	0.1738	. . .	. . .	. . .	SpT(~)
147	LHS 5156	M	145.706679	-63.632244	95.15	1.50	10.4265	31.3029	0.2019	. . .	. . .	. . .	SpT(~)
148	GJ 3564	M3.5	145.981801	26.969042	71.29	1.59	9.0398	31.8576	0.3651	. . .	. . .	. . .	SpT(~)
149	GJ 367	M1.0	146.124443	-45.776417	101.31	1.39	8.3494	32.1337	0.4852	. . .	. . .	. . .	SpT(14)
150	GJ 1129	M4.0	146.197145	-18.213593	90.93	1.59	9.7753	31.5634	0.2743	. . .	. . .	. . .	SpT(~)

No.	Star	SpT	RA* (J2000)	DEC* (J2000)	Plx° [mas]	(B-V)	M_{bol} [mag]	log L_{bol} [erg s^{-1}]	Mass [$M_{\odot}$]	P_{rot} [d]	t_{gyro} [Gyr]	t_{chromo}° [Gyr]	Reference
151	GJ 369	M2.0	147.790173	-12.329959	72.92	1.46	7.9283	32.3022	0.5560	. . .	. . .	. . .	SpT(12)
152	GJ 3571	M4.5	148.480133	20.946114	108.39	1.35	11.2088	30.9900	0.1337	. . .	. . .	. . .	SpT(12)
153	HIP 48659	M3.0	148.849460	-27.261274	88.32	1.60	9.5673	31.6466	0.2992	. . .	. . .	. . .	SpT(8)
154	GJ 373	M0.0	149.036200	62.788490	94.68	1.47	7.6517	32.4128	0.6379	. . .	. . .	1.6995	SpT(16)
155	GJ 378	M2.0	150.591010	48.089146	66.24	1.37	8.0753	32.2434	0.5982	. . .	. . .	. . .	SpT(6)
156	GJ 3586	M4.0	152.374861	51.288826	75.20	1.23	10.3382	31.3382	0.1789	. . .	. . .	. . .	SpT(~)
157	GJ 382	M2.0	153.073691	-3.745589	127.08	1.50	8.0887	32.2380	0.5411	21.56	**0.5467**	2.6729	SpT(12);P_{rot}(13)
158	GJ 1132	M3.5	153.716027	-47.156796	83.07	1.73	10.6244	31.2237	0.1775	. . .	. . .	. . .	SpT(~)
159	GJ 386	M3.0	154.191664	-11.961463	73.30	1.47	8.3872	32.1186	0.4914	. . .	. . .	. . .	SpT(14)
160	GJ 388	M4.5	154.901455	19.870068	204.60	1.54	9.0705	31.8453	0.4197	2.6	0.0089	. . .	SpT(16);P_{rot}(27)
161	GJ 390	M1.0	156.295335	-10.228726	81.00	1.49	8.0979	32.2344	0.5330	. . .	. . .	3.4896	SpT(16)
162	GJ 393	M2.5	157.231495	0.840983	141.50	1.53	8.6250	32.0235	0.4352	. . .	. . .	8.1578	SpT(12)
163	GJ 3612	M4.0	158.863572	69.449852	84.41	1.37	9.3283	31.7422	0.3111	. . .	. . .	. . .	SpT(20)
164	GJ 398	M3.5	159.005030	5.120226	68.80	1.39	-0.8342	35.8072	0.3122	. . .	. . .	. . .	SpT(16)
165	GJ 1134	M4.5	160.408746	37.611050	96.70	1.68	10.2036	31.3921	0.2041	. . .	. . .	. . .	SpT(12)
166	GJ 3618	M4.0	161.088833	-61.210678	208.95	1.82	12.1184	30.6261	0.0936	. . .	. . .	. . .	SpT(12)
167	HIP 52596	M1.5	161.319541	-30.807465	71.41	1.53	8.7926	31.9565	0.3991	. . .	. . .	. . .	SpT(8)
168	GJ 3622	M6.0	162.052429	-11.335619	220.30	2.10	12.5680	30.4463	0.0838	. . .	. . .	. . .	SpT(12)
169	GJ 403	M3.5	163.018357	13.997492	80.20	1.23	9.9165	31.5069	0.2403	96.8	13.7041	. . .	SpT(~);P_{rot}(11)
170	GJ 406	M6.0	164.120270	7.014658	419.10	2.00	12.1238	30.6240	0.0986	. . .	. . .	. . .	SpT(12)
171	GJ 408	M3.0	165.018017	22.833138	150.10	1.56	8.9754	31.8833	0.3786	. . .	. . .	9.5227	SpT(12)
172	GJ 3637	M4.0	165.331897	3.004777	71.80	1.75	10.9038	31.1120	0.1554	. . .	. . .	. . .	SpT(~)
173	GJ 410	M2.0	165.659701	21.967142	84.95	1.48	7.8125	32.3485	0.5837	2.935	0.0120	0.3311	SpT(16);P_{rot}(3)
174	GJ 411	M2.0	165.834327	35.969933	392.64	1.44	9.0013	31.8730	0.4057	48	**2.7310**	10.8169	SpT(12);P_{rot}(13)
175	GJ 413.1	M2.0	167.380771	-24.598579	93.00	1.53	8.5081	32.0702	0.4593	. . .	. . .	9.2960	SpT(14)
176	GJ 3647	M3.5	167.965670	33.536442	68.30	1.64	9.2951	31.7555	0.3302	7.79	0.0670	. . .	SpT(25);P_{rot}(11)
177	GJ 422	M3.5	169.000752	-57.547611	78.91	1.33	9.0894	31.8378	0.3542	. . .	. . .	. . .	SpT(14)
178	LHS 2395	M	169.877448	46.695480	97.00	1.54	12.0553	30.6514	0.1011	. . .	. . .	. . .	SpT(~)
179	HIP 56157	M3.0	172.674145	-8.095158	75.75	1.55	9.2220	31.7847	0.3495	. . .	. . .	. . .	SpT(8)
180	GJ 3668	M4.5	172.784826	-14.955598	85.00	1.93	10.8814	31.1209	0.1588	. . .	. . .	. . .	SpT(~)

No.	Star	SpT	RA* (J2000)	DEC* (J2000)	Plx° [mas]	(B-V)	M_{bol} [mag]	log L_{bol} [erg s^{-1}]	Mass [$M_\odot$]	P_{rot} [d]	t_{gyro} [Gyr]	t_{chromo}° [Gyr]	Reference
181	GJ 431	M3.5	172.943963	-41.046486	96.56	1.55	9.1406	31.8172	0.3686	14.31	**0.2367**	. . .	SpT(23);P_{rot}(13)
182	GJ 433	M1.5	173.862294	-32.539803	112.58	1.51	8.4168	32.1068	0.4709	. . .	. . .	. . .	SpT(14)
183	2MASS J11381671-7721484	M5.0	174.569647	-77.363464	122.27	. . .	11.7945	30.7557	0.1088	. . .	. . .	. . .	SpT(~)
184	GJ 1147	M3.0	174.604207	-41.375713	66.08	1.72	10.3481	31.3343	0.2039	. . .	. . .	. . .	SpT(~)
185	GJ 1148	M4.0	175.436318	42.752026	90.06	1.48	9.2954	31.7553	0.3421	. . .	. . .	. . .	SpT(21)
186	GJ 436	M3.5	175.545669	26.706980	98.61	1.52	8.6497	32.0136	0.4394	. . .	. . .	10.3759	SpT(12)
187	GJ 445	M4.0	176.922660	78.691208	186.86	1.59	10.2371	31.3787	0.2409	. . .	. . .	11.1914	SpT(12)
188	GJ 447	M4.5	176.935020	0.804568	298.04	1.74	10.7791	31.1618	0.1684	. . .	. . .	. . .	SpT(12)
189	GJ 1151	M4.5	177.741160	48.377666	115.36	1.84	10.6927	31.1964	0.1750	132	13.1610	. . .	SpT(12);P_{rot}(11)
190	GJ 450	M1.0	177.780727	35.271915	116.48	1.52	8.4696	32.0857	0.4597	. . .	. . .	3.4649	SpT(12)
191	GJ 3693	M8.0	178.469467	6.998918	70.30	1.72	12.5943	30.4358	0.0880	. . .	. . .	. . .	SpT(2)
192	GJ 452.1	M3.5	178.532852	9.806314	88.30	1.73	10.1424	31.4165	0.2082	. . .	. . .	. . .	SpT(~)
193	GJ 3707	M3.5	182.523321	-15.071017	77.93	1.52	9.0765	31.8429	0.3883	. . .	. . .	. . .	SpT(12)
194	GJ 1156	M5.0	184.747481	11.126083	152.90	1.83	11.2634	30.9681	0.1342	0.491	0.0003	. . .	SpT(12);P_{rot}(11)
195	GJ 465	M2.0	186.218463	-18.241770	112.98	1.59	9.7515	31.5729	0.2528	. . .	. . .	7.5435	SpT(14)
196	GJ 479	M3.0	189.467961	-52.001530	103.18	1.54	8.7191	31.9859	0.4309	. . .	. . .	. . .	SpT(28)
197	GJ 3737	M4.5	189.704754	-38.381332	156.78	1.69	11.0614	31.0489	0.1428	. . .	. . .	. . .	SpT(~)
198	GJ 480	M4.0	189.718410	11.696155	69.59	1.47	8.5643	32.0478	0.4663	. . .	. . .	6.0698	SpT(12)
199	GJ 480.1	M3.0	190.193042	-43.566536	128.52	1.73	10.5854	31.2394	0.1741	. . .	. . .	. . .	SpT(14)
200	LHS 2613	M	190.708177	41.896385	94.20	0.99	9.7655	31.5673	0.2662	. . .	. . .	. . .	SpT(~)
201	GJ 486	M4.0	191.986009	9.751397	119.47	1.56	9.4432	31.6962	0.3179	. . .	. . .	11.1095	SpT(12)
202	GJ 493.1	M5.0	195.139608	5.685586	123.10	1.75	10.8039	31.1519	0.1614	0.6	0.0004	. . .	SpT(12);P_{rot}(11)
203	GJ 3764	M3.5	197.334897	-40.157337	61.75	1.60	9.5924	31.6365	0.2893	. . .	. . .	. . .	SpT(~)
204	GJ 1167 A	M3.5	197.395632	28.985161	92.50	1.71	11.2133	30.9882	0.1374	. . .	. . .	. . .	SpT(23)
205	LHS 2686	M4.5	197.552869	47.755291	96.80	1.63	11.2475	30.9745	0.1267	. . .	. . .	. . .	SpT(23)
206	WT 392	~	198.289148	-41.511024	83.58	1.12	9.8005	31.5533	0.2781	. . .	. . .	. . .	SpT(-)
207	GJ 3777	M3.5	200.016320	-35.412148	73.04	1.20	9.9530	31.4923	0.2424	. . .	. . .	. . .	SpT(1)
208	GJ 3779	M4.0	200.736399	24.467621	73.10	1.62	9.7533	31.5722	0.2451	. . .	. . .	. . .	SpT(~)
209	GJ 3780	M3.5	200.908537	-25.912493	71.48	0.00	9.7395	31.5777	0.2741	. . .	. . .	. . .	SpT(23)
210	GJ 514	M1.0	202.499127	10.377120	130.62	1.50	8.1140	32.2279	0.5243	. . .	. . .	7.4345	SpT(12)

No.	Star	SpT	RA* (J2000)	DEC* (J2000)	Plx° [mas]	(B-V)	M_{bol} [mag]	log L_{bol} [erg s^{-1}]	Mass [$M_{\odot}$]	P_{rot} [d]	t_{gyro} [Gyr]	t_{chromo}° [Gyr]	Reference
211	GJ 1171	M4.5	202.629426	19.159454	68.70	1.79	10.7731	31.1643	0.1398	...	...	...	SpT(29)
212	GJ 521	M2.0	204.850438	46.186520	76.87	1.24	8.5146	32.0677	0.5045	...	...	...	SpT(12)
213	GJ 3801	M4.0	205.680362	33.290428	107.77	2.41	9.8118	31.5488	0.2618	...	...	...	SpT(20)
214	GJ 524	M2.5	206.203337	-54.121716	73.40	1.09	9.9259	31.5032	0.2308	...	...	...	SpT(~)
215	GJ 526	M4.0	206.431434	14.892165	185.49	1.39	8.2365	32.1789	0.4956	...	...	6.7852	SpT(12)
216	GJ 3804	M3.5	206.461457	-17.967993	97.62	1.55	9.5349	31.6595	0.3027	...	...	...	SpT(14)
217	GJ 3817	M3.0	209.558040	12.578835	88.40	1.66	9.7194	31.5857	0.2584	...	...	...	SpT(29)
218	GJ 3820	M4.5	209.793576	-19.834293	92.86	1.70	10.0263	31.4630	0.2442	...	...	...	SpT(~)
219	GJ 536	M1.5	210.263526	-2.655024	99.72	1.47	8.1749	32.2036	0.5118	...	...	6.3882	SpT(14)
220	GJ 2106	M2.0	213.303703	-56.742069	85.62	1.53	8.2937	32.1560	0.4871	...	...	...	SpT(14)
221	GJ 1182	M5.0	213.885570	4.658679	71.70	1.72	10.5106	31.2693	0.1796	...	...	...	SpT(12)
222	GJ 545	M3.5	215.030808	-9.620203	69.00	1.60	9.8318	31.5408	0.2585	...	...	...	SpT(~)
223	GJ 3843	M3.5	215.313034	-1.122204	74.66	0.95	10.1310	31.4211	0.2237	...	...	...	SpT(~)
224	GJ 3846	M2.5	216.233302	8.887656	70.03	1.60	9.4314	31.7009	0.3076	...	...	...	SpT(14)
225	LHS 2919	M6.5	217.017482	13.937150	82.80	2.45	12.6587	30.4100	0.0845	...	...	...	SpT(~)
226	GJ 3849	M9.0	217.180138	33.177540	90.80	1.46	13.6844	29.9998	0.0685	...	...	...	SpT(12)
227	GJ 552	M2.5	217.373821	15.532746	71.39	1.50	8.2168	32.1868	0.5150	...	...	4.0742	SpT(12)
228	GJ 3855	M6.5	217.657828	59.723595	103.80	1.82	12.9115	30.3089	0.0782	...	...	...	SpT(12)
229	GJ 553.1	M3.5	217.755009	-12.295886	92.44	1.59	9.4624	31.6885	0.3115	...	...	...	SpT(16)
230	GJ 555	M4.0	218.570143	-12.519636	164.99	1.60	9.7992	31.5538	0.2776	...	...	10.4100	SpT(12)
231	GJ 3877	M7.0	224.159642	-28.163160	159.20	1.34	12.9940	30.2759	0.0768	...	...	...	SpT(12)
232	GJ 1187	M5.5	224.473949	56.656734	89.00	1.95	11.4851	30.8795	0.1061	...	...	...	SpT(12)
233	2MASS J15010818+2250020	M9.0	225.284113	22.833900	94.40	...	13.7308	29.9812	0.0682	...	...	...	SpT(12)
234	GJ 3892	M3.0	227.398289	3.166880	69.19	1.51	8.6795	32.0017	0.4365	...	...	...	SpT(29)
235	GJ 3894	M4.5	227.961076	-10.238286	67.40	1.66	10.7815	31.1609	0.1696	...	...	...	SpT(~)
236	GJ 581	M5.0	229.862061	-7.722242	160.91	1.60	9.7790	31.5619	0.2997	...	...	10.8754	SpT(12)
237	GJ 9520	M1.5	230.470496	20.977634	87.63	1.52	8.0323	32.2606	0.5550	0.369	0.0002	...	SpT(25);P_{rot}(13)
238	GJ 585	M4.5	230.963040	17.465820	85.10	1.79	10.5638	31.2480	0.1767	...	...	...	SpT(12)
239	GJ 588	M2.5	233.054259	-41.275414	168.66	1.50	8.5122	32.0686	0.4682	...	...	...	SpT(14)
240	GJ 590	M4.0	234.143760	-37.906200	81.60	1.59	9.8737	31.5240	0.2510	...	...	...	SpT(1)

No.	Star	SpT	RA* (J2000)	DEC* (J2000)	Plx° [mas]	(B-V)	M_{bol} [mag]	log L_{bol} [erg s^{-1}]	Mass [$M_{\odot}$]	P_{rot} [d]	t_{gyro} [Gyr]	t_{chromo}° [Gyr]	Reference
241	GJ 592	M4.0	234.244513	-14.133502	74.90	1.58	9.6584	31.6101	0.2890	. . .	. . .	. . .	SpT(~)
242	GJ 606	M1.0	239.972382	-8.253167	71.95	1.51	8.1534	32.2121	0.5218	. . .	. . .	. . .	SpT(14)
243	GJ 609	M4.0	240.712436	20.589396	100.30	1.63	10.0706	31.4453	0.2333	. . .	. . .	. . .	SpT(20)
244	HIP 79431	M3.0	243.174086	-18.875483	69.46	1.51	8.6488	32.0140	0.4873	. . .	. . .	. . .	SpT(8)
245	GJ 625	M2.0	246.352474	54.304127	153.46	1.63	9.5813	31.6410	0.3156	. . .	. . .	11.1706	SpT(12)
246	GJ 3960	M3.5	248.220204	9.840550	77.40	1.69	10.1396	31.4177	0.2080	. . .	. . .	. . .	SpT(~)
247	GJ 3967	M4.0	250.024992	0.705230	89.00	1.31	10.6713	31.2050	0.1743	0.311	0.0002	. . .	SpT(~);P_{rot}(11)
248	GJ 3971	M5.0	250.086172	67.601295	74.70	1.95	11.0138	31.0680	0.1460	0.378	0.0002	. . .	SpT(15);P_{rot}(11)
249	GJ 633	M2.5	250.188507	-45.999733	59.47	0.97	9.5140	31.6679	0.2923	. . .	. . .	. . .	SpT(~)
250	GJ 1207	M4.0	254.273772	-4.348883	115.39	1.59	10.2132	31.3882	0.2269	. . .	. . .	. . .	SpT(20)
251	GJ 649	M2.0	254.536873	25.744230	96.67	1.48	8.0490	32.2539	0.5379	. . .	. . .	2.9972	SpT(12)
252	GJ 3988	M4.0	255.849368	51.406086	105.40	1.75	10.7453	31.1754	0.1676	. . .	. . .	. . .	SpT(20)
253	GJ 655	M3.0	256.781348	21.554008	74.84	1.57	9.0355	31.8593	0.3724	. . .	. . .	. . .	SpT(20)
254	HIP 84051	M1.0	257.746529	-52.515553	80.17	1.48	8.0415	32.2569	0.5389	. . .	. . .	. . .	SpT(14)
255	GJ 3992	M4.0	257.894674	38.442810	83.31	1.61	9.3023	31.7526	0.3738	. . .	. . .	. . .	SpT(20)
256	GJ 1214	M4.5	258.828924	4.963803	77.20	1.73	10.9025	31.1125	0.1530	53	2.4862	. . .	SpT(5);P_{rot}(17)
257	GJ 2128	M2.0	259.170747	8.058409	67.08	1.56	8.8166	31.9468	0.4030	. . .	. . .	. . .	SpT(14)
258	GJ 671	M3.0	259.969448	41.714188	80.77	1.56	9.2751	31.7634	0.3658	. . .	. . .	11.1860	SpT(6)
259	GJ 674	M3.0	262.166316	-46.895130	220.24	1.57	9.1680	31.8063	0.3461	33.29	**1.1817**	. . .	SpT(28);P_{rot}(13)
260	GJ 4004	M3.5	262.363717	-80.149254	79.95	1.40	9.5107	31.6692	0.3081	. . .	. . .	. . .	SpT(~)
261	GJ 678.1 A	M0.0	262.594695	5.548531	100.23	1.48	7.9144	32.3077	0.5639	. . .	. . .	4.7394	SpT(20)
262	GJ 1220	M4.0	262.821880	82.088844	70.90	1.77	10.4769	31.2828	0.1719	. . .	. . .	. . .	SpT(~)
263	GJ 680	M3.0	263.806765	-48.680843	102.83	1.55	8.4267	32.1028	0.4691	. . .	. . .	. . .	SpT(8)
264	GJ 682	M3.5	264.265327	-44.319118	196.90	1.65	9.8519	31.5327	0.2707	. . .	. . .	. . .	SpT(14)
265	GJ 686	M1.0	264.472102	18.591537	123.67	1.53	8.5164	32.0670	0.4412	. . .	. . .	8.3642	SpT(12)
266	GJ 694	M3.5	265.983134	43.378929	105.50	1.55	8.9451	31.8955	0.4323	. . .	. . .	3.9913	SpT(12)
267	GJ 4026	M3.5	266.519403	24.651379	68.70	0.93	9.5841	31.6399	0.2492	. . .	. . .	. . .	SpT(~)
268	GJ 693	M2.0	266.642824	-57.318924	171.48	1.64	9.8253	31.5434	0.2563	. . .	. . .	. . .	SpT(14)
269	GJ 4029	M6.0	267.497843	22.685270	67.90	-1.10	13.3603	30.1294	0.0693	. . .	. . .	. . .	SpT(~)
270	GJ 699	M4.0	269.452044	4.694597	548.31	1.73	10.8523	31.1326	0.1530	130	14.0237	11.1465	SpT(12);P_{rot}(13)

No.	Star	SpT	RA* (J2000)	DEC* (J2000)	Plx° [mas]	(B-V)	M_{bol} [mag]	log L_{bol} [erg s^{-1}]	Mass [$M_{\odot}$]	P_{rot} [d]	t_{gyro} [Gyr]	t_{chromo}° [Gyr]	Reference
271	GJ 4040	M1.0	269.462349	46.588390	70.99	1.56	9.1852	31.7994	0.3999	. . .	. . .	. . .	SpT(29)
272	GJ 1223	M5.0	270.692701	37.518021	83.50	1.79	11.2604	30.9693	0.1340	. . .	. . .	. . .	SpT(12)
273	GJ 701	M2.0	271.281491	-3.031218	128.89	1.52	8.3679	32.1263	0.4755	. . .	. . .	8.3692	SpT(12)
274	GJ 1224	M4.5	271.887196	-15.962905	132.60	1.83	11.2405	30.9773	0.1376	. . .	. . .	. . .	SpT(12)
275	GJ 4053	M4.5	274.738575	66.192558	137.50	1.83	11.2385	30.9781	0.1253	. . .	. . .	. . .	SpT(12)
276	GJ 712	M3.5	275.527967	6.343805	68.90	1.45	9.6166	31.6269	0.2642	. . .	. . .	. . .	SpT(~)
277	GJ 1227	M4.5	275.613297	62.050705	121.50	1.79	10.8662	31.1270	0.1571	. . .	. . .	. . .	SpT(12)
278	2MASS J18353790+3259545	M8.5	278.907925	32.998497	176.50	1.73	13.5275	30.0625	0.0697	. . .	. . .	. . .	SpT(24)
279	NLTT 46822	M6.5	279.887851	29.871227	85.38	1.00	12.7043	30.3918	0.0833	. . .	. . .	. . .	SpT(~)
280	GJ 4070	M3.0	280.496196	31.830513	87.36	1.54	9.0100	31.8695	0.3697	. . .	. . .	10.9889	SpT(29)
281	GJ 4071	M4.5	280.687455	13.904679	93.30	. . .	10.0497	31.4536	0.2304	. . .	. . .	. . .	SpT(15)
282	GJ 4073	M8.0	280.842225	40.672493	70.70	0.97	12.6526	30.4125	0.0863	. . .	. . .	. . .	SpT(24)
283	GJ 729	M3.0	282.455404	-23.836149	336.72	1.74	10.7012	31.1930	0.1700	2.869	0.0089	. . .	SpT(28);P_{rot}(13)
284	GJ 4078	M3.5	282.463308	-57.446835	82.21	1.18	9.8173	31.5466	0.2771	. . .	. . .	. . .	SpT(~)
285	GJ 740	M0.5	284.500585	5.908249	91.68	1.46	7.6514	32.4129	0.6191	. . .	. . .	3.6840	SpT(14)
286	GJ 739	M2.0	284.781066	-48.274433	70.95	1.47	8.5252	32.0634	0.4563	. . .	. . .	. . .	SpT(29)
287	GJ 1232	M4.5	287.462417	17.668736	93.60	1.89	10.5400	31.2575	0.1924	. . .	. . .	. . .	SpT(21)
288	GJ 754	M4.5	290.199811	-45.557869	169.03	1.70	10.7019	31.1928	0.1718	. . .	. . .	. . .	SpT(~)
289	GJ 4102	M3.0	290.226625	-82.554726	78.34	1.71	9.8365	31.5389	0.2603	. . .	. . .	. . .	SpT(~)
290	GJ 1235	M4.0	290.411164	20.867451	100.10	1.71	10.6991	31.1939	0.1759	. . .	. . .	. . .	SpT(20)
291	GJ 1236	M3.0	290.508605	7.041950	92.90	1.69	10.3286	31.3421	0.2160	. . .	. . .	. . .	SpT(~)
292	GJ 1238	M5.5	291.068089	75.553368	90.30	1.94	11.4327	30.9004	0.1196	114	9.1795	. . .	SpT(~);P_{rot}(11)
293	GJ 4117	M3.0	293.729061	53.256355	72.10	0.40	9.8905	31.5173	0.2849	. . .	. . .	. . .	SpT(29)
294	GJ 1243	M4.0	297.788774	46.483295	84.10	1.64	10.2025	31.3925	0.2308	0.593	0.0005	. . .	SpT(21);P_{rot}(11)
295	GJ 1248	M1.5	300.962441	5.995562	79.50	1.61	10.2729	31.3643	0.2339	. . .	. . .	. . .	SpT(~)
296	GJ 784	M0.0	303.472307	-45.164062	161.34	1.45	7.7311	32.3810	0.5867	. . .	. . .	. . .	SpT(28)
297	GJ 1253	M5.0	306.522037	58.572910	107.50	1.79	10.9284	31.1021	0.1506	. . .	. . .	. . .	SpT(12)
298	GJ 791	M3.0	306.923621	-27.747396	67.38	1.49	8.7492	31.9738	0.4463	. . .	. . .	. . .	SpT(14)
299	GJ 1251	M4.5	307.015952	-76.671227	79.02	1.72	10.8525	31.1325	0.1632	. . .	. . .	. . .	SpT(~)
300	GJ 793	M3.0	307.633655	65.449623	125.07	1.56	9.3402	31.7374	0.3713	. . .	. . .	4.1912	SpT(12)

No.	Star	SpT	RA* (J2000)	DEC* (J2000)	Plx° [mas]	(B-V)	M_{bol} [mag]	log L_{bol} [erg s^{-1}]	Mass [$M_{\odot}$]	P_{rot} [d]	t_{gyro} [Gyr]	t_{chromo}° [Gyr]	Reference
301	GJ 792	M4.0	307.856721	38.562012	67.10	1.82	10.1618	31.4088	0.2200	. . .	. . .	. . .	SpT(21)
302	GJ 1256	M4.5	310.140179	15.499227	102.00	1.72	10.5921	31.2366	0.1892	. . .	. . .	. . .	SpT(21)
303	GJ 4154	M2.5	311.655242	-81.720596	94.72	1.80	9.3295	31.7417	0.3241	. . .	. . .	. . .	SpT(~)
304	HIP 103039	M4.0	313.137687	-16.974718	175.03	1.57	10.1584	31.4102	0.2287	. . .	. . .	8.7262	SpT(8)
305	GJ 4169	M4.0	313.387677	10.617228	71.90	1.12	10.4476	31.2945	0.1918	. . .	. . .	. . .	SpT(~)
306	GJ 813	M2.0	314.355735	22.362701	72.58	1.61	9.4887	31.6780	0.2890	. . .	. . .	. . .	SpT(16)
307	GJ 816	M3.0	315.494406	-6.318637	69.53	1.51	8.5105	32.0693	0.4665	. . .	. . .	. . .	SpT(21)
308	GJ 2151	M4.0	315.807942	-56.963333	78.61	1.66	10.0360	31.4591	0.2328	. . .	. . .	. . .	SpT(14)
309	GJ 821	M1.0	317.322525	-13.302231	82.18	1.53	8.9340	31.8999	0.3605	. . .	. . .	10.0292	SpT(14)
310	GJ 9724	M1.0	317.956481	-43.613598	67.55	1.60	9.3656	31.7273	0.3078	. . .	. . .	. . .	SpT(14)
311	GJ 825	M0.0	319.313920	-38.867287	253.41	1.41	7.5011	32.4731	0.6297	. . .	. . .	. . .	SpT(28)
312	LHS 510	M4.0	322.698487	-40.708057	83.60	1.61	10.3777	31.3224	0.1937	. . .	. . .	. . .	SpT(30)
313	GJ 832	M1.5	323.391555	-49.008995	201.87	1.50	8.5249	32.0635	0.4425	. . .	. . .	8.1800	SpT(14)
314	WT 795	~	324.105504	-44.016811	69.53	1.85	10.5196	31.2657	0.1941	. . .	. . .	. . .	SpT(-)
315	GJ 4207	M3.5	324.682059	-33.665432	82.02	1.62	9.8251	31.5434	0.2619	. . .	. . .	. . .	SpT(~)
316	GJ 836	M4.0	324.753379	-24.157780	73.30	1.56	10.4167	31.3068	0.1997	. . .	. . .	. . .	SpT(~)
317	GJ 838.6	M2.5	328.688827	-46.992737	68.33	1.59	9.3087	31.7500	0.3178	. . .	. . .	. . .	SpT(14)
318	GJ 4239	M5.0	329.229735	-1.902793	74.80	1.76	11.2130	30.9883	0.1405	. . .	. . .	. . .	SpT(~)
319	GJ 842	M0.5	329.894982	-59.752914	83.43	1.47	7.8640	32.3279	0.5773	. . .	. . .	. . .	SpT(14)
320	GJ 4247	M4.0	330.304621	28.306915	112.33	1.72	9.9312	31.5010	0.2772	1.678	0.0032	. . .	SpT(26);P_{rot}(17)
321	GJ 843	M3.5	330.502926	-19.483128	78.20	1.27	9.2592	31.7698	0.3330	. . .	. . .	. . .	SpT(~)
322	GJ 846	M0.0	330.542766	1.400180	97.61	1.47	7.7335	32.3801	0.5974	. . .	. . .	4.0279	SpT(14)
323	GJ 4248	M3.5	330.622305	-37.080894	134.29	1.65	10.0425	31.4565	0.2353	. . .	. . .	. . .	SpT(~)
324	GJ 849	M3.5	332.417906	-4.640765	109.94	1.50	8.4657	32.0872	0.4869	. . .	. . .	7.5100	SpT(12)
325	GJ 851	M2.0	332.875335	18.426151	86.08	1.51	8.0911	32.2370	0.5490	. . .	. . .	3.3796	SpT(12)
326	GJ 9773	M3.0	333.149815	8.553080	66.84	1.50	9.1988	31.7940	0.3416	. . .	. . .	. . .	SpT(~)
327	GJ 1265	M4.0	333.428231	-17.685608	96.00	1.72	10.7995	31.1537	0.1683	. . .	. . .	. . .	SpT(29)
328	GJ 4274	M4.0	335.779023	-17.606953	134.40	1.84	10.7263	31.1830	0.1738	. . .	. . .	. . .	SpT(23)
329	GJ 4281	M6.5	337.226671	-13.421627	88.80	2.16	12.6276	30.4225	0.0854	. . .	. . .	. . .	SpT(12)
330	GJ 1270	M4.0	337.453574	41.479992	72.50	1.65	9.9959	31.4752	0.2374	. . .	. . .	. . .	SpT(~)

No.	Star	SpT	RA* (J2000)	DEC* (J2000)	Plx° [mas]	(B-V)	M_{bol} [mag]	log L_{bol} [erg s^{-1}]	Mass [$M_\odot$]	P_{rot} [d]	t_{gyro} [Gyr]	t_{chromo}° [Gyr]	Reference
331	GJ 863	M0.0	338.259378	9.378076	78.68	1.53	8.3308	32.1412	0.4798	. . .	. . .	9.4347	SpT(12)
332	GJ 873	M4.5	341.707530	44.334194	195.22	1.36	9.6699	31.6055	0.3174	4.38	0.0296	0.1777	SpT(12);P_{rot}(18)
333	GJ 875	M0.5	342.580966	-7.090146	70.77	1.47	7.8128	32.3484	0.5795	. . .	. . .	. . .	SpT(14)
334	GJ 875.1	M3.5	342.972871	31.754251	68.78	1.20	8.9770	31.8827	0.4359	1.64	0.0055	0.0855	SpT(12);P_{rot}(4)
335	GJ 876	M5.0	343.319676	-14.263586	213.28	1.57	9.3891	31.7178	0.3324	114.95	12.8100	9.4551	SpT(12);P_{rot}(17)
336	GJ 4302	M4.0	343.693576	-5.474021	40.60	1.33	9.5718	31.6448	0.3022	. . .	. . .	. . .	SpT(9)
337	GJ 877	M3.0	343.938857	-75.458916	116.07	1.50	8.7309	31.9811	0.4221	. . .	. . .	. . .	SpT(14)
338	GJ 880	M2.0	344.145710	16.553623	146.09	1.51	7.8695	32.3257	0.5810	. . .	. . .	2.7131	SpT(12)
339	GJ 887	M2.0	346.463814	-35.853634	305.26	1.48	8.3079	32.1504	0.4693	. . .	. . .	7.2993	SpT(28)
340	2MASS J23062928-0502285	M8.0	346.622013	-5.041274	82.58	. . .	12.9779	30.2823	0.0780	. . .	. . .	. . .	SpT(24)
341	GJ 4312	M3.5	346.875168	68.668091	63.50	1.54	9.3696	31.7256	0.2906	. . .	. . .	. . .	SpT(~)
342	GJ 4333	M4.0	350.406345	17.291241	91.00	1.53	9.0362	31.8590	0.3917	. . .	. . .	8.8027	SpT(14)
343	GJ 895	M2.0	351.127052	57.854256	77.15	1.51	8.0392	32.2578	0.5892	. . .	. . .	3.6197	SpT(6)
344	2MASS J23301612-4736459	M7.0	352.567168	-47.612759	72.71	. . .	12.6433	30.4162	0.0854	. . .	. . .	. . .	SpT(~)
345	2MASS J23312174-2749500	M7.5	352.840611	-27.830564	69.14	1.20	12.9246	30.3036	0.0787	. . .	. . .	. . .	SpT(7)
346	GJ 899	M2.5	353.513684	0.179235	71.54	1.48	8.6442	32.0158	0.4285	. . .	. . .	. . .	SpT(14)
347	GJ 1286	M5.5	353.793768	-2.389288	138.30	1.91	11.7636	30.7681	0.1121	. . .	. . .	. . .	SpT(12)
348	GJ 4350	M4.5	354.217798	-36.481056	86.23	1.62	10.8055	31.1513	0.1622	. . .	. . .	. . .	SpT(~)
349	GJ 905	M6.0	355.479122	44.177994	316.00	1.91	11.3361	30.9391	0.1384	115	9.5504	. . .	SpT(12);P_{rot}(17)
350	GJ 1288	M4.5	355.719762	30.822752	81.80	1.77	11.0451	31.0555	0.1417	. . .	. . .	. . .	SpT(~)
351	GJ 1289	M4.0	355.776205	36.537010	123.50	1.60	10.4165	31.3069	0.1997	. . .	. . .	. . .	SpT(12)
352	GJ 908	M2.0	357.302331	2.401053	167.29	1.46	8.6128	32.0284	0.4174	. . .	. . .	10.9409	SpT(28)
353	HIP 117828	M	358.459062	-75.632645	100.07	1.49	8.1597	32.2096	0.5379	. . .	. . .	. . .	SpT(10)
354	GJ 1292	M3.5	359.433750	23.304714	72.80	1.54	8.9632	31.8882	0.3796	. . .	. . .	. . .	SpT(~)
355	GJ 4380	M3.5	359.438198	19.769785	67.30	1.69	9.8931	31.5163	0.2421	. . .	. . .	. . .	SpT(~)

Table 2.1: lists the names, positions and distances of the used M type stars' sample as well as several stellar parameters which were either taken from the given references or calculated. (*) in [deg] and taken from *Skrutskie et al.* 2006; (°) taken from *Odert* 2012, in preparation; (1) *Bidelman* 1985, (2) *Bochanski et al.* 2011, (3) *Bopp et al.* 1983, (4) *Carrasco et al.* 1980, (5) *Ehrenreich & Desert* 2011, (6) *Endl et al.* 2006, (7) *Faherty et al.* 2009, (8) *Gray et al.* 2006, (9) *Hawley et al.* 1996, (10) *Houk & Cowley* 1975, (11) *Irwin et al.* 2011, (12) *Jenkins et al.* 2009, (13) *Kiraga & Stépien* 2007, (14) *Koen et al.* 2010, (15) *Law et al.* 2008, (16) *Montes et al.* 2001, (17) *Odert* 2012, in preparation, (18) *Pettersen* 1980, (19) *Pizzolato et al.* 2003, (20) *Reid et al.* 1995, (21) *Reid et al.* 2004, (22) *Reyle et al.* 2006, (23) *Riaz et al.* 2006, (24) *Schmidt et al.* 2007, (25) *Shkolnik et al.* 2009, (26) *Strassmeier* 2009, (27) *Torres et al.* 1983, (28) *Torres etal.* 2006, (29) *Van Altena et al.* 1995, (30) *Walker* 1983, (31) *West et al.* 2008; (~) taken from *Simbad* (October 14th, 2011); (-) no spectral type available; Col. 12: values marked bold meet all criteria given by *Barnes* (2007). All other values were calculated as explained in chapter 2.

Table 2.2: G Star Sample

No.	Star	SpT	RA* (J2000)	DEC* (J2000)	Plx* [mas]	(B-V)	M_{bol} [mag]	log L_{bol} [erg s^{-1}]	Mass [$M_{\odot}$]	P_{rot} [d]	t_{gyro} [Gyr]	t_{iso}° [Gyr]	Reference
1	HD 2071	G2V	6.177285	-53.983998	36.72	0.60	5.1635	33.4081	0.9029	. . .	. . .	8	SpT(2)
2	HD 12846	G2V	31.626014	24.333993	43.91	0.66	4.9998	33.4736	0.9376	. . .	. . .	0.2	SpT(3)
3	HD 14082B	G2V	34.353059	28.741759	36.58	0.59	5.5012	33.2730	0.8354	. . .	. . .	8.4	SpT(7)
4	HD 20619	G2V	49.757893	-2.843194	39.65	0.66	4.9322	33.5006	0.9523	. . .	. . .	2.7	SpT(3)
5	HD 25874	G2V	60.612369	-61.356939	38.59	0.68	4.5514	33.6530	1.0396	. . .	. . .	9.1	SpT(2)
6	HD 29587	G2V	70.401316	42.118474	36.27	0.61	5.0107	33.4692	0.9352	. . .	. . .	11.7	SpT(~)
7	HD 42807	G2V	93.302093	10.627142	55.71	0.68	5.0587	33.4500	0.9250	7.8	0.486	. . .	SpT(4);P_{rot}(1)
8	HD 45289	G2V	96.101459	-42.847517	35.81	0.68	4.3290	33.7419	1.0942	. . .	. . .	10.7	SpT(2)
9	HD 48189	G2V	99.501524	-61.533387	46.96	0.57	4.4956	33.6752	1.0530	. . .	. . .	9.2	SpT(5)
10	HD 102365	G2V	176.629469	-40.500353	108.45	0.66	4.9641	33.4878	0.9453	. . .	. . .	7.1	SpT(2)
11	HD 107146	G2V	184.777093	16.548295	36.42	0.62	4.8037	33.5520	0.9809	. . .	. . .	2.4	SpT(6)
12	HD 108309	G2V	186.700588	-48.913192	37.58	0.68	4.0238	33.8640	1.1739	. . .	. . .	10.5	SpT(2)
13	HD 115043	G2V	198.404202	56.708270	39.53	0.57	4.7576	33.5704	0.9914	6	0.495	5.6	SpT(4);P_{rot}(1)
14	HD 137107J	G2V	230.801272	30.287825	55.98	0.56	3.7212	33.9850	1.2586	. . .	. . .	4.1	SpT(~)
15	HD 164595	G2V	270.162060	29.571922	35.26	0.64	4.7314	33.5809	0.9974	. . .	. . .	10.7	SpT(~)
16	HD 168009	G2V	273.885267	45.209318	43.82	0.60	4.4564	33.6910	1.0626	. . .	. . .	9.1	SpT(~)
17	HD 177082	G2V	285.658588	14.567014	36.81	0.70	4.5058	33.6712	1.0506	. . .	. . .	4.9	SpT(~)
18	HD 181321	G2V	290.373952	-34.983464	53.10	0.59	5.0605	33.4493	0.9246	. . .	. . .	0.2	SpT(5)
19	HD 189567	G2V	301.386519	-67.320894	56.41	0.63	4.7518	33.5728	0.9927	. . .	. . .	9.1	SpT(2)
20	HD 205905	G2V	324.792298	-27.306574	38.99	0.62	4.6218	33.6248	1.0229	. . .	. . .	. . .	SpT(5)
21	HD 207129	G2V	327.065627	-47.303616	62.52	0.60	4.4991	33.6739	1.0522	. . .	. . .	5.2	SpT(5)
22	HD 210918	G2V	333.661056	-41.381663	45.35	0.62	4.4699	33.6855	1.0593	. . .	. . .	12.4	SpT(2)

Table 2.2: lists the names, positions and distances of the used G2V stars' sample as well as several stellar parameters which were either taken from the given references or calculated. (*) in [deg] and taken from *Van Leeuwen* 2007; (°) taken from *Holmberg et al.* 2009; (1) *Barnes* 2007, (2) *Gray et al.* 2006, (3) *Koen et al.* 2010, (4) *Montes et al.* 2001, (5) *Torres et al.* 2006, (6) *White et al.* 2007, (7) *Zuckerman & Song* 2004; (~) taken from *Simbad* (October 14th, 2011). All other values were calculated as explained in chapter 2.

3 Results and Discussion

The electromagnetic radiation of 355 M-type stars was studied in twelve different wavelengths and compared to the radiation of 22 Sun-like (G2V) stars. These wavelength ranges are X-ray, EUV, FUV, NUV, U, B, V, R, I, J, H and K. Furthermore, the emission of the spectral line Hα was investigated.

The most interesting ranges concerning M-type stars and their space weather are, of course, the short-wavelengths ranges (X-ray, EUV, FUV and NUV) and the emission in the spectral line Hα. The longer wavelengths are included for completeness and will be explained first, before the most significant part will be treated in detail.

Finally the examination of the M- and G-type stars' Hα emissions will be discussed. Hα is a very important proxy concerning a dwarf star's chromospheric activity and thus can be used as an indicator of the intensity of chromospheric events such as flares.

For each wavelength range at least two diagrams[23] were compiled, one plotting the stellar masses against the luminosity of the studied wavelength, the second plotting the stellar masses against the ratios of the particular filter's to the bolometric luminosity. In the diagrams on the following pages the M-type stars are marked as red diamonds, while the G2V stars are green. This applies for all upcoming diagrams, unless other descriptions are given.

Additionally the luminosities of the short-wavelength ranges, as well as of the spectral line Hα, were not only investigated in terms of the stellar masses, but also as a function of the stars' spectral subtypes and their ages.

In summary, this work presents an almost complete coverage of the electromagnetic radiation emitted by 355 M-type stars as well as 22 Sun-like (G2V) stars over a wavelength range from 0.5 to 2300 nm and thus illustrates the characteristics over a large part of the electromagnetic spectrum.

[23] There is a prominent outlier clearly below all other stars in all diagrams where magnitude I was used for calculations. This star is GJ 398 (No. 164), which has a far too high value in this passband (*Monet et al.*, 2003; I=17.9). It was kept in the sample for completeness. Further discussions about outliers do not concern this one.

3.1 The Johnson UBV

3.1.1 The U Band

The U filter is sensitive to ultraviolet rays in a wavelength range from 325-395 nm *(Reid & Hawley,* 2005). The M-type stars' apparent magnitudes in U were available for 124 stars and mainly taken from *Simbad* (except two values). As far as reference papers[24] were stated, they are quoted below. The G2V stars' apparent magnitudes in U were available for 3 stars and also taken from *Simbad*. The corresponding references[25] are cited below as well.

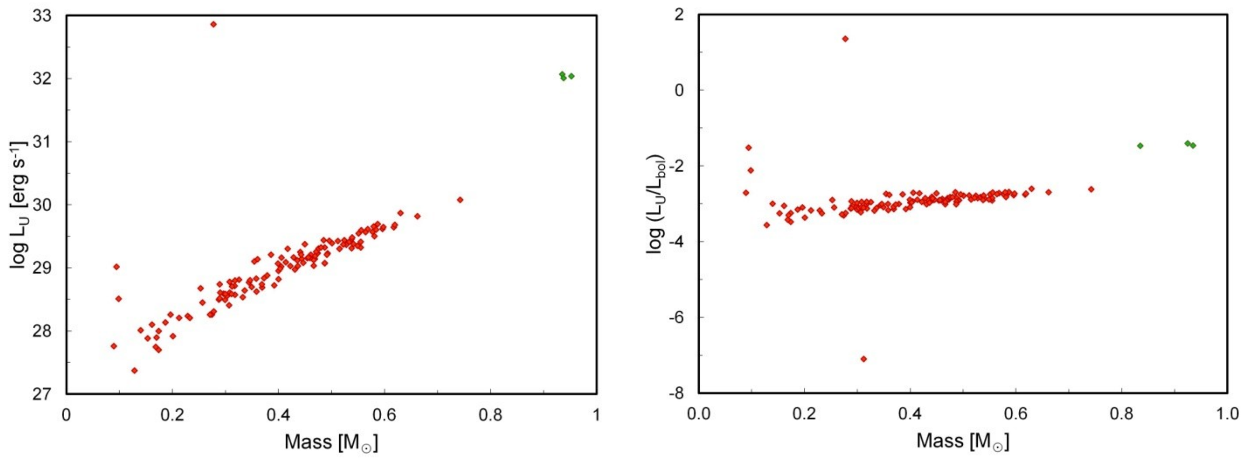

Figure 3.1. The relationship between mass and luminosity in passband U for the studied M and G stars sample in this work. M stars are marked red as the G stars are green.

In Figure 3.1 (right) the amount of radiation in U compared to the bolometric only slightly increases with increasing stellar mass. Further it can be seen that Sun-like stars have higher U luminosities than M-type stars, which is clear as they are more luminous in the blue part of the spectrum. In the left diagram in Fig. 3.1 there is an obvious linear relationship between mass and the log of U filter luminosity. The outliers in both Figures could represent bad data and/or flaring stars as flares are a phenomenon of chromospheric activity and the main amount of the chromosphere's radiation consists of UV radiation (*Hanslmeier,* 2007).

---

[24] **M stars:** *Henry* (2002): Stars no. 139, 146, 150; *Koen* (2010): Stars no. 1, 10, 18, 22, 25, 31, 34, 35, 41, 43, 45, 47,48, 60, 70, 74, 76, 78, 80, 82, 86, 88, 89, 91, 93, 94, 99, 105, 111, 112, 116-118, 123, 140, 141, 143, 145, 149, 151, 153, 157, 159, 161, 162, 167, 171, 173, 175, 177, 179, 181, 182, 188, 195, 196, 198, 199, 201, 210, 215, 216, 219, 220, 224, 227, 229, 230, 234, 236, 237, 239, 242, 244, 251, 253, 254, 257, 259, 261, 263-265, 268, 270, 273, 283, 285, 286, 296, 298, 304, 306, 307-310, 313, 317, 319, 322, 324, 325, 331, 333, 335, 337, 338, 342, 346, 352, 353; *Oja* (1985): Star no. 174; *Samus* (2003): Stars no. 27, 126, 130, 164, 170, 202, 311, 320.

[25] **G2V stars:** *Koen* (2010): Stars no. 2, 4; *Oja* (1991): Star no. 6.

3.1.2 The B Band

The B filter is sensitive to blue light and covers a wavelength range from 390-490 nm (*Reid & Hawley,* 2005). The M-type stars' apparent magnitudes in B were available for 347 stars and taken from *Simbad*. As far as a reference paper[26] was stated, it is quoted below. The G2V stars' apparent magnitudes in B were available for all 22 stars and also taken from *Simbad*, referenced[27] below as far as available.

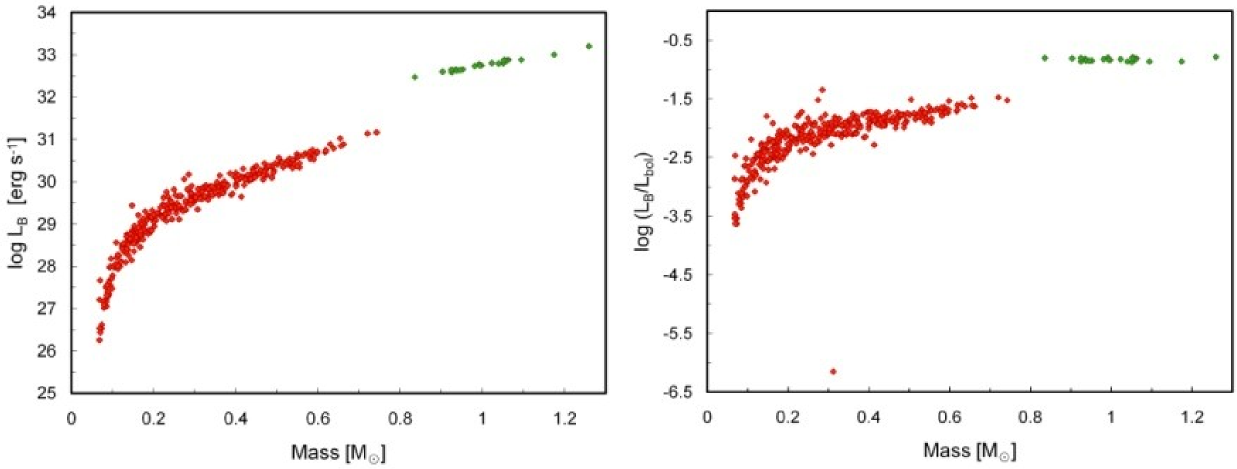

Figure 3.2. The relationship between mass and luminosity in passband B for the studied M and G stars sample in this work. M stars are marked red as the G stars are green.

Figure 3.2 shows clearly that the amount of B radiation in M dwarfs increases with increasing mass and is obviously less than in the compared Sun-like stars. Besides, it demonstrates a steep increase of radiation in B at the lower mass end of M-type stars. Compared to Figure 3.1, the intensity of B filter luminosity at the lower mass end illustrates the higher chromospheric activity in U present in late M-type stars lower than 0.2 $M_\odot$, as there is a significant break-point in Figure 3.2, but a rather flat slope in Figure 3.1.

[26] **M stars:** *Bessell* (1990): Star no. 240. *Casagrande* (2008): Stars no. 44, 241. *Hog* (2000): Stars no. 26, 28, 110, 114, 142, 212, 245, 255, 334. *Kharchenko* (2001): Stars no. 12, 58, 90, 127, 148, 176, 185, 204, 205, 213, 280, 320. *Koen* (2010): Stars no. 1, 10, 18, 25, 31, 34, 35, 41, 43, 45, 47, 48, 60, 70, 74, 76, 78, 80, 82, 86, 88, 89, 91, 93, 94, 99, 105, 111, 112, 116-118, 123, 140, 141, 143, 145, 149, 151, 153, 157, 159, 161, 162, 167, 171, 173, 175, 177, 179, 181, 182, 188, 195, 196, 198, 199, 201, 210, 215, 216, 219, 220, 224, 227, 229, 230, 234, 236, 237, 239, 242, 244, 251, 253, 254, 257, 259, 261, 263, 264, 265, 268, 270, 273, 283, 285, 286, 296, 298, 304, 306-310, 313, 317, 319, 322, 324, 325, 331, 333, 335, 337, 338, 342, 346, 352, 353. *Lasker* (2008): Star no. 249. *Mermilliod* (2006): Star no. 15. *Monet* (2003): Stars no. 3, 4, 21, 22, 37, 57, 59, 62, 68, 72, 77, 102, 119, 136, 138, 152, 156, 164, 178, 200, 214, 225, 228, 247, 260, 267, 269, 278, 279, 281, 282, 293, 305, 355. *Oja* (1985): Star no. 174. *Oppenheimer* (2001): Star no. 20. *Reid* (2004): Stars no. 36, 103, 122, 124, 294. *Space Telescope Science Institute* (2001): Star no. 284.

[27] **G2V stars:** *Hog* (2000): Stars no. 10, 19; *Koen* (2010): Stars no. 2, 4; *Oja* (1991): Star no. 6.

3.1.3 The V Band

The V filter is sensitive to visual light and ranges from 500-590 nm *(Reid & Hawley,* 2005). The M-type stars' apparent magnitudes in V were available for 350 stars and mainly taken from *Simbad*. Because of the importance of V values for several calculations, additional catalogs were searched, to find even more values in V. The G2V stars' apparent magnitudes in V were available for all 22 stars and taken from *Simbad*. As far as reference papers[28,29] for these values were stated, they are quoted below.

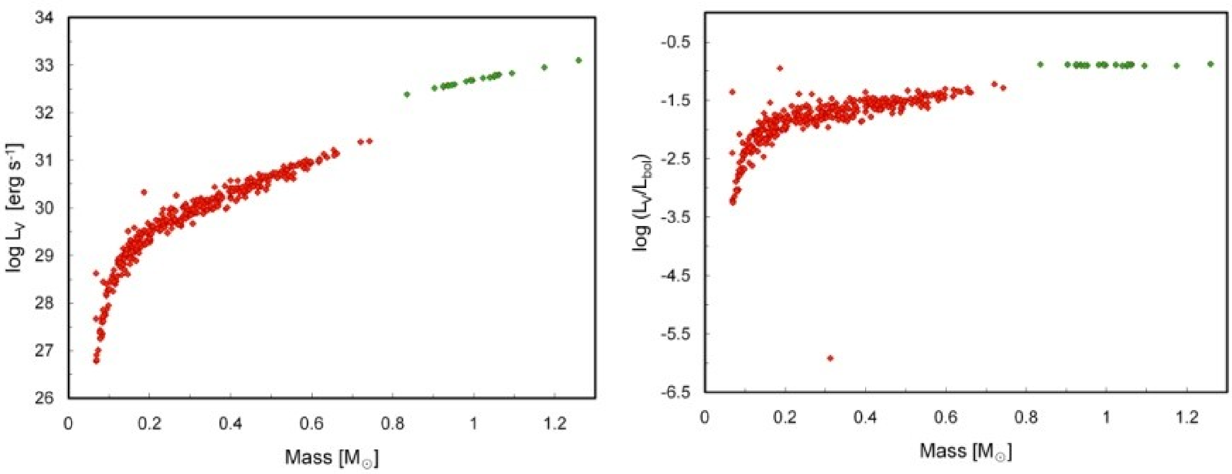

Figure 3.3. The relationship between mass and luminosity in passband V for the studied M and G stars sample in this work. M stars are marked red as the G stars are green.

Passband V, like the other visual passbands B and R, demonstrates the same break-point at 0.2 $M_\odot$. This is the last filter range going redwards, where the ratio of the filter to bolometric luminosity is unambiguously higher for the G2V stars than for the M stars. Again a steep increase of the M stars luminosity from the lower mass limit up to 0.2 $M_\odot$ can be seen in both diagrams of Fig. 3.3, which afterwards flattens its slope.

---

[28] **M stars:** *Bessell* (1990): Star no. 240. *Casagrande* (2008): Stars no. 2, 32, 44, 136, 166, 180, 183, 193, 241. *Costa* (2005): Stars no. 14, 38. *Costa* (2006): Star no. 340. *Hog* (2000): Stars no. 26, 28, 110, 114, 142, 212, 245, 255, 334. *Jao* (2011): Star no. 289. *Jenkins* (2009): Stars no. 5, 9, 13, 16, 27, 52, 55, 57, 65, 83, 98, 104, 107, 108, 120, 121, 144, 152, 160, 165, 168, 170, 186, 187, 189, 190, 194, 202, 221, 232, 238, 266, 272, 275, 300, 332, 349, 351. *Kharchenko* (2001): Stars no. 12, 58, 90, 127, 148, 176, 185, 204, 205, 213, 280, 320. *Koen* (2010): Stars no. 1, 10, 18, 22, 25, 31, 34, 35, 41, 43, 45, 47, 48, 60, 70, 74, 76, 78, 80, 82, 86, 88, 89, 91, 93, 94, 99, 105, 111, 112, 116-118, 123, 140, 141, 143, 145, 149, 151, 153, 157, 159, 161, 162, 167, 171, 173, 175, 177, 179, 181, 182, 188, 195, 196, 198, 199, 201, 210, 216, 219, 220, 224, 227, 229, 230, 234, 236, 237, 239, 242, 244, 251, 253, 254, 257, 259, 261, 263-265, 268, 270, 273, 283, 285, 286, 296, 298, 304, 306-310, 313, 317, 319, 322, 324, 325, 331, 333, 335, 337, 338, 342, 346, 352, 353. *Lépine* (2009): Stars no. 3, 59, 77, 178, 225. *Mermilliod* (2006): Star no. 15. *Oja* (1985): Star no. 174. *Patterson* (1998): Star no. 206. *Reid* (2004): Stars no. 7, 36, 85, 103, 122, 124, 130, 228, 274, 178, 294, 301. *Riedel* (2010): Stars no. 33, 147, 303, 314. *Van Altena* (1995): Stars no. 4, 6, 19-21, 23, 30, 37, 40, 46, 50, 66-68, 72, 92, 96, 119, 131-134, 137, 138, 156, 163, 164, 169, 172, 191, 200, 214, 226, 231, 233, 235, 247-249, 252, 267, 269, 277, 282, 292, 293, 297, 305, 318, 321, 328, 329, 336, 347, 350, 355. *Van Belle* (2009): Star no. 215.

[29] **G2V stars:** *Hog* (2000): Stars no. 10,19. *Koen* (2003): Stars no. 2, 4. *Oja* (1991): Star no. 1.

3.2 An Extension into the Red

3.2.1 The R Band

Passband R is sensitive to red light and ranges from 565-725 nm (*Reid & Hawley,* 2005). The M-type stars' apparent magnitudes in R were available for 332 stars and mainly taken from *Simbad* but also from other references. The G2V stars' apparent magnitudes in R were available for 9 stars and taken from *Simbad*. As far as reference papers[30,31] were stated, they are quoted below.

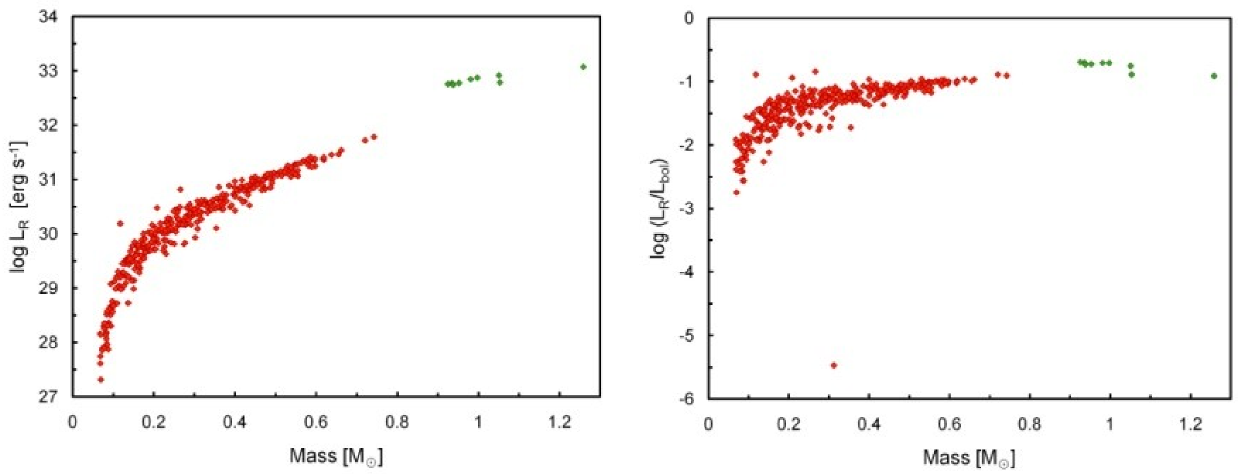

Figure 3.4. The relationship between mass and luminosity in passband R for the studied M and G stars sample in this work. M stars are marked red as the G stars are green.

As in filters B and V, Figure 3.4 shows a significant break-point at 0.2 $M_\odot$. This break-point demonstrates the redshift of a star's spectrum at lower masses, and when compared with the U filter, the higher chromospheric activity of these stars. At this point the G2V stars luminosity ratio, right diagram, approaches that of the M stars.

[30] **M stars:** *Casagrande* (2008): Stars no. 2, 16, 32, 44, 136, 139, 146, 166, 180, 183, 193, 241. *Costa* (2005): Stars no. 17, 38, 92, 133. *Costa* (2006): Stars no. 344, 345. *Cvetkovic* (2011): Star no. 150. *Henry* (2006): Stars no. 24, 42, 61, 83, 197, 323. *Jao* (2005): Stars no. 11, 71, 158, 203, 206, 222, 288, 299, 312, 315, 348. *Jao* (2011): Stars no. 87, 289. *Koen* (2010): Stars no. 1, 10, 18, 22, 25, 31, 34, 35, 41, 43, 45, 47, 48, 60, 70, 74, 76, 78, 80, 82, 86, 88, 89, 91, 93, 94, 99, 105, 111, 112, 116-118, 123, 140, 141, 143, 145, 149, 151, 153, 157, 159, 161, 162, 167, 171, 173, 175, 177, 179, 181, 182, 188, 195, 196, 198, 199, 201, 210, 215, 216, 219, 220, 224, 227, 229, 230, 234, 236, 237, 239, 242, 244, 251, 253, 254, 257, 259, 261, 263-265, 268, 270, 273, 283, 285, 286, 296, 298, 304, 306-310, 313, 317, 319, 322, 324, 325, 331, 333, 335, 337, 338, 342, 346, 352, 353. *Lasker* (2008): Star no. 14. *Liebert* (2006): Stars no. 7, 231, 340. *Monet* (2003): Stars no. 3, 4, 5, 6, 9, 12, 13, 19, 21, 26, 28, 29, 30, 36, 37, 39, 40, 46, 49, 52, 53, 55, 56, 57, 58, 59, 62, 64, 65, 68, 72, 77, 79, 85, 90, 95, 96, 98, 100, 102, 104, 106-110, 113,114, 119-121, 124, 126, 127, 129, 130, 132, 135, 137, 138, 142, 144, 148, 152, 154-156, 160, 163-165, 169, 170, 172, 174, 176, 178, 187, 189, 191, 192, 194, 200, 202, 204, 205, 208, 211-213, 217, 221, 225, 226, 228, 232, 238, 245-248, 252, 255, 256, 258, 262, 266, 267, 269, 271, 272, 275-282, 291-295, 297, 300, 305, 320, 330, 332, 341, 343, 349-351, 354, 355. *Norton* (2007): Star no. 334. *Patterson* (1998): Star no. 168. *Reid* (2004): Stars no. 27, 69, 75, 81, 84, 103, 122, 185, 186, 190, 274, 287, 290, 301, 302. *Reid* (2007): Star no. 128. *Riedel* (2010): Stars no. 33, 51, 97, 101, 125, 147, 184, 218, 303, 314. *Wheatley* (2008): Stars no. 243, 250. *Zacharias* (2009): Stars no. 15, 20, 207, 209, 214, 223, 240, 249, 260, 284, 336.

[31] **G2V stars:** *Cutri* (2003): Star no. 9. *Koen* (2010): Stars no. 2, 4. *Monet* (2003): Stars no. 6, 7, 11, 14, 15, 17.

3.2.2 The I Band

Passband I is sensitive to radiation that ranges from 730-880 nm (*Reid & Hawley,* 2005). The M-type stars' apparent magnitudes in I were available for 326 stars and mainly taken from *Simbad* but also other catalogs. All available references[32] are cited below. The G2V stars' apparent magnitudes in I were available for 8 stars and taken from *Simbad*, referenced[33] below.

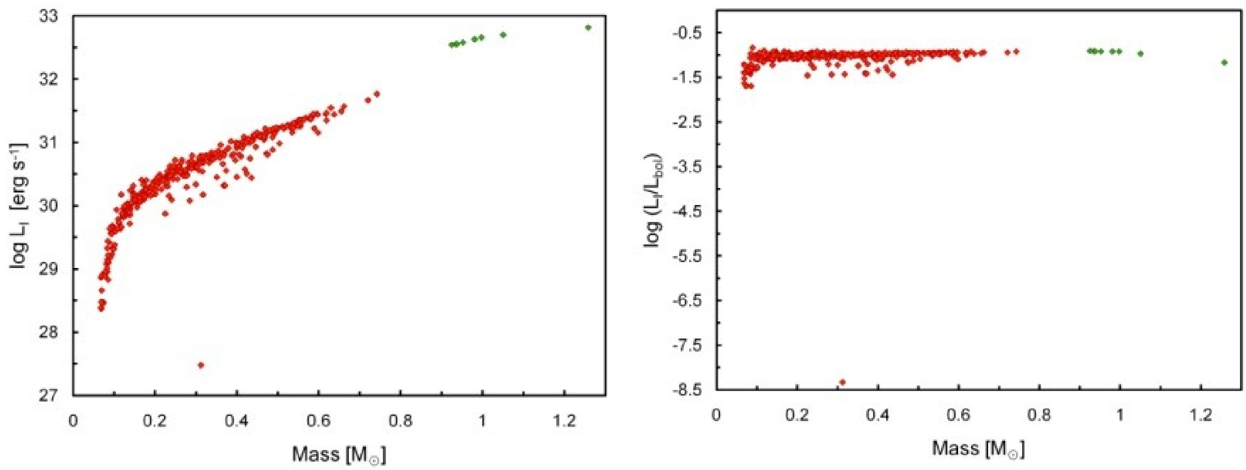

Figure 3.5. The relationship between mass and luminosity in passband I for the studied M and G stars sample in this work. M stars are marked red as the G stars are green.

Figure 3.5 illustrates that the break-point, that was at 0.2 $M_\odot$ in the visual passbands, has moved to stellar masses of about 0.1 $M_\odot$. Independent of the stellar mass and spectral type (M or G), the radiation amount in I compared to the bolometric remains at the same level except for stars with masses lower than 0.1 $M_\odot$, where a short decrease can be seen in Figure 3.5.

---

[32] **M stars:** *Casagrande* (2008): Stars no. 2, 32, 44, 136, 139, 146, 166, 183, 193, 241. *Costa* (2006): Stars no. 344, 345. *Cvetkovic* (2011): Star no. 150. *Henry* (2002): Star no. 38. *Henry* (2006): Stars no. 24, 42, 61, 83, 197, 323. *Jao* (2005): Stars no. 11, 71, 92, 158, 203, 206, 299, 315, 348. *Jao* (2011): Stars no. 87, 289. *Koen* (2010): Stars no. 1, 10, 18, 22, 25, 31, 34, 35, 41, 43, 45, 47, 48, 60, 70, 74, 76, 78, 80, 82, 86, 88, 89, 91, 93, 94, 99, 105, 111, 112, 116-118, 123, 140, 141, 143, 145, 149, 151, 153, 157, 159, 161, 162, 167, 171, 173, 175, 177, 179, 181, 182, 188, 195, 196, 198, 199, 201, 210, 215, 216, 219, 220, 224, 227, 229, 230, 234, 236, 237, 239, 242, 251, 253, 254, 257, 259, 261, 263-265, 268, 270, 273, 283, 285, 286, 296, 304, 306-310, 313, 317, 319, 322, 324, 325, 331, 333, 335, 337, 338, 342, 346, 352, 353. *Lasker* (2008): Star no. 15. *Leggett* (1992): Stars no. 52, 55, 121, 133, 134, 168, 170, 311, 329, 339. *Liebert* (2006): Stars no. 7, 231, 288, 340. *Monet* (2003): Stars no. 3, 5, 6, 9, 12, 13, 16, 19, 21, 28, 30, 36, 37, 39, 40, 46, 49, 53, 56-59, 62, 64, 65, 68, 72, 77, 85, 90, 95, 96, 98, 100, 102, 104, 106-110, 113, 114, 119, 124, 126, 127, 129, 132, 135, 142, 144, 152, 154-156, 160, 163-165, 172, 174, 176, 178, 187, 189, 191, 194, 200, 202, 204, 205, 208, 211, 212, 217, 221, 225, 226, 228, 232, 238, 245-248, 252, 255, 256, 258, 262, 266, 267, 269, 271, 272, 275-279, 281, 282, 291-295, 297, 300, 305, 320, 330, 332, 334, 341, 343, 349, 350, 354, 355. *Oppenheimer* (2001): Star no. 20. *Reid* (2004): Stars no. 27, 69, 75, 81, 84, 103, 122, 130, 185, 186, 190, 274, 287, 290, 301, 302. *Riedel* (2010): Stars no. 51, 97, 101, 125, 147, 184, 207, 218, 223, 303, 314. *Smart* (2007): Stars no. 4, 138, 169, 180, 192, 222, 336. *The Denise Consortium* (2005): Stars no. 14, 33, 209, 214, 240, 244, 249, 260, 284, 298, 312. *Wheatley* (2008): Star no. 250.

[33] **G2V stars:** *Koen* (2010): Stars no. 2, 4. *Monet* (2003): Stars no. 6, 7, 11, 14, 15, 17.

3.3 An Extension into the Near-Infrared

The passbands JHK are an extension of the Johnson UBV system to near-infrared wavelengths.

3.3.1 The J Band

Passband J is sensitive in the wavelength range from 1160-1350 nm (*Reid & Hawley,* 2005). The apparent magnitudes in J were available for all 355 M-type stars as well as for all 22 G2V stars and were taken from *Cutri et al.* (2003).

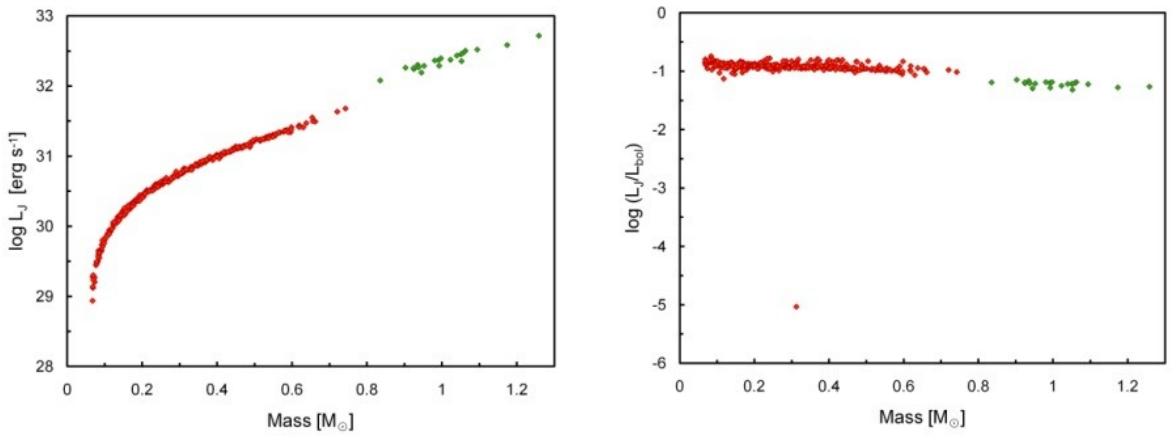

Figure 3.6. The relationship between mass and luminosity in passband J for the studied M and G stars sample in this work. M stars are marked red as the G stars are green.

In Figure 3.6 the M stars show almost no scatter or deviation along the curve, as this is to be expected in the H and K bands as well. This is due to the fact, that all measurements were obtained using the same instrumentation in the same mission, and the K band, which lies near resp. next to passbands J and H, was used to determine the stellar masses for all M stars. The luminosity ratio in the right diagram illustrates the opposite behavior as in the previous passbands, UBVRI, namely a negative slope. Going redwards the Sun-like stars, G2V, for the first time show a smaller fraction of total luminosity in this passband than all M stars in the sample. All in all the luminosity ratio demonstrates, that with increasing stellar masses the luminosity in J as a fraction of the bolometric decreases.

3.3.2 The H Band

Passband H is sensitive to wavelength ranges from 1490-1800 nm (*Reid & Hawley,* 2005). The apparent magnitudes in H were available for all 355 M-type stars as well as for all 22 G2V stars and were taken from *Cutri et al.* (2003).

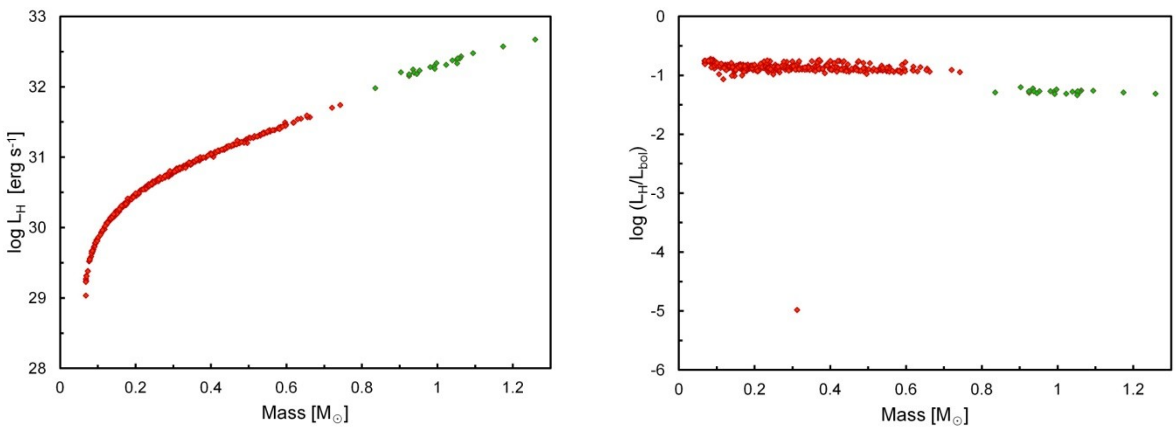

Figure 3.7. The relationship between mass and luminosity in passband H for the studied M and G stars sample in this work. M stars are marked red as the G stars are green.

As already mentioned in 3.3.1, Figure 3.7 shows a smooth curve with almost no scatter as was expected. The gap between red dwarfs and Sun-like stars would be the position for stars of spectral type K as well as for mid- and late-type G stars. Despite this gap, it can clearly be seen that the G2V stars' luminosity in H follows exactly along the same curve defined by the M stars.

As opposed to previous luminosity ratio diagrams, the ratio of H band luminosity to bolometric shows a slight increase at the very end of the lower M star masses at 0.1 $M_\odot$. Figure 3.7 illustrates even clearer, that in passband H the G2V stars have a smaller fraction of total luminosity than the red dwarfs. This is in agreement with the well-known fact that red dwarfs are literally redder than yellow dwarfs and the chosen sample of M stars conforms perfectly with this fact.

3.3.3 The K Band

Passband K is sensitive for wavelength ranges between 2000-2300 nm (*Reid & Hawley,* 2005). The apparent magnitudes in K were available for all 355 M-type stars as well as for all 22 G2V stars and were taken from *Cutri et al.* (2003).

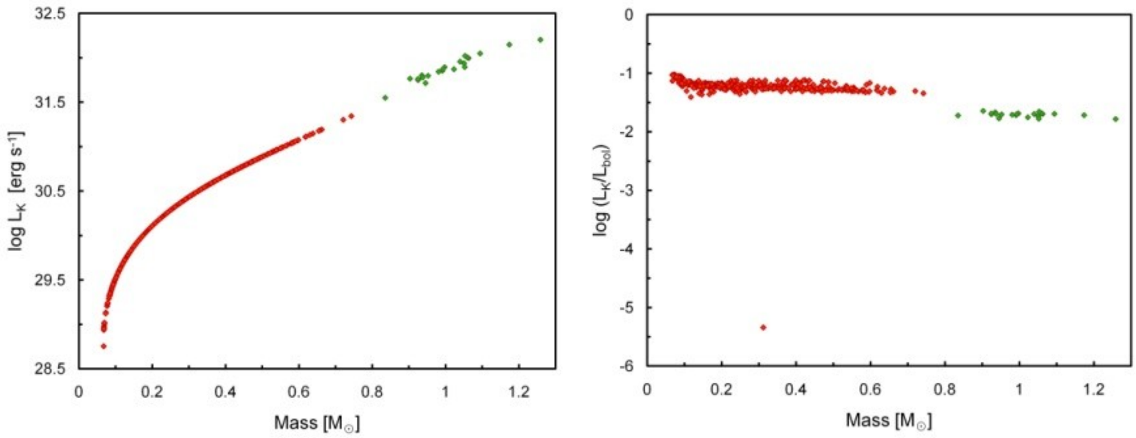

Figure 3.8. The relationship between mass and luminosity in passband K for the studied M and G stars sample in this work. M stars are marked red as the G stars are green.

Since the M star's masses were determined using the K band it was no surprise that the result of plotting stellar mass against luminosity in K revealed a smooth curve with no scatter at all (Figure 3.8, left diagram), while the G2V stars, calculated using a different method, show a little scatter. Nevertheless, the Sun-like stars follow the same direction that the M stars have shaped, demonstrating that the higher a star's mass the higher its luminosity in K. The right diagram illustrates results very similar to the previous luminosity ratio in passband H with a slight increase at 0.1 solar masses followed by a smooth trend for the M-type stars and a fractionally lower K versus bolometric luminosity ratio.

3.4 The Short-Wavelengths

The wavelength ranges NUV, FUV, EUV and X-ray are arranged at the bluer end of the visible spectrum and are short-wavelengths. Down from about 150 nm they become ionizing, which might impact habitable planetary atmospheres in different ways. For example, strong ionizing radiation could erode a planet's atmosphere through stellar winds. From all main sequence stars, M dwarfs are one of the most luminous at short-wavelengths (*Reid & Hawley,* 2005).

3.4.1 NUV - Near Ultraviolet

The NUV passband of *GALEX* is sensitive to radiation from 175-280 nm (*Hanslmeier,* 2009). All used values in NUV were given in AB magnitudes and taken from *GALEX*[34]. Altogether 200 values for the M stars' sample and 15 values for the G2V stars' sample were available.

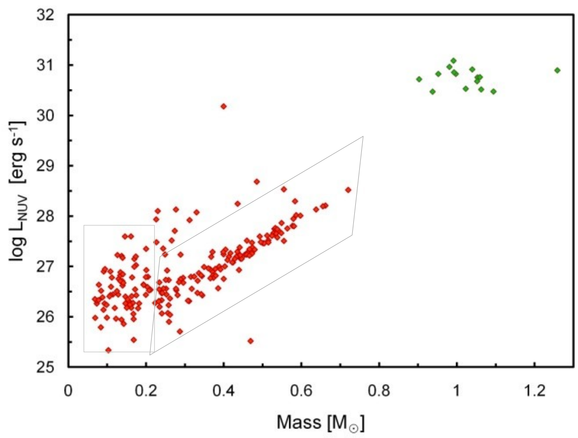

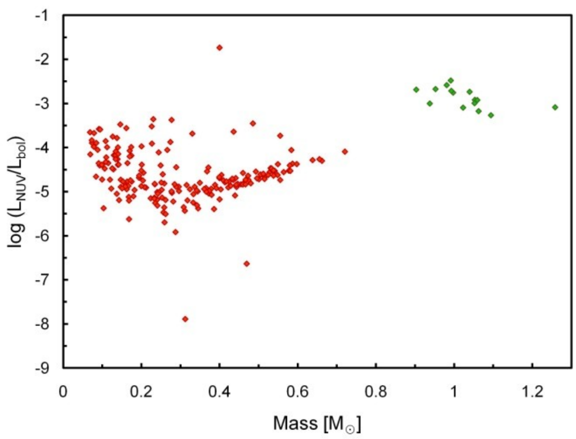

Figure 3.9. The relationship between mass and luminosity in passband NUV for the studied M and G stars sample in this work. M stars are marked red as the G stars are green.

In comparison to all previous passbands, NUV shows two differing groups of M stars (Figure 3.9, left diagram), which are separated at approximately 0.2 $M_\odot$. In the first group of very low mass stars there seems to be no apparent relationship between mass and radiation in NUV. The second group demonstrates a linear relationship with mass above which the stars in the first group show large scatter. This phenomenon is even more obvious in the diagram on the right.

[34] Data products see: http://galex.stsci.edu/ (Data release GR6)

The scattering above both groups could be caused by flaring events or general activity. Possible explanations for the existence of these two groups will be discussed later.

In Figure 3.9 the ratio of NUV to bolometric luminosity demonstrates that almost all M stars have lower values than the G2V stars. Even the most active M stars at very low mass, first group, show a lower ratio of about three times than all G stars in the sample. The M star outlier slightly above [-2] on the y-axis is most likely a measurement during a strong flaring event. As it is clear to which masses these two groups belong, it is necessary to inspect the corresponding spectral subtypes.

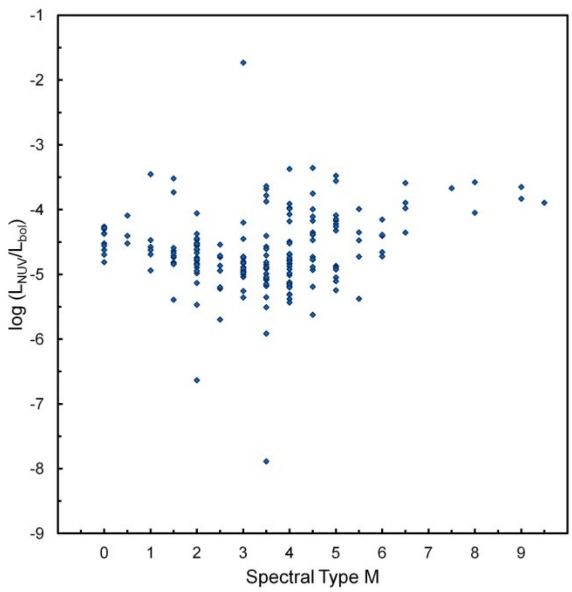

Figure 3.10. The relationship between spectral type and the NUV luminosity ratio defined by M stars from the sample.

Figure 3.10 illustrates the luminosity ratio in NUV versus the spectral subtype only for the M stars sample. Taking a closer look, it shows a transition around spectral class M4. From M0-M4 there is a downwards trend, but after the minimal turning point the curve increases strongly and even passes the highest NUV ratio level at M0. This leads to the presumption that the more massive early-type M stars belong to the second group from above. Those stars of the first group appear to belong to spectral types M3.5 and later, which exactly correlates with the stellar mass, where stars change from a radiative zone surrounded by a convective envelope to a fully convective energy transport.

The previous figures in NUV (Fig. 3.9 and Fig 3.10) showed different activity levels depending on mass and spectral subtype. To make a statement about activity changes during stellar evolution, age is a fundamental parameter.

Therefore, estimated stellar ages using different methods were plotted against the NUV luminosity ratio (Figure 3.11), which showed that there is a correlation between fractional NUV emission and stellar age. This can be seen for the ages estimated by chromospheric as well as by gyrochronological method, which are in good agreement, especially for ages above several million years. The G2V stars do not show such a behavior as they scatter around the same level through billions of years. However, this could be caused by the domination of the NUV flux by the photospheric emission or the uncertainties of the isochrone method discussed in chapter 1.4.3.

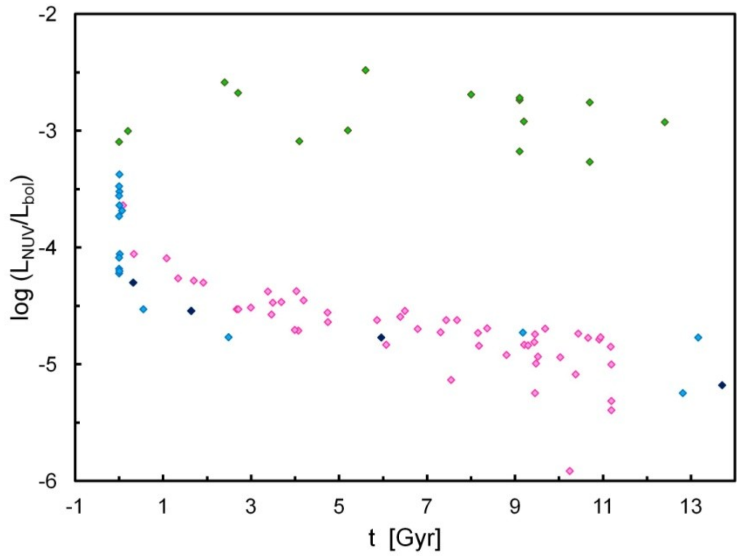

Figure 3.11. The relationship between age and NUV luminosity ratio. M star ages estimated by the chromospheric method are marked pink while the gyrochronological ages are illustrated in light and dark blue. The dark blue stars represent those that roughly fulfill the criteria given by *Barnes* (2007). G2V star ages estimated by the isochrone method are marked green.

3.4.2 FUV - Far Ultraviolet

The FUV passband from *GALEX* is sensitive in a wavelength range from 135-175 nm (*Hanslmeier,* 2009). All values in FUV were given in AB magnitudes and taken from *GALEX*[35]*.* Overall 92 values for the M and 15 values for the G2V stars were available.

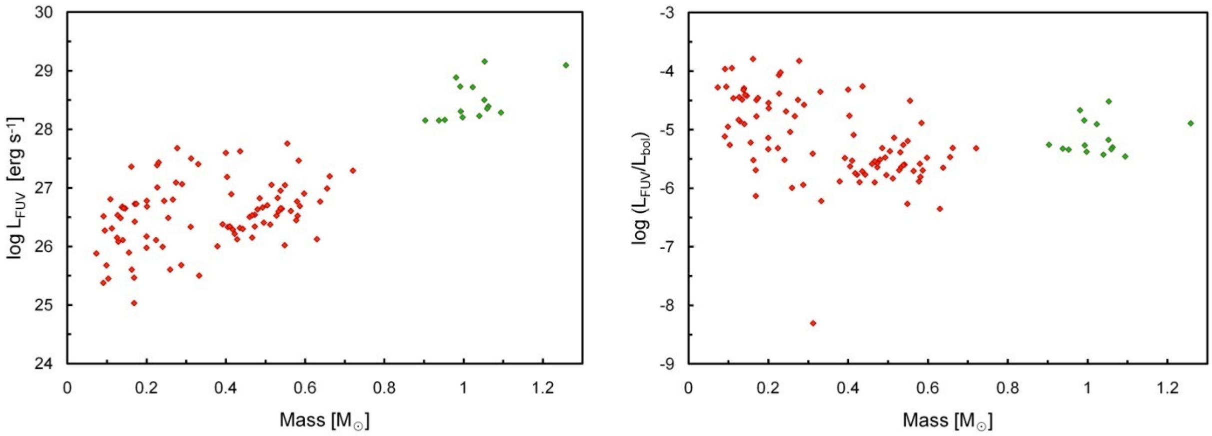

Figure 3.12. The relationship between mass and luminosity in passband FUV for the studied M and G stars sample in this work. M stars are marked red as the G stars are green.

Compared to the results in NUV, Figure 3.12 illustrates that the linear mass-luminosity relationship of the second group has dispersed. Still the presence of two groups in FUV with a separation at around 0.3 $M_\odot$ can be observed. Apparently at higher energy radiation there is a larger scatter when compared to lower energy bands, i.e. NUV and U.

The diagram on the right of fig. 3.12 demonstrates a higher FUV emission for lower mass stars, which decreases with increasing stellar mass. At this wavelength G stars and less active M stars scatter around the same level.

Due to a lack of data in FUV for stars later than M6 it is difficult to demonstrate the presumption of two existing groups with different activity levels based on spectral type (Figure 3.13). Nevertheless, a trend starting between M3.5 and M4 can be noticed, where later stars seem to be more active in FUV.

[35] Data products see: http://galex.stsci.edu/ (Data release GR6)

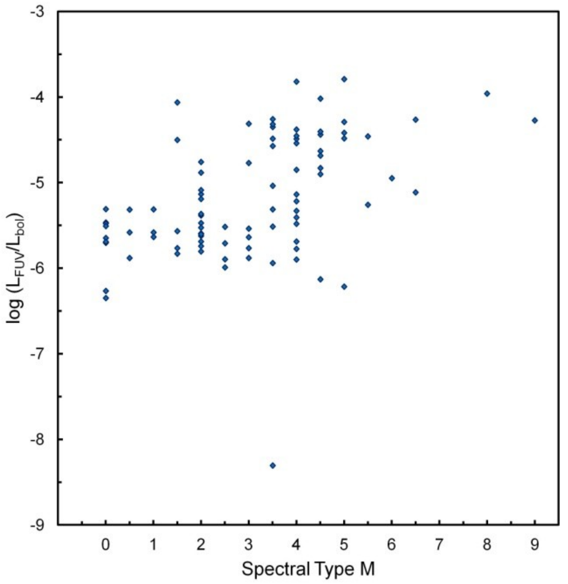

Figure 3.13. The relationship between spectral type and the FUV luminosity ratio defined by M stars from the sample.

Concerning FUV emission over time, Figure 3.14 illustrates that there is a very high activity for stars younger than 500 million years. Older stars appear to be less active in FUV. A reason for this could be that estimating stellar ages by the chromospheric method requires measurements of the Ca II K line, which lies within the bluer end of passband B. As demonstrated in Figure 3.2, the B luminosity of low mass (< 0.2 $M_\odot$) stars is very faint und thus could be a reason why/that there are no measurements of Ca II K for these stars.

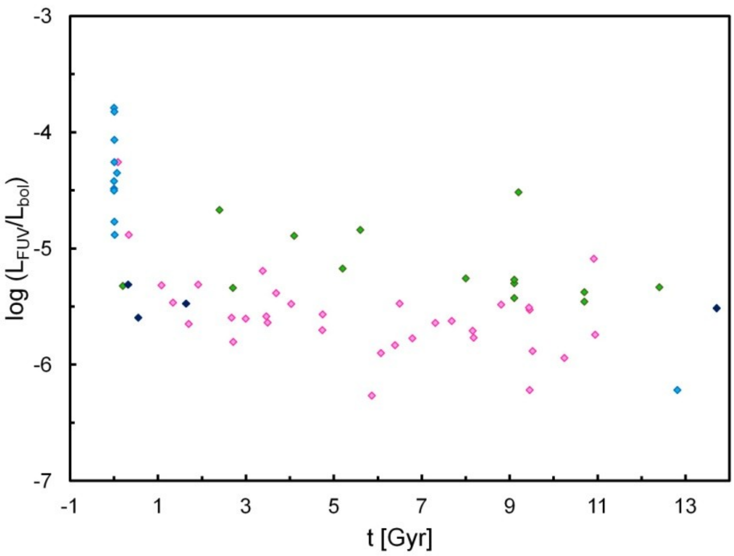

Figure 3.14. The relationship between age and FUV luminosity ratio. M star ages estimated by the chromospheric method are marked pink while the gyrochronological ages are illustrated in light and dark blue. The dark blue stars represent those that roughly fulfill the criteria given by *Barnes* (2007). G2V star ages estimated by the isochrone method are marked green.

In fact, when plotting the stellar masses against chromospheric ages (Figure 3.15) it showed that there is a mass-age dependence. Whether this has to do with limitations of the chromospheric method or that only for young early-type M stars, ages can be determined as their activity is lower than that of later-type M stars anyway and even decreases further with increasing age.

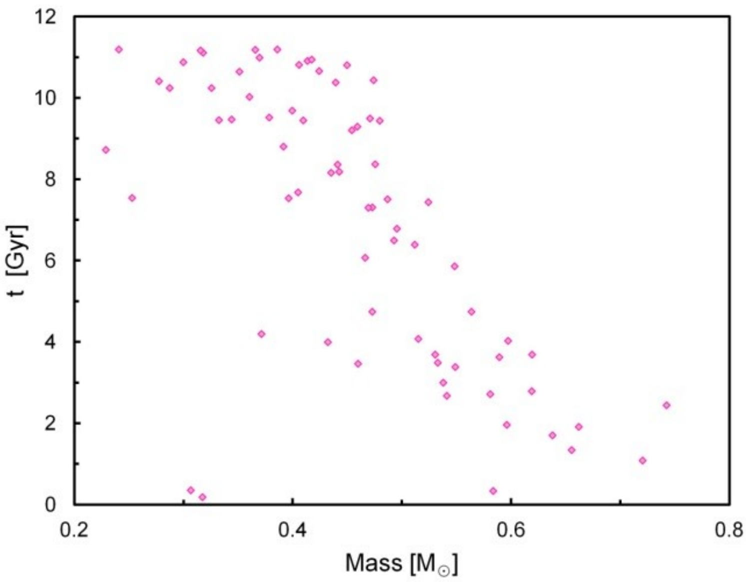

Figure 3.15. The relationship between mass and chromospheric age of the here studied M stars' sample.

Another rather unlikely explanation could be a gradient in stellar evolution within 15 pc of the Sun, namely that there are only young early-type and old late-type M stars. However, the comparison between M and G stars illustrates (Figure 3.14), that Sun-like stars have higher FUV emissions than coeval red dwarfs.

3.4.3 EUV - Extreme Ultraviolet

The passbands in EUV are sensitive in wavelength ranges from 5.8-17.4 nm (Lexan/B *EUVE*) (*Christian et al.,* 1999) and 6.0-14.0 nm (S1 *ROSAT*) (*Pye et al.,* 1995). All EUV values were given in counts per second and mainly taken from the EUV Master Catalog[36], supplemented with the catalog from *Hodgkin & Pye* (1994) .

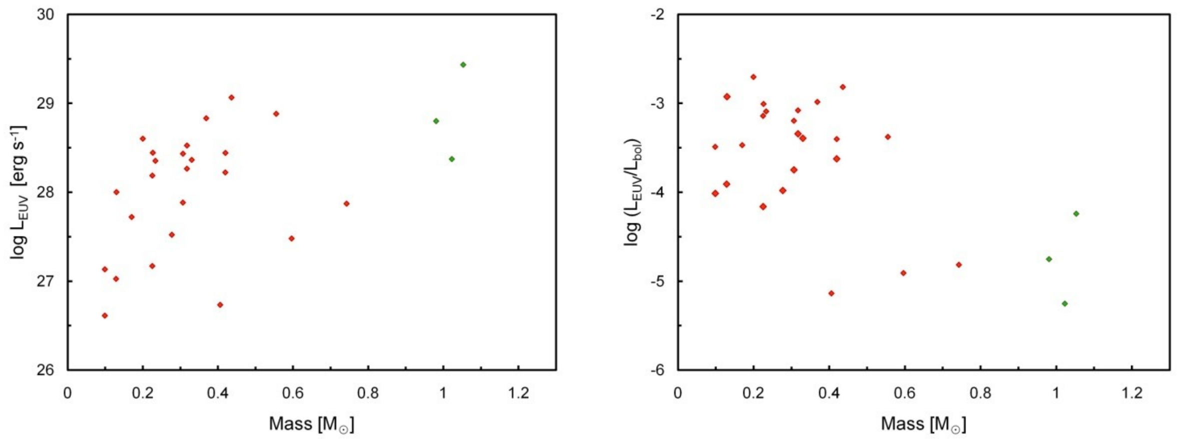

Figure 3.16. The relationship between mass and luminosity in passband EUV for the studied M and G stars sample in this work. M stars are marked red as the G stars are green.

As there were very few measurements in EUV available for the complete sample, it is difficult to draw a conclusion. Nevertheless, Figure 3.16 in EUV shows the same existence of two groups as the other short-wavelengths did before. One being more active at lower masses and another with lower activity at higher masses. However, in the second group there are only three data points. This might be due to the limits of the instruments' sensitivity as stars in this sample later than M6.5 have no corresponding EUV data (see Figure 3.17). These three stars in the lower activity group belong to early-type M stars as Figure 3.17 identifies.

Again, the M stars demonstrate a clearly higher activity than the G2V stars, except the lower activity group. Besides, this confirms the trend of lower mass M dwarfs radiating a comparatively higher fraction of their bolometric luminosity in the higher energy ranges than the G2V stars.

[36] The EUV Master Catalog is a compendium of seven catalogs from which the six following were used in this work: EUVEBSL (*Malina et al.* 1994), EUVECAT2 (*Bowyer et al.* 1996), ROSWFC2RE (*Pye et al.* 1995), ROSATXUV (*Kreysing et al.* 1995), EUVERAP2 (*Christian et al.* 1999) and EUVEXRTCAT (*Lampton et al.* 1997).

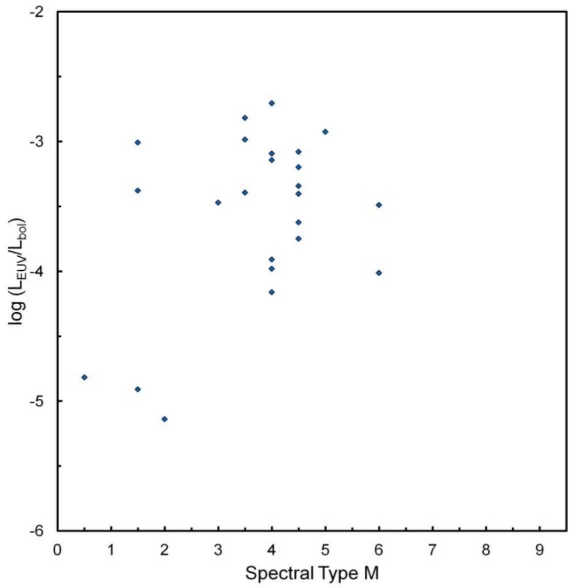

Figure 3.17. The relationship between spectral type and the EUV luminosity ratio defined by M stars from the sample.

Due to the lack of data in EUV almost no conclusion can be reached when studying age versus luminosity ratio (see Figure 3.18). The single statement that can be made without any doubts is that very young stars have a much higher EUV fraction than older stars in this sample.

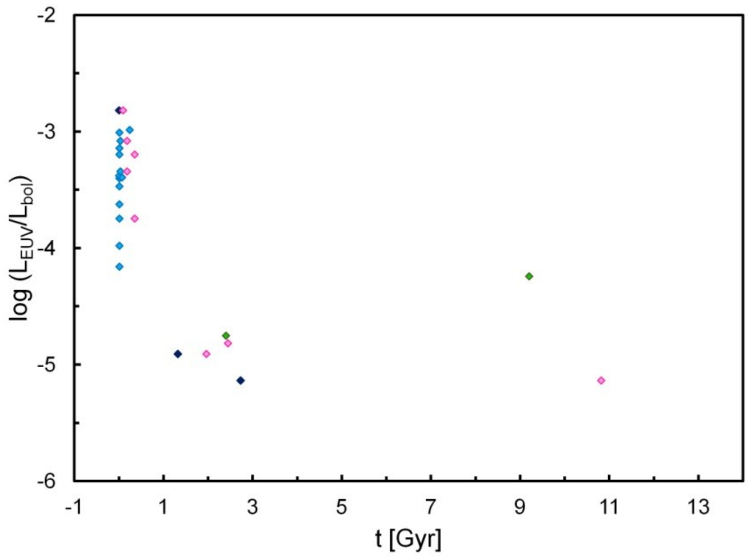

Figure 3.18. The relationship between age and EUV luminosity ratio. M star ages estimated by the chromospheric method are marked pink while the gyrochronological ages are illustrated in light and dark blue. The dark blue stars represent those that roughly fulfill the criteria given by *Barnes* (2007). G2V star ages estimated by the isochrone method are marked green.

3.4.4 X-ray

The X-ray detector from *ROSAT* (PSPC) is sensitive to a wavelength range from 0.52-12.4 nm (*Voges et al.,* 1999). The X-ray luminosities [erg s^{-1}] for the M stars' sample were already calculated and taken from *Odert* (2012, in preparation). The X-ray values [cts s^{-1}] for the G2V stars were derived from *ROSAT* bright and faint source catalogs (*Voges et al.,* 1999; *Voges et al.,* 2000) and available for 11 G2V stars.

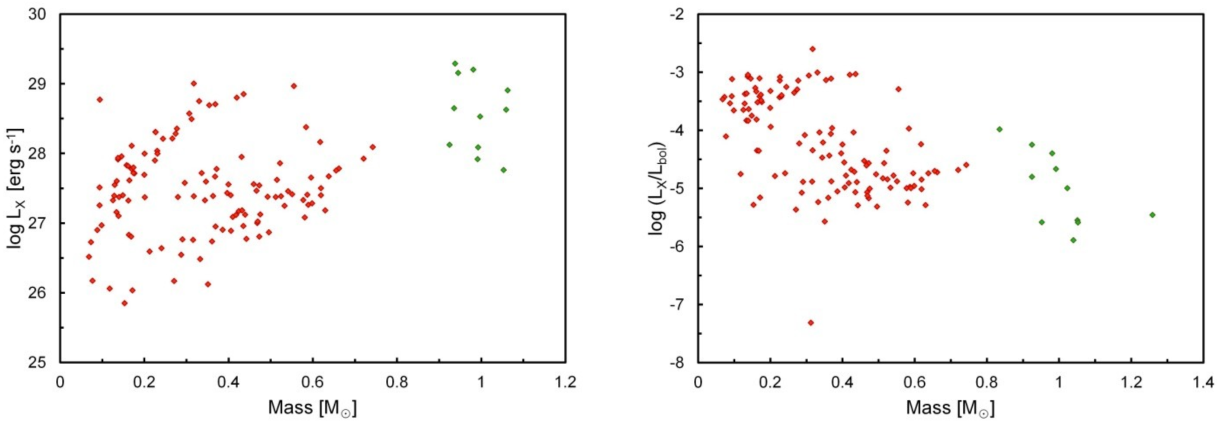

Figure 3.19. The relationship between mass and luminosity in X-ray wavelength for the studied M and G stars sample in this work. M stars are marked red as the G stars are green.

In the preceding mass-luminosity figures of short-wavelengths, the existence of two groups might have been difficult to notice. Coming to the shortest wavelength range studied in this work, X-ray, their existence can no longer be doubted. Taking a look at Figure 3.19, two strong concentrations of stars can be seen immediately and prove that the M stars in the here studied sample contain two groups of different activity.

Comparing stars of spectral type M and G, it shows that many M-type stars have a much higher energy output at X-ray wavelengths relative to their bolometric, especially those at the lower mass end. *Reid & Hawley* (2005) claim that X-ray luminosity when compared to the visual (L_X/L_V) can reach a ratio of 10% in M dwarfs and this is about 1000 times higher than the G star ratio. Figures 3.3 and 3.19, when compared, perfectly confirm this statement. *Kiraga & Stépien* (2007) state that the most active M-type stars show a ratio of L_X/L_{bol} of about 10^{-3}, which is in very good agreement with Fig. 3.19, right diagram.

Concluding, it turns out that later-type M stars have a relatively higher coronal emission than G stars. This is also illustrated in Figure 3.20, where the spectral subtype is plotted against the luminosity ratio in X-ray wavelengths. Beginning at approximately M3.5 the stars almost exclusively belong to the higher activity group.

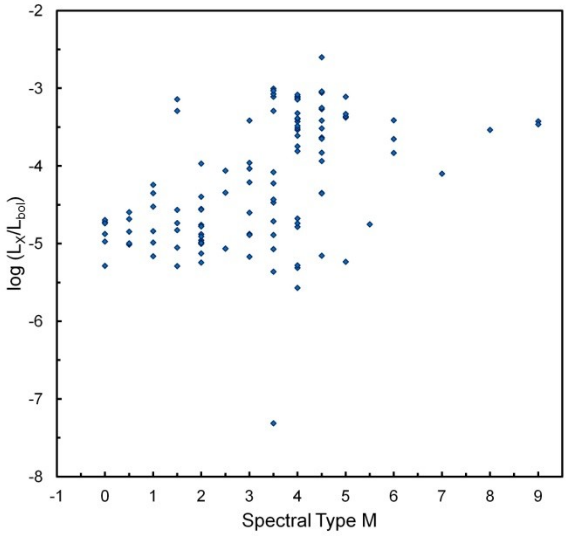

Figure 3.20. The relationship between spectral type and the X-ray luminosity ratio defined by M stars from the sample.

When comparing the X-ray luminosity ratio to age, there is no significant dependence observable at ages higher than a few hundred million years (Figure 3.21). In contrast to the previous age figures, the M and G stars scatter at the same levels.

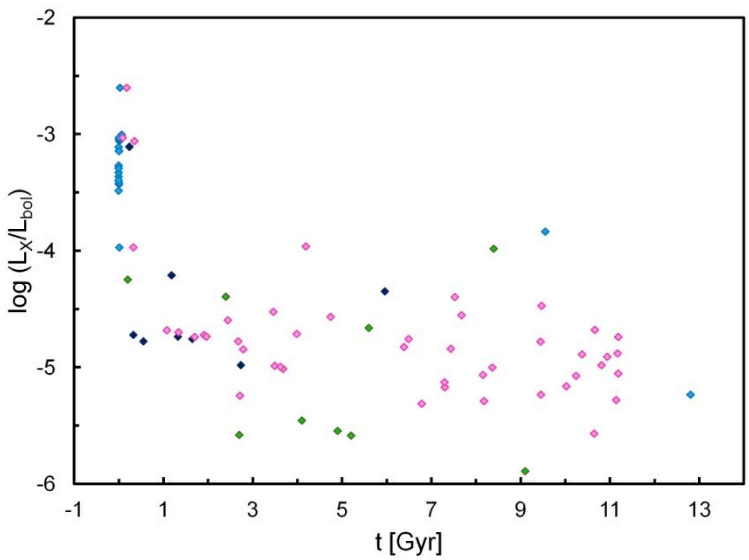

Figure 3.21. The relationship between age and X-ray luminosity ratio. M star ages estimated by the chromospheric method are marked pink while the gyrochronological ages are illustrated in light and dark blue. The dark blue stars represent those that roughly fulfill the criteria given by *Barnes* (2007). G2V star ages estimated by the isochrone method are marked green.

3.5 The Spectral Line Hα

The spectral line Hα is the strongest line of ionized hydrogen with a wavelength of 656.28 nm. When an electron falls from the third to the second lowest energy level, the Hα line emission occurs, emitting red light. To detect this released emission, special Hα filters or spectroscopy are used to visualize the structure of the chromosphere. The equivalent widths of Hα emission were available for 59 M stars and derived from several catalogs[37], referenced below. The surface fluxes in Hα for 10 G stars were found in several articles[38]. However, as the I band was needed to calculate Hα luminosities for the M stars (see section 2.2.5) and data was not available in this band for all stars with an equivalent width in Hα, only 52 M stars could be processed.

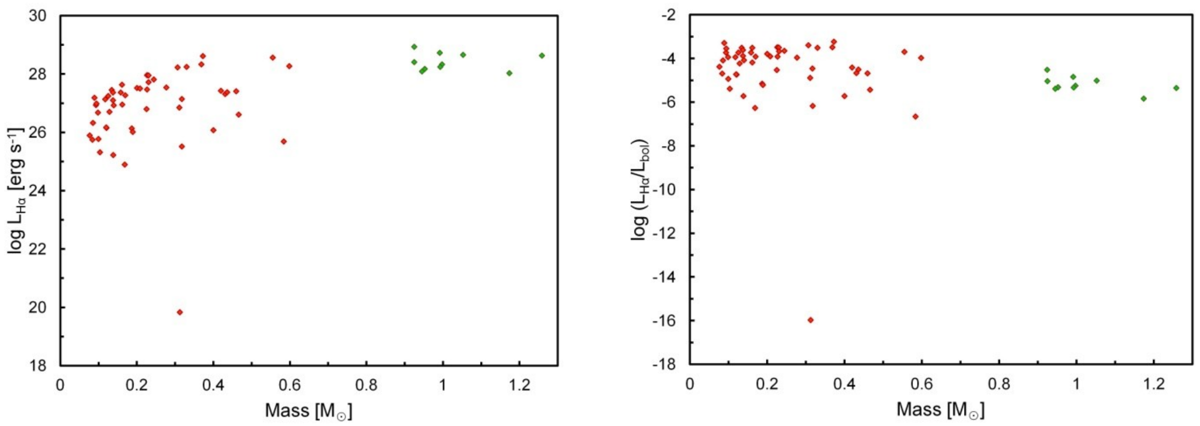

Figure 3.22. The relationship between mass and luminosity in Hα for the studied M and G stars sample in this work. M stars are marked red as the G stars are green.

The examination of the Hα emission of stars is of prime importance when trying to get information about a star's chromospheric activity. In the figures of the previous short-wavelength ranges two groups could be identified probably based on different activities. Looking at Figure 3.22, it seems that one group is missing. This can be easily explained as only the emission of Hα was studied, while stars with Hα in absorption were excluded.

[37] **M stars:** *Gizis et al.* (2002): Stars no.: 2, 18, 27, 30, 36, 40, 75, 83, 95, 108, 118, 119, 126, 132, 137, 168, 170, 173, 192, 194, 202, 218, 274, 275, 281, 283, 292, 294, 302, 320, 328, 347, 349, 351. *Mohanty & Basri* (2003): Stars no.: 231, 329. *Panagi & Mathioudakis* (1993): Stars no.: 181, 188, 196. *Shkolnik* et al. (2009): Stars no.: 26, 130, 176, 204, 237, 332, 334. *Walkowicz & Hawley* (2009): Stars no.: 88, 160, 163, 164, 198, 201, 250, 271. *West et al.* (2008): Stars no.: 67, 155, 253. *West et al.* (2011): Stars no.: 190, 233.

[38] **G2V stars:** *Herbig* (1985): Stars no.: 13, 14. *Lyra & Porto de Mello* (2005): Stars no.: 10, 12, 15, 18, 19, 21. *Martinez-Arnaiz et al.* (2010): Stars no.: 4, 7.

Further, it illustrates that the G2V stars are on the same level as the more active M stars' group, which is probably explained through taking measurements during or shortly after flaring events as G stars normally absorb in Hα and only emit during strong flares. When viewed against spectral subtype one can conclude that the vast majority of Hα emitting stars belong to M3 and later (Figure 3.23).

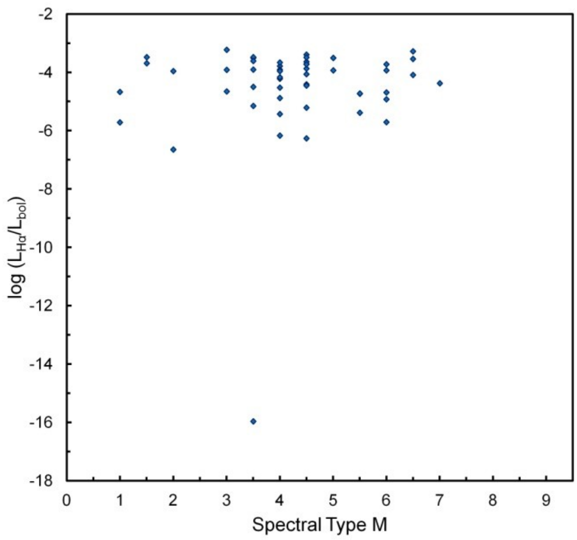

Figure 3.23. The relationship between spectral type and the Hα luminosity ratio defined by M stars from the sample.

Even the comparison with age (Figure 3.24) allows no significant statement of Hα evolution with age, as there were too few stars with Hα emission and corresponding age available.

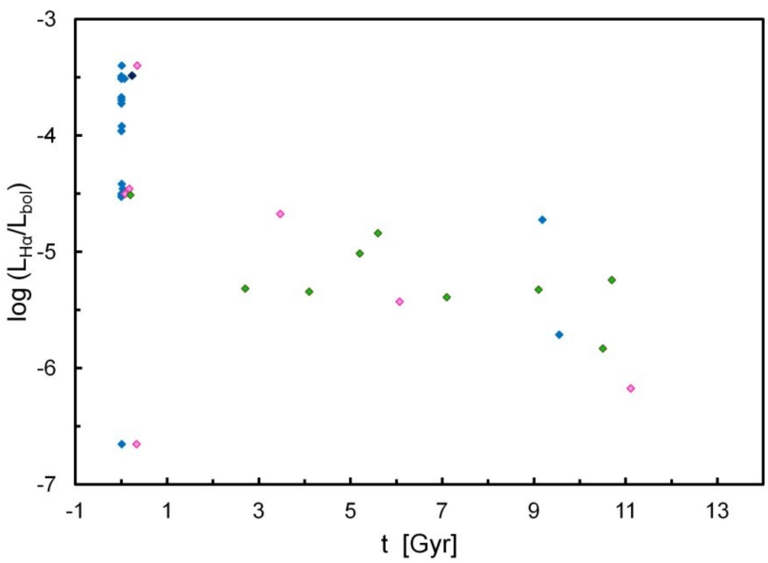

Figure 3.24. The relationship between age and Hα luminosity ratio. M star ages estimated by the chromospheric method are marked pink while the gyrochronological ages are illustrated in light and dark blue. The dark blue stars represent those that roughly fulfill the criteria given by *Barnes* (2007). G2V star ages estimated by the isochrone method are marked green.

3.6 Why look far when the good is so NEAR?

The two groups of M dwarfs in this sample can be seen in NUV, FUV, EUV and X-ray wavelengths. These two groups seem to separate the sample into active late-type stars and inactive early-type stars. This could simply indicate the length of time necessary for late-type M dwarf star evolution. As an example, if the rate of star formation is independent of the subtype, then more stars of late-type will remain active before scaling down to less activity. A further explanation could be that at different times different subtypes formed. Also the two groups could have formed within a short period of time at some point in the past and evolve in different time frames.

Irrespective of these thoughts, there is a dramatic change in activity at or around the point at which the full-convective model begins, and this significant shift can only be explained by large differences in the periods of stellar evolution, with early-types taking hundreds of millions of years to reach a point when the activity scales down, whereas later types require billions of years.

The discussion above clearly shows how urgent an accurate age determination method is needed to estimate ages from very young up to very old M dwarfs precisely. All current age determinations existing for M-type stars do not achieve satisfying results as they are connected with too many limitations.

As there was a good agreement between chromospheric and gyrochronological ages in NUV (see Fig. 3.11), the idea of using NUV as an age proxy came to mind. Since a dependency between age, activity and mass seems to exist, it was attempted to find a color which would give satisfying results as an age proxy. Hence the K band was included as it was used to determine the stellar masses for the M stars' sample, and demonstrates a reverse relationship to mass compared to the NUV passband.

Searching through the literature did not show anything comparable to this idea besides one article by *Findeisen et al.* (2011), where NUV-J is used to predict ages. In their work very young stars from moving groups are chosen for calibration. This method was not tried on M-type stars but only on earlier spectral classes (B8-K5).

Findeisen et al. (2011) come to the conclusion that there exists a correlation between NUV flux and activity or age. However, they describe this effect as slight, particularly for stars older than 1 Gyr.

As opposed to *Findeisen et al.* (2011), the here presumed proxy demonstrates a correlation between NUV-K and chromospheric ages from hundreds of millions to billions of years (Figure 3.25). A correlation between activity and NUV-K can be seen in the short-wavelength ranges FUV and X-ray as well as in the emission line Hα. Due to a lack of data in EUV the existence of such a correlation could not be proved. However, it is believed that one exists as it is embedded between X-ray and FUV wavelengths.

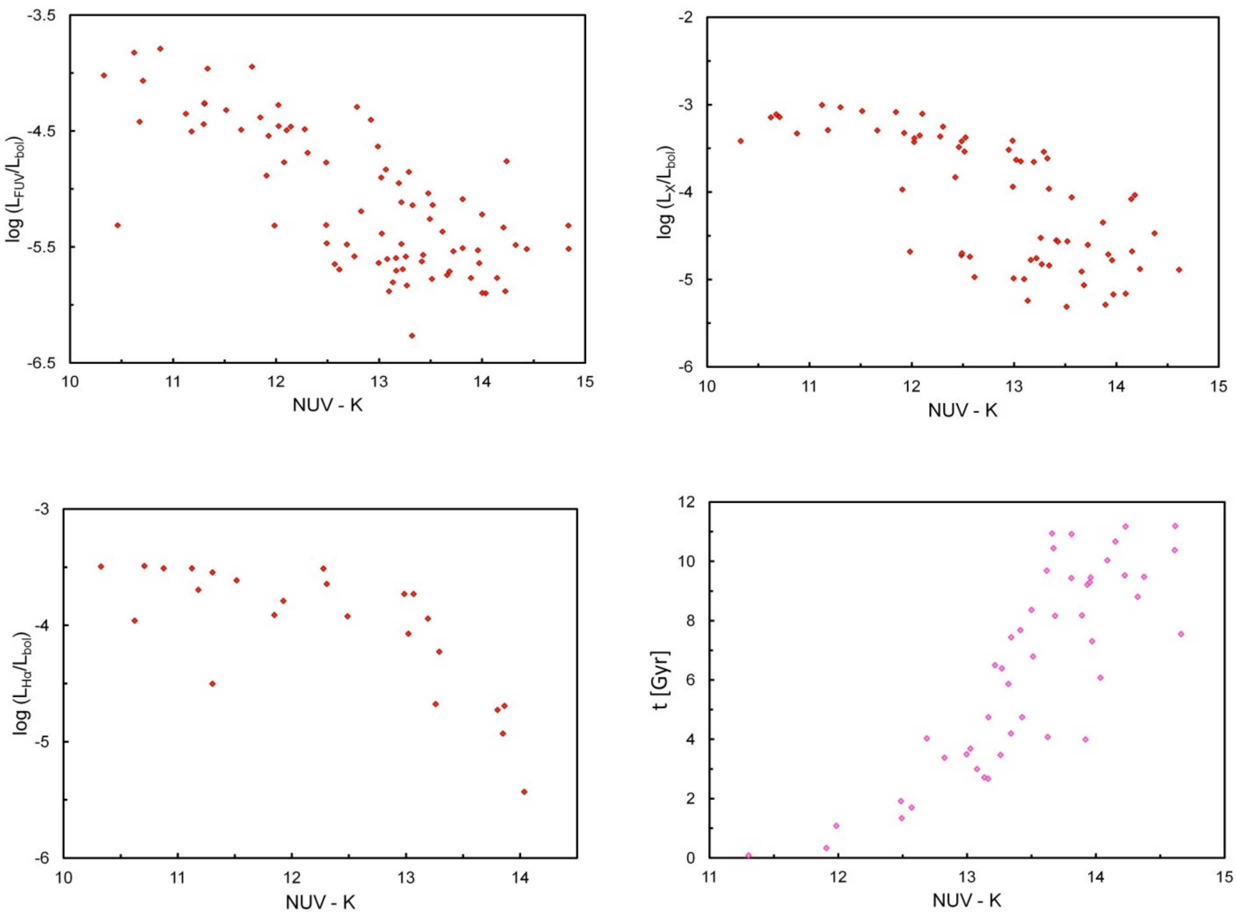

Figure 3.25. The relationship between NUV-K and the short-wavelengths FUV resp. X-ray as well as the spectral line Hα (upper diagrams and lower left). Lower right: Relationship between NUV-K and chromospheric ages. All data points are stars of the M stars' sample.

NUV emission can be related to the magnetic field of stars. *Vazquez & Hanslmeier* (2006) state that the largest proportion of chromospheric heating is accomplished by the magnetic fields of the star. Through heating of the chromosphere, UV radiation is emitted. These low energy wavelengths of UV radiation could be indicative of long-term heating of the chromosphere, since their generation does not require high energies as shorter wavelengths do. Therefore, NUV could be an indicator of long-term magnetic field strength in dwarf stars. Accounting for mass-specific influences, this could be a strong proxy of baseline magnetic field strength through activity and therefore age. Of course, this theory must be tested, e.g. with moving group ages.

4 Red Dwarfs as Host Stars

Already in the 1980's, the first extrasolar planets were discovered but wrongly classified as brown dwarfs. In 1992, the existence of two or more exoplanets orbiting the pulsar star PSR 1257+12 was published (*Wolszczan & Frail*, 1992). In 1995, the first exoplanet hosted by a Sun-like star was discovered by Michel Mayor and Didier Queloz using the radial velocity method (*Mayor & Queloz*, 1995). Since then the search for planets orbiting other stars than the Sun is one of the most pulsating topics in modern astronomy.

First the focus was laid on F, G and K stars, which means stars with spectral classes like the Sun, as well as one subclass up and down. Since more and more exoplanets have been found orbiting M-type stars - especially small, terrestrial planets - they finally have become targets for exoplanetary search missions and topic for theories discussing the possibility of a planet's habitability around such a red dwarf.

4.1 Habitability of Exoplanets Orbiting M-Type Stars

The importance of M dwarfs as host stars for habitable planets had been neglected for a long time as there were many considerations that argued against them.

The smaller a star, the closer is its habitable zone. Calculations for determining the extensions of habitable zones were made by *Kaltenegger et al.* (2010). Since M dwarfs have such low masses, their habitable zones are located much closer to the star. For spectral subtype M0, the perfect orbit for liquid water on a planet's surface is 0.1-0.35 AU and moves even closer to the host star with later M-types (*Tarter et al.,* 2007). M-type stars' habitable zones may remain stable clearly longer than the Solar System's HZ as the star does not change its luminosity significantly due to its slow evolution. Further, this means that a larger fraction of this zone is continuously habitable, wherein a planet could remain for up to 100 Gyr (*Tarter et al.*, 2007).

Despite this, one of the main concerns is the fact that planets orbiting their host stars at very close distances can become tidally locked.

This means that one side of the planet is always facing the host star receiving X-ray and UV emission over a long time scale and the other side is dark and cold. If water exists on the planet, then it is probably frozen on the nightside. *Tarter et al.* (2007) state that not all close-in planets become tidally locked, as a large initial eccentricity or a third body that perturbs the orbit could prevent the planet from becoming that.

Besides, different theories of heat transport and heat dissipation already exist, which attempt to explain how heat can be transported to the frozen side of the planet to become habitable (*Selsis et al.,* 2007). *Haberle et al.* (1996) presented a solution based on an energy-balance model. These authors argued that atmospheric heat-transport in the form of strong cloud coverage could prevent the planet's dark side from freezing. Further, they showed that a pure CO_2 atmosphere of 150 mbar could be sufficient to transport heat to the dark side of a tidally locked planet to maintain temperatures above the freezing point of CO_2. For liquid water 1-1.5 bar would be necessary.

Similar ideas derive from *Joshi & Haberle* (1997). They claim, that a dense and opaque atmosphere in the IR could transport heat to the dark side of the planet. Another method of heat transport, and thus preventing the planet's dark side from freezing, is the idea of a global ocean. Further, *Joshi et al.* (1997) presented a three-dimensional simulation of exoplanets' atmospheres, where it was attempted to estimate the climate of a tidally locked planet around an M-type star. Several factors were taken into account, for example the presence of clouds. In conclusion, *Joshi* (2003) claims that even synchronously rotating planets are suitable for life as long as they reside in the habitable zone around their host star.

But there is a further concern about tidally locked planets as it is not clear whether non-rotating planets can generate magnetic fields. *Lammer et al.* (2007) presumed that a reduced magnetic field can lead to the loss of the planetary atmosphere. This low magnetic moment, as well as the continuous impacts of CMEs experienced by the planet over a very long period of time, would lead to the exposure of these planets to a dense flow of CME plasma (*Khodachenko et al.,* 2007). This would cause strong erosion of the planet‘s atmosphere within the very close HZ of active M-type stars (*Khodachenko et al.,* 2007).

On the other hand, *Lammer et al*. (2007) claim that even weak magnetic moments of exoplanets can prevent major erosion of the atmosphere. Further, *Lammer et al.* (2007) state that an Earth-like exoplanet orbiting an M-type star with 0.5 $M_{\odot}$ can preserve its atmosphere if its orbit is less than or equal to 0.1 AU and the EUV radiation is not higher than 50-70 times that of the Sun. The crucial parameter for atmospheric loss is the EUV flux exposure as well as the thermal heating and expansion that would take place. Larger planets could be more effective at protecting their atmospheres against erosion (*Lammer et al*., 2007).

As M dwarfs are smaller than Sun-like stars, their protoplanetary disks are less massive. Therefore, it is expected that planets orbiting such stars are Neptune-sized and smaller (*Oshagh et al.,* 2010). Observations of protoplanetary disks have shown that M dwarfs also have such disks with sufficient material to form Earth-sized planets (*Andrews & Williams,* 2005). Nevertheless, it is not known whether small planets are preferably formed around M-type stars or more massive ones. Regardless of this discussion, with the current detection methods it should be easier to discover small planets around M-type stars than around stars of the more massive spectral classes.

Another concern besides tidal locking, is the magnetic activity which, among other things, becomes noticeable through heavily spotted surfaces, strong flares and powerful CMEs. M dwarfs are covered by much more starspots than Sun-like stars (e.g. *Reid & Hawley*, 2005). The heavy covering can lead to a radiation decrease of up to 40 % (*Joshi et al*., 1997) and an M star flare can double the incoming radiation in several wavelengths within minutes (*Tarter et al*., 2007, and references therein). During all these space weather phenomena, strong short-wavelength radiation is emitted and planets in the close-in habitable zone would be exposed to it.

This raises the question, how long the high activity period for M-type stars lasts. Although the magnetic dynamo is not fully understood, especially for fully convective stars, it is well-known that the level of activity and its duration depend on the stellar mass and further, that young stars are more likely to flare. That means, if focusing on early-type M stars with ages higher than one billion years, similar conditions to that of the young Sun could be expected.

Later-type M stars should be excluded as they show chromospheric activity levels too high, even at higher ages, as their magnetic dynamo scales down more slowly. This statement is also supported by different authors (e.g *Turnball & Tarter*, 2003). However, *Segura et al.* (2005) presume that atmospheric ozone could defuse the strong radiation coming from flaring events and this ozone can be produced abiotically.

So if we want to say something about a planet's habitability, it is crucial to understand the effects of space weather. The magnetic dynamo has to be understood and also the size of a star's astrosphere has to be taken into account, which turns out to be very complicated, as even the precise extensions of the heliosphere are not yet known.

Discussing the pros and cons of M-type stars as hosts for habitable planets, it must not be forgotten how adaptable life is to the extremest conditions. On earth such organisms are called extremophiles and biologists are surprised each time anew when unknown species existing under incredible conditions are discovered. Several exoplanetary search missions require lists for so-called "Habstars", in which all nearby early M-type stars with ages higher than one billion years should be absolutely included.

4.2 M-Type Stars of this Sample Hosting Exoplanets

Since 1995, there exists an online catalog which is called “The Extrasolar Planets Encyclopaedia” by Jean Schneider[39]. It contains 716 exoplanets[40], which were detected either by radial velocity, astrometry, transit, microlensing, imaging or timing method. Within this catalog 14 of the 355 M stars in this sample are listed to date as host stars with a total number of 21 exoplanets.

The following table (Table 4.1) lists the names of these stars, the stars' spectral subtypes as well as the number of so far detected orbiting planets.

[39] www.exoplanet.eu

[40] January 14th, 2012

Table 4.1: Exoplanets

Star	SpT	Planets	No. in Tab. 2.1
GJ 176	M2.0	1	78
GJ 179	M3.5	1	80
GJ 317	M3.5	2	131
GJ 433	M1.5	1	182
GJ 436	M3.5	1	186
GJ 581	M5.0	4	236
GJ 649	M2.0	1	251
GJ 674	M3.0	1	259
GJ 832	M1.5	1	313
GJ 849	M3.5	1	324
GJ 876	M5.0	4	335
GJ 1148	M4.0	1	185
GJ 1214	M4.5	1	256
HIP 79431	M3.0	1	244

Table 4.1: lists the stars of the here studied M stars' sample orbited by so far detected exoplanets.

5 Conclusion

The close proximity of M stars in this work, lying within a radius of 15 pc of the Sun, allowed the extensive study of even low mass M dwarfs in a wide wavelength range from X-ray to NIR. Further, it permitted the decrease of biases introduced by limitations in the detection of faint objects. This work attempted to characterize M-type stars over a large range of the electromagnetic spectrum, as well as a dependency of several activity indicators on age.

M-type stars make up the overwhelming majority of stars in the galaxy with lifetimes long enough for habitable conditions to form and life to evolve. Due to concerns about long periods of high activity and tidal locking of planets within the habitable zone, they were neglected for a long time, and exoplanetary search missions largely concentrated on the spectral classes FGK as host stars.

When considering the habitability of exoplanets, one must also consider the "hospitality" of the host star itself. In particular, the long period of initial high activity must be regarded and its potential to erode a planet's atmosphere, where due to tidal locking possibly no protective magnetic field exists.

West et al. (2008) and this work demonstrate that the long lifetimes of high activity in M stars may in fact not necessarily be long enough to erode a planetary atmosphere. Atmospheric erosion models for planets in the habitable zone around red dwarfs have shown this to be the case (*Lammer et al.,* 2009). In *West et al.* (2008) and here, data is presented that shows for at least the early-type M stars up to spectral subtype M3.5 that this lifetime may be about several hundred million years.

Actually, M stars should be treated as two separate groups when considering candidates for habitable exoplanet searches, namely early till mid-type and mid- till late-type stars. The border separating these two is the upper mass limit for a fully convective energy transport. This seems to be, from the data presented here, 0.3 $M_{\odot}$, if not in fact lower.

The first group of M dwarfs with short activity lifetimes has a mass range of 0.3-0.6 $M_{\odot}$, while the second group of high activity stars range from 0.08-0.3 $M_{\odot}$.

In all mass-luminosity diagrams in the UBVRIJHK passbands, there is an interesting transition beginning at 0.2-0.3 $M_{\odot}$. This transition can also be observed in the shorter wavelength ranges, X-ray, EUV, FUV and NUV and could be the mass limit for full convection.

All activity indicators plotted against ages demonstrate, at least for early and mid-type red dwarfs, a decrease of activity after several hundred million years. If these lifetimes are as low as shown, then the viability of these stars to host habitable planets has greatly increased, as well as the quantity of potential candidate stars. Therefore, it is very important to improve the age determination methods of early to mid-type M stars to allow an empirical study of their high activity lifetimes and evolution.

Currently, there are no age determination methods specifically for M-type stars. The here presented age proxy (NUV-K) could very well be of interest for at least early-type M dwarfs. Both chromospheric and gyrochronology age determination are hampered by limits even in the most massive M-type stars. As could be observed in Fig. 3.15, the chromospheric ages appear to be mass dependent, indicating the limits of this method.

Continued work must be done to improve the understanding of M-type dwarf evolution. Early and mid-type stars, a large portion of the masses of this spectral class, require more intensive study. Their viability for hosting habitable planets must be determined as their quantity in the galaxy and advantages for exoplanet discovery over more massive stars lend this class to closer examination. Further, much more work needs to be done to understand the transition between the dynamo generation in fully convective and interface stars.

Early-type M stars are extremely interesting in the search for Earth-sized planets in the habitable zones of their host stars.

They have several advantages in terms of mass and luminosity over their more massive relatives for current detection methods, and allow even direct imaging of candidate planets.

With the current exoplanet detection methods it is feasible to discover Earth-sized planets hosted by M stars. Within the coming years presumably many exoplanets around M stars will be discovered thanks to missions like CoRoT, Kepler, Gaia, TESS, PLATO and so on.

If enough importance is given to M-type stars, then the majority of terrestrial exoplanets will likely be discovered around red dwarfs. This also means that studying the influence of space weather phenomena on a planet's potential habitability cannot be taken seriously enough.

The present state of scientific and technical knowledge does not allow precise determination of several fundamental stellar parameters to make explicit predictions concerning the future evolution of red dwarfs. At the current age of the universe it seems that mid and late-type M stars are still too young to offer conditions for life as we know it as their activity and thus their radiation in certain wavelengths is far too strong. But we should always keep in mind that even M stars older than 10 Gyr are still very young compared to their expected lifetimes. Maybe one day, several billions of years in the future, when human beings will have disappeared from Earth and the Sun will have expanded to a red giant, a myriad of M-type stars could be host stars for other livable worlds.

6 Bibliography

Andrews, S.M., Williams, J.P. 2005. Circumstellar Dust Disks in Taurus-Auriga: The Submillimeter Perspective. ApJ 631, 1134.

Barnes, S.A. 2003. On the rotational evolution of solar- and late-type stars, its magnetic origins and the possibility of stellar gyrochronology. ApJ 586, 464.

Barnes, S.A. 2007. Ages for illustrative field stars using gyrochronology: viability, limitations, and errors. ApJ 669, 1167.

Bercik, D.J., Fisher, G.H., Johns-Krull, C.M., Abbett, W.P. 2005. Convective Dynamos and the Minimum X-ray Flux in Main-Sequence Stars. ApJ 631, 529.

Bessell, M.S. 1990. BVRI photometry of the Gliese catalogue stars. A&A Suppl. Ser. 83, 357.

Bidelman, W.P. 1985. G.P. Kuiper's spectral classifications of proper-motion stars. ApJ Suppl. Ser. 59, 197.

Bochanski, J.J., Hawley, S.L., West, A.A. 2011. The Sloan digital sky survey data release 7 spectroscopic M dwarf catalog. II. Statistical parallax analysis. AJ 141, 98.

Bopp, B.W., Africano, J.L., Stencel, R.E., Noah, P.V., Klimke, A. 1983. Observations of Active Chromosphere Stars. ApJ 275, 691.

Bowyer, S., Lampton, M., Lewis J., Wu, X., Jelinsky, P., Malina, R.F. 1996. The Second Extreme-Ultraviolet Explorer Source Catalog. ApJ 102, 129.

Browning, M.K., Basri, G., Marcy, G.W., West, A.A., Zhang, J. 2010. Rotation and magnetic activity in a sample of M-dwarfs. AJ 139, 404.

Carrasco, L., Franco, J., Roth, M. 1980. On the initial distribution and evolution of angular momentum for main sequence stars. A&A 86, 217.

Casagrande, L., Flynn, C., Bessell, M. 2008. M dwarfs: effective temperatures, radii and metallicities. MNRAS 389, 585.

Chabrier, G., Gallardo, J., Baraffe, I. 2007. Evolution of low-mass star and brown dwarf eclipsing binaries. A&A 472, L17.

Christian, D.J., Craig, N., Cahill, W., Roberts, B., Malina, R.F. 1999. The Second Extreme Ultraviolet Explorer Right Angle Program Catalog. AJ 117, 2466.

Costa, E., Mendez, R.A., Jao,W.-C., Henry, T.J., Subasavage, J.P., Brown, M.A., Ianna, P.A., Bartlett, J.2005. The Solar Neighborhood. XIV. Parallaxes from the Cerro Tololo Inter-American Observatory Parallax Investigation - First Results from the 1.5 m Telescope Program. AJ 130, 337.

Costa, E., Mendez, R.A., Jao, W.-C., Henry, T.J., Subasavage, J.P., Ianna, P.A. 2006. The Solar Neighborhood. XVI. Parallaxes from CTIOPI: Final Results from the 1.5 m Telescope Program. AJ 132, 1234.

Cutri, R.M., Skrutskie, M.F., Van Dyk, S., Beichman, C.A., Carpenter, J.M., Chester, T., Cambresy, L., Evans, T., Fowler, J., Gizis, J., Howard, E., Huchra, J., Jarrett, T., Kopan, E.L., Kirkpatrick, J.D., Light, R.M., Marsh, K.A., McCallon, H., Schneider, S., Stiening, R., Sykes, M., Weinberg, M., Wheaton, W.A., Wheelock, S., Zacarias, N. 2003. 2MASS All Sky Catalog of point sources. CDS/ADC Collection of Electronic Catalogues 2246, 0.

Cvetkovic, Z. 2011. Four first and two recalculated orbits for binaries. AJ 141, 116.

Delfosse, X., Forveille, T., Perrier, C. 1998. Rotation of Field M Dwarfs. ASP Conference Series 134, 102.

Delfosse, X., Forveille, T., Ségransan, D., Beuzit, J.-L., Udry, S., Perrier, C., Mayor, M. 2000. Accurate masses of very low mass stars IV. Improved mass-luminosity relations. A&A 364, 217.

Donahue, R.A. 1998. Stellar Ages Using the Chromospheric Activity of Field Binary Stars. ASP Conference Series 154, 1235.

Duric, N. 2004. Advanced Astrophysics. Cambridge University Press.

Ehrenreich, D., Desert, J.-M. 2011. Mass-loss rates for transiting exoplanets. A&A 529A, 136.

Endl, M., Cochran, W.D., Kurster, M., Paulson, D.B., Wittenmyer, R.A., MacQueen, P.J., Tull, R.G. 2006. Exploring the frequency of close-in Jovian planets around M dwarfs. ApJ 649, 436.

Faherty, J.K., Burgasser, A.J., Cruz, K.L., Shara, M.M., Walter, F.M., Gelino, C.R. 2009. The brown dwarf kinematics project I. Proper motions and tangential velocities for a large sample of late-type M, L, and T dwarfs. AJ 137, 1.

Findeisen, K., Hillenbrand, L., Soderblom, D. 2011. Stellar activity in the Broad-Band Ultraviolet. AJ 142, 23.

Flower, P.J. 1996. Transformations from Theoretical Hertzsprung-Russell Diagrams to Color-Magnitude Diagrams: Effective Temperatures, B-V Colors, and Bolometric Corrections. AJ 469, 355.

Gizis, J. E., Reid, I. N., Hawley, S. L. 2002. The Palomar/MSU Nearby Star Spectroscopic Survey. III. Chromospheric Activity, M Dwarf Ages, and the Local Star Formation History. AJ 123, 3356.

Golimowski, D.A., Leggett, S.K., Marley, M.S., Fan, X., Geballe, T.R., Knapp, G.R., Vrba, F.J., Henden, A.A., Luginbuhl, C.B., Guetter, H.H., Munn, J.A., Canzian, B., Zheng, W., Tsvetanov, Z.I., Chiu, K., Glazebrook, K., Hoversten, E.A., Schneider, D.P., Brinkmann, J. 2004. L' and M' Photometry of Ultracool Dwarfs. AJ 127, 3516.

Gray, R.O., Corbally, C.J., Garrison, R.F., McFadden, M.T., Bubar, E.J., McGahee, C.E., O'Donoghue, A.A., Knox, E.R. 2006. Contributions to the nearby stars (NStars) project: spectroscopy of stars earlier than M0 within 40 pc--The southern sample. AJ 132, 161.

Gurzadyan, G.A. 1970. On some Properties of Flare Stars in Orion. Boletín de los Observatorios de Tonantzintla y Tacubaya 5, 263.

Haberle, R.M., McKay, C.P., Tyler, D., Reynolds, R.T. 1996. Can Synchronously Rotating Planets Support An Atmosphere? Circumstellar Habitable Zones, Proceedings of The First International Conference. Travis House Publications 1996, 29.

Hanslmeier, A. 2007. The sun and space weather. Vol. 347. Springer-Verlag.

Hanslmeier, A. 2009. Habitability and Cosmic Catastrophes. Springer-Verlag Berlin Heidelberg.

Hartmann, L.W., Noyes, R.W. 1987. Rotation and Magnetic Activity in Main-Sequence Stars. ARAA 25, 271.

Hawley, S.L., Gizis, J.E., Reid, I.N. 1996. The Palomar/MSU nearby star spectroscopic survey. II. The southern M dwarfs and investigations of magnetic activity. AJ 112, 2799.

Henry, T. J., Walkowicz, L.M., Barto, T.C., Golimowski, D.A. 2002. The Solar Neighborhood. VI. New Southern Nearby Stars Identified by Optical Spectroscopy. AJ 123, 2002.

Henry, T. J., Jao, Wei-Chun, Subasavage, J.P., Beaulieu, T. D., Ianna, P. A., Costa, E., Méndez, R. A. 2006. The Solar Neighborhood. XVII. Parallax Results from the CTIOPI 0.9 m Program: 20 New Members of the RECONS 10 Parsec Sample. AJ 132, 2360.

Herbig, G.H. 1985. Chromospheric Hα Emission in F8-G3 Dwarfs and its Connection with the T Tauri Stars. ApJ 289, 269.

Hodgkin, S.T., Pye, J.P. 1994. ROSAT Extreme Ultraviolet / EUV Luminosity Functions of Nearby Late Type Stars. MNRAS 267, 840.

Hog, E., Fabricius, C., Makarov, V.V., Urban, S., Corbin, T., Wycoff, G., Bastian, U., Schwekendiek, P., Wicenec, A. 2000. The Tycho-2 catalogue of the 2.5 million brightest stars. A&A 355, L27-30.

Holmberg, J., Nordström, B., Andersen, J. 2009. The Geneva Copenhagen Survey of the Solar Neighbourhood. III. Improved distances, ages, and kinematics. A&A 501, 941.

Houk, N., Cowley, A.P. 1975. Catalogue of two dimensional spectral types for the HD stars, Vol. 1. Michigan Spectral Survey, Ann Arbor, Dep. Astron., Univ. Michigan, 1, 0.

Irwin, J., Berta, Z.K., Burke, C.J., Charbonneau, D., Nutzman, P., West, A.A., Falco, E.E. 2011. On the Angular Momentum Evolution of Fully Convective Stars: Rotation Periods for Field M-dwarfs from the MEarth Transit Survey. AJ 727, 56.

Jao, W.C., Henry, T.J., Subasavage, J.P., Brown, M.A., Ianna, P.A., Bartlett, J.L., Costa, E., Méndez, R.A. 2005. The solar neighborhood. XIII. Parallax results from the CTIOPI 0.9 meter program: stars with μ > 1.0"/yr (MOTION sample). AJ 129, 1954.

Jao, W.C., Henry, T.J., Subasavage, J.P., Winters, J.G., Riedel, A.R., Ianna, P.A. 2011. The solar neighborhood. XXIV. Parallax results from the CTIOPI 0.9 M program: stars with μ > 1".0/yr (MOTION sample) and subdwarfs. AJ 141, 117.

Jenkins, J.S., Ramsey, L.W., Jones, H.R.A., Pavlenko, Y., Gallardo, J., Barnes, J.R., Pinfield, D.J. 2009. Rotational velocities for M dwarfs. AJ 704, 975.

Joshi, M.M., Haberle, R.M., Reynolds, R.T. 1997. Simulations of the Atmospheres of Synchronously Rotating Terrestrial Planets Orbiting M Dwarfs: Conditions for Atmospheric Collapse and the Implications for Habitability. Icarus 129, 450.

Joshi, M.M., Haberle, R.M. 1997. On the Ability of Synchronously Rotating Planets to Support Atmospheres. Astronomical and Biochemical Origins and the Search for Life in the Universe, IAU Colloquium 161, 351.

Joshi, M.M. 2003. Climate Model Studies of Synchronously Rotating Planets. Astrobiology 3, 415.

Kaltenegger, L., Eiroa, C., Ribas, I., Paresce, F., Leitzinger, M., Odert, P., Hanslmeier, A., Fridlund, M., Lammer, H., Beichman, C., Danchi, W., Henning, T., Herbst, T., Léger, A., Liseau, R., Lunine, J., Penny, A., Quirrenbach, A., Röttgering, H., Selsis, F., Schneider, J., Stam, D., Tinetti, G., White, G.J. 2010. Stellar Aspects of Habitability - Characterizing Target Stars for Terrestrial Planet-Finding Missions. Astrobiology 10, 103.

Karttunen, H., Kröger, P., Oja, H., Poutanen, M., Donner, K.J. 2007. Fundamental Astronomy. Springer.

Kasting, J.F., Whitmire, D.P., Reynolds, R.T. 1993. Habitable Zones around Main Sequence Stars. Icarus 101, 108.

Kharchenko N.V. 2001. All-sky Compiled Catalogue of 2.5 million stars (ASCC-2.5). Kinematika Fiz. Nebesn. Tel., 17, part no 5, 409 .

Khodachenko, M.L., Ribas, I., Lammer, H., Grießmeier, J.-M., Leitner, M., Selsis, F., Eiroa, C., Hanslmeier, A., Biernat, H.K., Farrugia, C.J., Rucker, H.O. 2007. Coronal Mass Ejection (CME) Activity of Low Mass M Stars as an Important Factor for the Habitability of Terrestrial Exoplanets. I. CME Impact on Expected Magnetospheres of Earth-Like Exoplanets in Close-In Habitable Zones. Astrobiology 7, 167.

Kiraga, M., Stepien, K. 2007. Age-Rotation-Activity Relations for M Dwarf Stars Based on ASAS Photometric Data. Acta Astronomica 57, 149.

Koen, C., Kilkenny, D., Van Wyk, F., Marang, F. 2010. UBV(RI)$_C$JHK observations of Hipparcos-selected nearby stars. MNRAS 403, 1949.

Kreysing, H.-C., Brunner, H., Staubert, R. 1995. A ROSAT XUV pointed phase source catalogue. A&A 114, 465.

Lammer, H., Lichtenegger, H.I.M., Kulikov, Y.N., Grießmeier, J.-M., Terada, N., Erkaev, N.V., Biernat, H.K., Khodachenko, M.L., Ribas, I., Penz, T., Selsis F. 2007. Coronal Mass Ejection (CME) Activity of Low Mass M Stars as an Important Factor for the Habitability of Terrestrial Exoplanets. II. CME - Induced Ion Pick Up of Earth-Like Exoplanets in Close-In Habitable Zones. Astrobiology 7, 185.

Lammer, H., Odert, P., Leitzinger, M., Khodachenko, M.L., Panchenko, M., Kulikov, Yu.N., Zhang, T.L., Lichtenegger, H.I.M., Erkaev, N.V., Wuchterl, G., Micela, G., Penz, T., Biernat, H.K., Weingrill, J., Stellar, M., Ottacher, H., Hasiba, J., Hanslmeier, A. 2009. Determining the mass loss limit for close-in exoplanets: what can we learn from the transit observations? A&A 506, 399.

Lampton, M., Lieu, R., Schmitt, J.H.M.M., Bowyer, S., Voges, W., Lewis, J., Wu, X. 1997. An All-Sky Catalog of Faint Extreme Ultraviolet Sources. ApJ 108, 545.

Lasker, B.M., Lattanzi, M.G., McLean, B.J., Bucciarelli, B., Drimmel, R., Garcia, J., Greene, G., Guglielmetti, F., Hanley, C., Hawkins, G., Laidler, V.G., Loomis, C., Meakes, M., Mignani, R., Morbidelli, R., Morrison, J., Pannunzio, R., Rosenberg, A., Sarasso, M., Smart, R.L., Spagna, A., Sturch, C.R., Volpicelli, A., White, R.L., Wolfe, D., Zacchei, A. 2008. The second-generation guide star catalog: description and properties. AJ 136, 735.

Law, N.M., Hodgkin, S.T., MacKay, C.D. 2008. The LuckyCam survey for very low mass binaries - II. 13 new M4.5-M6.0 binaries. MNRAS 384, 150.

Leggett, S.K. 1992. Infrared Colors of Low-Mass Stars. AJ Suppl. Ser. 82, 351.

Lépine S., Shara M.M. 2005. A catalog of northern stars with annual proper motions larger than 0".15 (LSPM-NORTH catalog). AJ 129, 1483.

Lépine, S., Thorstensen, J.R., Shara, M.M., Rich, R.M. 2009. New Neighbors: Parallaxes of 18 Nearby Stars Selected from the LSPM-North Catalog. AJ 137, 4109.

Liebert, J., Gizis, J.E. 2006. RI photometry of 2MASS-selected late M and L dwarfs. Publ. Astron. Soc. Pac. 118, 659.

Lopez-Santiago, J., Micela, G. Montes, D. 2009. Quantifying the contamination by old main-sequence stars in young groups: the case of the Local Association. A&A 499, 129.

Lyra, W., Porto de Mello, G.F. 2005. Fine structure of the chromospheric activity in Solar-type stars - The Hα line. A&A 431, 329.

Malina, R.F., Marshall, H.L., Antia, B., Christian, C.A., Dobson, C.A., Finley, D.S., Fruscione, A., Girouard, F.R., Hawkins, I., Jelinsky, P., Lewis, J.W., McDonald, J.S., McDonald, K., Patterer, R.J., Saba, W.W., Sirk, M., Stroozas, B.A., Vallerga, J.V., Vedder, P.W., Wiercigroch, A., Bowyer, S. 1994. Extreme Ultraviolet Explorer Bright Source List. AJ 107, 751.

Mamajek, E.E., Hillenbrand, L.A.. 2008. Improved age estimation for solar-type dwarfs using activity-rotation diagnostics. ApJ 687, 1264.

Martinez-Arnaiz, R., Maldonado, J., Montes, D., Eiroa, C., Montesinos, B. 2010. Chromospheric activity and rotation of FGK stars in the solar vicinity. A&A 520, 79.

Matt, S., Pudritz, R.E. 2008. Accretion-powered Stellar Winds. II. Numerical Solutions for Stellar Wind Torques. ApJ 678, 1109.

Mayor, M., Queloz, D. 1995. A Jupiter-mass companion to a solar-type star. Nature 378, 355.

Mermilliod, J. C. 2006. Homogeneous Means in the UBV System. VizieR On-line Data Catalog: II/168.

Mohanty, S., Basri, G. 2003. Rotation and Activity in Mid-M to L Field Dwarfs. ApJ 583, 451.

Monet, D.G., Levine, S.E., Canzian, B., Ables, H.D., Bird, A.R., Dahn, C.C., Guetter, H.H., Harris, H.C., Henden, A.A., Leggett, S.K., Levison, H.F., Luginbuhl, C.B., Martini, J., Monet, A.K.B., Munn, J.A., Pier, J.R., Rhodes, A.R., Riepe, B., Sell, S., Stone, R.C., Vrba, F.J., Walker, R.L., Westerhout, G., Brucato, R.J., Reid, I.N., Schoening, W., Hartley, M., Read, M.A., Tritton, S.B. 2003. The USNO-B catalog. AJ 125, 984.

Montes, D., Lopez-Santiago, J., Galvez, M.C., Fernandez-Figueroa, M.J., De Castro, E., Cornide, M. 2001. Late-type members of young stellar kinematic groups - I. Single stars. MNRAS 328, 45.

Mullan, D.J. 1974. Starspots on Flare Stars. ApJ 192, 149.

Norton, A.J., Wheatley, P.J., West, R.G., Haswell, C.A., Street, R.A., Collier Cameron, A., Christian, D.J., Clarkson, W.I., Enoch, B., Gallaway, M., Hellier, C., Horne, K., Irwin, J., Kane, S.R., Lister, T.A., Nicholas, J.P., Parley, N., Pollacco, D., Ryans, R., Skillen, I., Wilson, D.M. 2007. New periodic variable stars coincident with ROSAT sources discovered using SuperWASP. A&A 467, 785.

Noyes, R.W., Hartmann, L.W., Baliunas, S.L., Duncan, D.K., Vaughan, A.H. 1984. Rotation, convection, and magnetic activity in lower main-sequence stars. ApJ 279, 763.

Odert, P., Leitzinger, M., Hanslmeier, A., Lammer, H., Khodachenko, M.L., Ribas, I. 2010. M-Type Stars as Hosts for Habitbale Planets: Ages of Nearby M Dwarfs. Cent. Eur. Astrophys. Bull. 34, 129.

Odert, P. 2012 (in preparation). Activity of M-type stars and the influence on planetary atmospheres. PhD Thesis, University of Graz.

Oja, T. 1985. Photoelectric photometry of stars near the North Galactic Pole. II. A&A Suppl. Ser. 61, 331.

Oja, T. 1991. UBV photometry of stars whose positions are accurately known. VI. A&A Suppl. Ser. 89, 415.

Oke, J.B. 1974. Absolute Spectral Energy Distributions for White Dwarfs. ApJS 27, 21.

Oppenheimer, B.R., Hambly, N.C., Digby, A.P., Hodgkin, S.T., Saumon, D. 2001. Direct detection of Galactic halo dark matter. Science 292, 698.

Oshagh, M., Haghighipour, N., Santos, N.C. 2010. A survey of M stars in the field of view of Kepler space telescope. Proceedings of the International Astronomocial Union 6, 448.

Panagi, P. M., Mathioudakis, M. 1993. The importance of surface inhomogeneities for K and M dwarf chromospheric fluxes. A&A Suppl. Ser. 100, 343.

Parker, E.N. 1955. Hydromagnetic Dynamo Models. ApJ 122, 293.

Parker, E.N. 1993. A solar dynamo surface wave at the interface between convection and nonuniform rotation. ApJ 408, 707.

Patterson, R.J., Ianna, P.A., Begam, M.C. 1998. The Solar Neighborhood. V. VRI Photometry of Southern Nearby Star Candidates. AJ 115, 1648.

Pettersen, B.R. 1980. Starspots and the rotation of the flare star EV Lac. AJ 85, 871.

Pizzolato, N., Maggio, A., Micela, G., Sciortino, S., Ventura, P. 2003. Activity-rotation Relationship: Interpretation of an X-ray Derived Rossby Number. The Future of Cool-Star Astrophysics: 12th Cambridge Workshop on Cool Stars, Stellar Sytems, and the Sun, eds. Brown, A., Harper, G.M. Ayres, T.R. 2003, 887.

Pye, J.P., McGale, P.A., Allan, D.J., Barber, C.R., Bertram, D., Denby, M., Page, C.G., Ricketts, M.J., Stewart, B.C., West, R.G. 1995. The ROSAT Wide Field Camera all-sky survey of extreme-ultraviolet sources – II. The 2RE Source Catalogue. MNRAS 274, 1165.

Reid, I.N., Hawley, S.L., Gizis, J.E. 1995. The Palomar/MSU nearby-star spectroscopic survey. I. The northern M dwarfs-band strengths and kinematics. AJ 110, 1838.

Reid, I.N., Cruz, K.L., Allen, P., Mungall, F., Kilkenny, D., Liebert, J., Hawley, S.L., Fraser, O.J., Covey, K.R., Lowrance, P., Kirkpatrick, J.D., Burgasser, A.J. 2004. Meeting the cool neighbors. VIII. A preliminary 20 parsec census from the NLTT catalogue. AJ 128, 463.

Reid, N., Hawley, S.L. 2005. New Light On Dark Stars: Red Dwarfs, Low Mass Stars, Brown Dwarfs. Chichester: Praxis Publishing.

Reid, I.N., Cruz, K.L., Allen, P.R. 2007. Meeting the cool neighbors. XI. Beyond the NLTT catalog. AJ 133, 2825.

Reiners, A., Basri, G. 2009. On the magnetic topology of partially and fully convective stars. A&A 496, 787.

Reyle, C., Scholz, R.-D., Schultheis, M., Robin, A.C., Irwin, M. 2006. Optical spectroscopy of high proper motion stars: new M dwarfs within 10 pc and the closest pair of subdwarfs. MNRAS 373, 705.

Riaz, B., Gizis, J.E., Harvin, J. 2006. Identification of new M dwarfs in the solar neighborhood. AJ 132, 866.

Riedel, A.R., Subasavage, J.P., Finch, C.T., Jao, W.-C., Henry, T.J., Winters, J.G., Brown, M.A., Ianna, P.A., Costa, E., and Rene A. Mendez. 2010. The Solar Neighborhood. XXII. Parallax Results from the CTIOPI 0.9 m Program: Trigonometric Parallaxes of 64 Nearby Systems with 0".5 ≤ μ ≤1".0 yr^{-1} (SLOWMO Sample). AJ 140, 897.

Samus, N.N., Goranskii, V.P., Durlevich, O.V., Zharova, A.V., Kazarovets, E.V., Kireeva, N.N., Pastukhova, E.N., Williams, D.B., Hazen, M.L. 2003. Astron. Lett. 29, 468.

Scalo, J., Kaltenegger, L., Segura, A., Fridlund, M., Ribas, I., Kulikov, J.N., Grenfell, JL., Rauer, H., Odert, P., Leitzinger, M., Selsis, F., Khodachenko, M.L., Eiroa, C., Kasting, J., Lammer, H. 2007. M Stars as Targets for Terrestrial Exoplanet Searches and Biosignature Detection. Astrobiology 7, 85.

Schmidt, S.J., Cruz, K.L., Bongiorno, B.J., Liebert, J., Reid, I.N. 2007. Activity and kinematics of ultracool dwarfs, including an amazing flare observation. AJ 133, 2258.

Schuh, S.L., Handler, G. Drechsel, H., Hauschildt, P., Dreizler, S., Medupe, R., Karl, C., Napiwotzki, R., Kim, S.-L., Park, B.-G., Wood, M.A., Paparó, M., Szeidl, B., Virághalmy, G., Zsuffa, D., Hashimoto, O., Kinugasa, K., Taguchi, H., Kambe, E., Leibowitz, E., Ibbetson, P., Lipkin, Y., Nagel, T., Göhler, E., Pretorius, M.L. 2003. 2MASS J0516288+260738: Discovery of the first eclipsing late K + Brown dwarf binary system? A&A 410, 649.

Segura, A., Kasting, J.F., Meadows, V., Cohen, M., Scalo, J., Crisp, D., Butler, R.A.H., Tinetti, G. 2005. Biosignatures from Earth-Like Planets Around M Dwarfs. Astrobiology 5, 706.

Selsis, F., Kasting, J.F., Levrard, B., Paillet, J., Ribas, I., Delfosse, X. 2007. Habitable Planets around the star Gliese 581? A&A 476, 1373.

Shkolnik, E., Liu, M.C., Reid, I.N. 2009. Identifying the young low-mass stars within 25 pc. I. Spectroscopic observations. ApJ 699, 649.

Simon, T., Drake, S.A., Kim, P.D. 1995. The X-Ray Emission of A-Type stars. PASP 107, 1034.

Skrutskie, M. F., Cutri, R. M., Stiening, M-D., Weinberg, M. D., Schneider, S., Carpenter, J. M., Beichman, C., Capps, R., Chester, T., Elias, J., Huchra, J., Liebert, J., Lonsdale, C., Monet, D. G., Pice, S., Seitzer, P., Jarrett, T., Kirkpatrick, J. D., Gizis, J., Howard, E., Evans, T., Fowler, J., Fullmer, L., Hurt, R., Light, R., Kopan, E. L., Marsh, K. A., McCallon, H. L., Tam, R., Van Dyk, S., Wheelock, S. 2006. The Two Micron All Sky Survey (2MASS). AJ 131, 1163.

Skumanich, A. 1972. Time Scales for Ca II Emission Decay, Rotational Braking, and Lithium Depletion. ApJ 171, 565.

Smart, R.L., Lattanzi, M.G., Jahreiss, H., Bucciarelli, B., Massone, G. 2007. Nearby star candidates in the Torino observatory parallax program. A&A 464, 787.

Soderblom, D.R. 2010. The Ages of Stars. ARAA 48, 581.

Soon, W.H., Baliunas, S.L., Zhang, Q. 1993. An Interpretation of Cycle Periods of Stellar Chromospheric Activity. ApJ 414, L33.

Space Telescope Science Institute; Osservatorio Astronomico di Torino. 2001. The Guide Star Catalog, Version 2.2 (GSC2.2). CDS/ADC Collection of Electronic Catalogues 1271, 0.

Strassmeier, K.G. 2009. Starspots. A&A Rev., 17, 251.

Tarter, J.C., Backus, P.R., Mancinelli, R.L., Aurnou, J.M., Backman, D.E., Basri, G.S., Boss, A.P., Clarke, A., Deming, D., Doyle, L.R., Feigelson, E.D., Freund, F., Grinspoon, D.H., Haberle, R.M., Hauck, II, S.A., Heath, M.J., Henry, T.J., Hollingsworth, J.L., Joshi, M.M., Kilston, S., Liu, M.C., Meikle, E., Reid, I.N., Rothschild, L.J., Scalo, J., Segura, A., Tang, C.M., Tiedje, J.M., Turnbull, M.C., Walkowicz, L.M., Weber, A.L., Young, R.E. 2007. A Reappraisal of the Habitability of Planets Around M Dwarf Stars. Astrobiology 7, 30.

The Denis Consortium. 2005. The DENIS database, 3rd Release. CDS/ADC Collection of Electronic Catalogues 2263, 0.

Torres, C.A.O., Busko, I.C., Quast, G.R. 1983. Activity in Red Dwarf Stars. Eds. Byrne, P.B., Rodono, M. Reidel, Dordrecht, p.175.

Torres, C.A.O., Quast, G.R., Da Silva, L., De La Reza, R., Melo, C.H.F., Sterzik, M. 2006. Search for containing young stars (SACY). I. Sample and searching method. A&A 460, 695.

Turnball, M.C., Tarter, J.C. 2003. Target Selection for SETI. I. A Catalog of Nearby Habitable Systems. ApJ Suppl. Ser. 145, 181.

Unsöld, A., Baschek, B. 2001. The New Cosmos. 5th ed. Springer-Verlag Berlin Heidelberg.

Van Altena, W.F., Lee, J.T., Hoffleit, E.D. 1995. The General Catalogue of Trigonometric Stellar Parallaxes, Fourth Edition. General Cat. Trigo. Parallaxes, 0.

Van Belle, G.T., Von Braun, K. 2009. Directly determined linear radii and effective temperatures of exoplanet host stars. AJ 694, 1085.

Van Leeuwen, F. 2007. Validation of the new Hipparcos reduction. A&A 474, 653.

Vazquez, M., Hanslmeier, A. 2006. Ultraviolet Radiation in the Solar System. Springer. Dordrecht.

Veeder, G.J. 1974. Luminosities and temperatures of M dwarf stars from infrared photometry. AJ 79, 1056.

Voges, W., Aschenbach, B., Boller, T., Bräuninger, H, Briel, U., Burkert, W., Dennerl, K., Englhauser, J., Gruber, R., Haberl, F., Hartner, G., Hasinger, G., Kürster, M., Pfeffermann, E., Pietsch, W., Predehl, P., Rosso, C., Schmitt, J.H.M.M., Trümper, J., Zimmermann, H.-U. 1999. The ROSAT All-Sky Survey Bright Source Catalogue (1RXS). A&A 349, 389.

Voges, W., Aschenbach, B., Boller, T., Bräuninger, H, Briel, U., Burkert, W., Dennerl, K., Englhauser, J., Gruber, R., Haberl, F., Hartner, G., Hasinger, G., Pfeffermann, E., Pietsch, W., Predehl, P., Schmitt, J.H.M.M., Trümper, J., Zimmermann, H.-U. 2000. ROSAT All-Sky Survey Faint Source Catalog (RASS-FSC). IAUC 7432, R1.

Walker, A.R. 1983. A spectroscopic survey of 113 nearby red dwarf stars. South African Astron. Obs. Circ., 7, 106.

Walkowicz, L.M., Hawley, S.L., West, A.A. 2004. The χ Factor: Determining the Strength of Activity in Low-Mass Dwarfs. PASP 116, 1105.

Walkowicz, L. M., Hawley, S. L. 2009. Tracers of Chromospheric Structure. I. Observations of Ca II K and Hα in M Dwarfs. AJ 137, 3297.

West, A.A., Hawley, S.L., Walkowicz, L.M., Covey, K.R., Silvestri, N.M., Raymond, S.N., Harris, H.C., Munn, J.A., McGehee, P.M., Ivezic, Z., Brinkmann, J. 2004. Spectroscopic Properties of Cool Stars in the Sloan Digital Sky Survey: An Analysis of Magnetic Activity and a Search for Subdwarfs. AJ 128, 426.

West, A.A., Hawley, S.L., Bochanski, J.J., Covey, K.R., Reid, I.N., Dhital, S., Hilton, E.J., Masuda, M. 2008. Constraining the age-activity relation for cool stars: the Sloan Digital Sky Survey Data Release 5 low-mass star spectroscopic sample. AJ 135, 785.

West, A.A., Basri, G. 2009. A first look at rotation in active late-type M dwarfs. ApJ 693, 1283.

West, A.A., Morgan, D.P., Bochanski, J.J., Andersen. J.M., Bell, K.J., Kowalski, A.F., Davenprot, J.R.A., Hawley, S.L., Schmidt, S.J., Bernat, D., Hitlon, E.J., Muirhead, P., Covey, K.R., Rojas-Ayala, B., Schlawin, E., Gooding, M., Schluns, K., Dhital, S., Pineda, S., Jones, D.O. 2011. The Sloan Digital Sky Survey Data Release 7 Spectroscopic M Dwarf Catalog I: Data. AJ 141, 97.

Wheatley, J.M., Welsh, B.Y., Browne, S.E. 2008. The second GALEX ultraviolet variability (GUVV-2) catalog. AJ 136, 259.

White, R.J., Gabor, J.M., Hillenbrand, L.A. 2007. High-dispersion optical spectra of nearby stars younger than the Sun. AJ 133, 2524.

Wolszczan, A., Frail, D. A. 1992. A planetary system around the millisecond pulsar PSR1257 + 12. Nature 355, 145.

Wood, B.E., Brown, A., Linsky, J.L. 1995. Determination of Plasma Temperatures and Luminosities Using Multiple Extreme-Ultraviolet and X-Ray Filters. ApJ 438, 350.

Zacharias, N., Finch, C., Girard, T., Hambly, N., Wycoff, G., Zacharias, M.I., Castillo, D., Corbin, T., Di Vittorio, M., Dutta, S., Gaume, R., Gauss, S., Germain, M., Hall, D., Hartkopf, W., Hsu D., Holdenried, E., Makarov, V., Martines, M., Mason, B., Monet, D., Rafferty, T., Rhodes, A., Siemers, T., Smith, D., Tilleman, T., Urban, S., Wieder, G., Winter, L., Young, A. 2009. Third U.S. Naval Observatory CCD Astrograph Catalog (UCAC3). CDS/ADC Collection of Electronic Catalogues 1315, 0.

Zuckerman B., Song, I. 2004. Young stars near the Sun. Annual Rev. A&A 42, 685.

Abstract

The term space weather was originally introduced to describe temporal changes of the Sun's activity and their influence on the planets of the Solar System. Due to numerous discoveries of exoplanets in the past decades, this term is also used today to describe the activity of other stars than the Sun. In the present work a large sample of M-type stars within 15 parsec of the Sun was studied directing the main focus on their activity in comparison to Sun-like stars. In summary, an almost complete coverage of the electromagnetic radiation emitted by 355 M-type stars as well as 22 Sun-like stars over a wavelength range from 0.5 to 2300 nm was performed and thus illustrates their characteristics over a large part of the electromagnetic spectrum. It turned out that the high activity lifetime of ionizing short radiation is not as long as expected, especially for early-type M stars. Furthermore, the mass limit for fully convective energy transport seems to be lower than it has been postulated in earlier articles. Finally, a possibly new age indicator for stars of spectral class M is discussed.

Zusammenfassung

Der Begriff Space Weather wurde ursprünglich eingeführt, um zeitliche Änderungen der Sonnenaktivität und deren Einfluss auf die Planeten des Sonnensystems zu beschreiben. Aufgrund zahlreicher Entdeckungen von Exoplaneten in den vergangenen Jahrzehnten wird dieser Begriff nun auch zur Beschreibung der Aktivität anderer Sterne als der Sonne verwendet. In der vorliegenden Arbeit wurde ein großes Sample von Sternen der Spektralklasse M, die sich in einem Radius von 15 pc um die Sonne befinden, untersucht, wobei der Fokus auf ihre Aktivität im Vergleich zu sonnenähnlichen Sternen gerichtet wurde. Zusammenfassend wurde die elektromagnetische Strahlung von 355 M sowie 22 sonnenähnlichen Sternen im Wellenlängenbereich von 0.5 bis 2300 nm nahezu vollständig untersucht und somit die jeweiligen Besonderheiten über einen großen Teil des elektromagnetischen Spektrums dargelegt. Dabei zeigte sich, dass die hohe Aktivitätszeit der ionisierenden kurzwelligen Strahlung nicht so lange anzudauern scheint wie bislang vermutet. Dies gilt besonders für frühe M Sterne. Des Weiteren scheint die Grenzmasse für einen völlig konvektiven Strahlungstransport niedriger zu sein als sie in früheren Artikeln eingeschätzt wird. Darüber hinaus wird ein möglicher neuer Altersindikator für Sterne der Spektralklasse M diskutiert.

Acknowledgements

I want to thank my supervisor Univ.-Prof. Dr. Arnold Hanslmeier for giving me the chance to work on a combination of two topics that I absolutely wanted to work on. He took the time to discuss several ways and ideas until the perfect match was found. Furthermore, I really appreciate having been taught by such a didactically great professor, who never loses sight of the practical aspects next to a fundamental scientific education. Further, he supports his students in many different ways, for example inviting me to the Central European Solar Physics Meeting V in Bairisch Kölldorf, Austria, where I was allowed to present my first scientific poster. His feedback was always constructive and motivating and so guided me through the process of writing a master's thesis.

I acknowledge Mag. Petra Odert for allowing me access to various calculated results from her PhD thesis in advance of publication. Further, I would like to thank her for advice and many helpful suggestions during the writing of this work. She put so much effort into supporting me and not one single of my numerous e-mails or questions was left unanswered.

There are two other persons, that I would like to quote in particular: David Horner and Barbara Kaschel. Thank you, for accompanying me for the last ten years and that I can always count on you.

In addition, I am very grateful to all my friends, who were truly interested in my master's thesis' topic and never stopped questioning about it. This really helped not to lose the thread. Besides, I would like to thank everyone, who offered valuable comments on this work, supported me in any way or just was understanding when I had no time during the writing process. Listing all your names would fill several pages. Please feel mentioned, remembered and appreciated!

Finally, I want to thank my parents for supporting me financially over the main part of my studies.

CURRICULUM VITAE Traude Rochowanski

PERSONAL INFORMATION

Date, place of birth: September 9th, 1983, Vienna, Austria

E-mail: t.rochowanski@yahoo.de

EDUCATION

10/2008 - 04/2012	University of Vienna, Master of Astronomy (Magisterstudium) Majors: Stellar Astrophysics, Structure and Evolution of the Milky Way Master's thesis: M-Type Stars and their Space Weather
10/2004 - 10/2007	University of Vienna, Bachelor of Astronomy (Bakkalaureatsstudium)
09/1993 - 06/2001	Secondary School (AHS), BG VIII, Vienna, Austria School Leaving Examination (Matura) June 21st, 2001

WORK EXPERIENCE

02/2010 - present	Trainer for German as a second and English as a foreign language Project ISIS, Adult Education Centers of Vienna (VHS). ISIS is a project to support migrant youth. Tasks: Conducting lessons, developing curricula and teaching material, empowerment and motivation
01/2011 - present	Project manager for the project uni4you Private initiative in collaboration with the Adult Education Centers of Vienna Content: Integration of young immigrants into the higher education sector. Responsible for selection of staff, conducting workshops, networking and collaborating with project partners (universities, schools, NGOs), development of material, project documentation and evaluation

AWARDS

Project ISIS	Austrian National Award for adult education. Section: Integration through education (in the framework of the Dynamo network), 2010
Project uni4you	Vielfalter Award. Awarded with 5000€, 2012

VOLUNTARY ENGAGEMENT

09/1989 - present	Active scout member at the scout group 23 "St. Calasanz", Vienna, Austria Since 2009 scout leader. Main tasks: working with 13-16 year old adolescents on different topics (environmental protection, first aid, social behavior, politics etc.), organizing weekly meetings, scout camps and other events

POSTER

10/2011	M-Type Stars and their Space Weather Central European Solar Physics Meeting V; Bairisch Kölldorf, Styria, Austria